Study commissioned by the Defra Flood Management Division, the Health and Safety Executive and the Geological Survey of Ireland.

Tsunamis – Assessing the Hazard for the UK and Irish Coasts

June 2006

HR Wallingford
Working with water
British Geological Survey
NATURAL ENVIRONMENT RESEARCH COUNCIL
Proudman Oceanographic Laboratory
NATURAL ENVIRONMENT RESEARCH COUNCIL

Statement of use
This report is the result of further research studies on the potential impacts of Tsunamis on the coasts of UK and Ireland. It should be read in conjunction with the previous study, lead by BGS and published by Defra. It is designed to provide general background analysis for use by those planning for the impact of such extreme but plausible events.

Dissemination status
Agreed by the sponsors for public release as a report of scientific research.

Keywords: tsunami, earthquake, numerical modelling, hazard, UK coastline

Research contractor:
HR Wallingford
Howbery Park
Wallingford
Oxon
OX10 8BA
Project Manager: Dr Stephen Richardson, s.r.richardson@hrwallingford.co.uk
This project is reported as HR Wallingford Report EX 5364.

The project was carried out by a consortium with the following membership:
HR Wallingford
British Geological Survey
Proudman Oceanographic Laboratory

Defra project officer:
Mr David Richardson, david.richardson@defra.gsi.gov.uk

Publishing organisation
Department for Environment, Food and Rural Affairs
Flood Management Division,
Ergon House,
Horseferry Road
London SW1P 2AL

Tel: 020 7238 3000 Fax: 020 7238 6187
www.defra.gov.uk/environ/fcd

Published by the Department for Environment, Food and Rural Affairs. Printed in the UK, (March, 2006) on recycled material containing 80% post-consumer waste and 20% chlorine-free virgin pulp.

PB No. *xxxxx* ISBN: *xxxxxx*

Executive summary

Following completion of the 2005 Department for Environment, Food and Rural Affairs (Defra) commissioned study "The threat posed by tsunamis to the UK", this study was undertaken to investigate more specific questions raised from the previous report. This study has been commissioned by Defra, the Health and Safety Executive and the Geological survey of Ireland.

The original Defra study identified four potential tsunami sources origins (North Sea, Celtic Sea, offshore of Lisbon and La Palma in the Canary Islands), and provided first estimates for wave conditions at the UK coast for tsunamigenic events of very high, high and moderate likelihood.

Two of these source origins are now reviewed in more detail, the North Sea event and a Lisbon-type event, with their consequence compared to an assessment of hazard. The objectives of this study are as follows:

- Refinement of the potential impact envelope in South West England, South Wales, the Bristol Channel, southern and western Ireland from Lisbon-type events;
- Further consideration of the difference between tsunami-type events and storm surge waves in terms of coastal impact;
- Investigation of typical impacts of near-coast events e.g. North Sea beaches and other facilities seaward of defences including expected wave heights, celerities and therefore degree of hazard.

The first task was to review the tectonics in the area between Gibraltar and the Azores. A review of existing literature led to three models being proposed:

Model A	Epicentre of the 1969 earthquake in the Horseshoe Abyssal Plain, southeast of the Gorringe Bank. The orientation of the fault is southwest-northeast;
Model B	Epicentre north of the Gorringe Bank, related to the tectonic uplift of the region. The orientation of the fault is west-east;
Model C	Epicentre is located southwest of Lisbon, offshore but closer to the Iberian coast than model A and model B. The fault orientation is north-south.

Previous literature suggests that the magnitude of the 1755 earthquake was in the range from 8.5 to 9.0 M_W. Extreme magnitudes of ≥ 9.0 M_W were excluded, since earthquakes of this size are only likely to occur in subduction zones. There is no credible evidence of a subduction zone off the southwest coast of Lisbon. This led to source magnitudes of $M_W = 8.5 \pm 0.2$ being used in the models A – C. Estimates of the surface displacement were then calculated for each model.

The six source conditions were entered into the POL CS3 12km model as initial surface displacements. The propagation of the resulting tsunami waves was performed by solving the shallow water equations. The 8.3 M_W earthquakes produced maximum wave elevations of approximately 0.1m at the UK continental shelf. As might be expected, the larger magnitude earthquakes (8.7 M_W) produced larger tsunami waves of up to 0.5m at the continental shelf. The orientation of the original source fault was also found to be of importance with regard to approach

wave elevation. Model C has a north-south orientation; therefore the majority of the wave energy is directed into the Atlantic Ocean or onto the Iberian coast. The fault orientation of model A and B are similar, although the resulting leading tsunami wave from model A is positive and model B leads with a depression wave. Results of the Lisbon-type events performed indicate that no matter whether the tsunami leads with a positive wave or a depression (noted at the coast by a withdrawal of the sea), the wave elevation at the continental shelf would be similar.

The resulting waves at the continental shelf were propagated to the UK and Irish coasts by TELEMAC-2D. The computational model allowed the processes of refraction and diffraction, up the shelf and over the shallow bathymetry, to be modelled on a variable resolution mesh, enabling a constant number of cells per wavelength.

Results of the TELEMAC flow model indicated that model B (8.7 M_W) produced the highest wave elevations along the UK and Irish coastline, specifically the Cornish coast and southern Ireland. The model run produced maximum wave values of 1-2m around the majority of Cornwall, with 3-4m identified between Penzance and Lizard Point. Along the south coast of Ireland, wave elevations were also consistently 1-2m, with a number of areas (Ross Carbery and Kinsale) recording wave elevations of greater than 2.5m.

An investigation into the typical impact of a near-coast event in the North Sea was also performed. The event was centred on the location of the 1931 earthquake, with an assumed magnitude of 6.0 M_W. The predicted surface rupture length was 8km, of maximum displacement 0.3m for a northwest-southeast fault orientation. The resulting tsunami was propagated from source using the POL N10 3.5km resolution model, the wave had an assumed wave period of approximately 20-30 minutes. Close to the coast, wave data was extracted from the N10 model and wave run-up and inundation simulated using the TELEMAC flow model.

Results of these model runs confirmed that the type of numerical model used (finite volume or finite element) had no significant impact on run-up level predictions for the 1:60 and 1:200 sloping beaches modelled. Run-up levels were in the region 2.5 – 3.0 times the offshore tsunami wave elevation.

The model results were then used to assess hazard at the coastline. As the tide level generally had little effect on the overall tsunami wave elevation, the tsunamis arrival was assumed initially to coincide with mean high water springs and latterly with mean high water neaps. The tsunami elevations around the coast were compared against 50 year and 100 year extreme sea level. Only the most south-westerly coast of the UK may incur sea level elevations marginally in excess of the 1:100 year extreme sea level predictions.

A further assessment of hazard reviewed the wave elevation and flow velocity at the still water level for the tsunami wave as it ran-up and down the beach. A simple formula used these parameters to assess the hazard level. Results indicated that the North Sea event hazard level could be classified as “low”. For an 8.7 M_W Lisbon-type event the tsunami waves reaching the Cornish and southern Irish coasts could be classified as “extreme”, dangerous for all.

Finally, travel times from the origin of the tsunami source to the UK coast were reviewed. If the North Sea event occurred, the wave would reach the coast in approximately 30 minutes, probably too short a time to issue a warning. This said, the level of hazard on the beaches for such an event could be classified as low. For the Lisbon-type tsunami, travel times are approximately four and a half hours to the Cornish coast, allowing enough time for the general public to be notified of the potential hazard providing a suitable mechanism were in place.

Contents

Tables

Figures

Appendices

1 Introduction

In early 2005, the Department for Environment, Food and Rural Affairs (Defra) commissioned the study "The threat posed by tsunamis to the UK" (Kerridge 2005) following the earthquake off the northwest coast of Sumatra and the consequent devastating tsunami of the 26 December 2004. The study, completed in May 2005, provided first estimates for wave conditions at the coast for tsunamigenic events that had a very high, high or moderate likelihood of reaching the UK. In this previous study four origins for the tsunami source were examined:

- Near field earthquake in the North Sea (cf. Dogger Bank, 1931);
- Passive margin earthquake in the western Celtic Sea;
- Plate boundary west of Gibraltar (Lisbon, 1755);
- La Palma slide (Canary Island).

Results from the study indicated that the most likely scenario, for a significantly damaging tsunami, would be a large, relatively close earthquake producing a tsunami that would be severe only locally. These sources would either be in the North Sea or western Celtic Sea, although such earthquakes are rare and should such an event occur would probably not be tsunamigenic.

There is evidence of tsunami sources, further a field, which have impacted on the UK coast. Specifically the earthquake of 1755 (Borlase 1755, 1758), which had a source in the region of the Azores-Gibraltar fault zone and which devastated Lisbon. There have been other large earthquakes in this region, which have been tsunamigenic, although non-have produced any significant impact on the UK coast.

Another potential far field source would be the collapse of the western flank of the Cumbre Vieja, La Palma. It has been hypothesised that such a collapse would generate a wave, tens of metres high, which would propagate across the Atlantic and devastate the east coast of America (Ward and Day, 2001). The assumption for the collapse mechanism, assumed to be a whole of the western flank is questionable. There is evidence from surveys of material deposited from previous landslides in the Canary Islands that collapses take place as multiple events, over a period of time (Kerridge, 2005). Consequently if this is the collapse mechanism, the tsunamigenic potential is significantly reduced.

This second study was commissioned by Defra in August 2005, with the following objectives:

- Refinement of the potential impact envelope in South West England, South Wales, the Bristol Channel and Southern Ireland (later extended to the west coast of Ireland) from Lisbon-type events;
- Further consideration of the difference between tsunami-type events and storm surge waves in terms of coastal impact;
- Investigation of typical impacts of near-coast events e.g. North Sea beaches and other facilities seaward of defences including expected wave heights, celerities and therefore degree of hazard.

It was noted in the previous Defra study (Kerridge, 2005) that when modelling tsunami events several standard numerical techniques can be used to simulate the wave propagation, but confidently predicting the sea surface deformation and final run-up levels present a greater challenge. This work develops the previous analysis to consider the seismic generation and run-up components in more detail.

The first stage of this report (Chapter 2) reviews the impact of a Lisbon-type event on the UK and Irish coastline. The derivation of the source for such an event is discussed in Section 2.1. Aside from prehistoric tsunamis caused by submarine slides on the continental margin of Northwest Europe, the largest tsunami to impact on the shores of the British Isles was that caused by the great Lisbon earthquake of 1 November 1755. This tsunami was well observed in Southwest Britain, especially in Cornwall (Borlase, 1755, 1758). It caused no damage, but there are reports that state it was sufficiently strong to displace boulders (Edmonds, 1846). In considering tsunami risk to the UK and Ireland, it is therefore imperative to consider what would be the consequences of a repeat of the 1755 earthquake. Modelling this requires knowledge, or at least an estimate, of the source parameters of such a tsunamigenic earthquake.

Since the Lisbon earthquake occurred 250 years ago, the main source of information is documentary records, and some way has to be found to estimate earthquake parameters from descriptions of what occurred in terms of human impact. This is complicated further by the fact that the earthquake occurred offshore, and observations are restricted to the land area. Baptista *et al*. (1998a) present a compilation of almost all the available historical data for the 1755 earthquake from countries affected by the tsunami. From this dataset, the authors infer tsunami travel time, polarity of the first movement, maximum run-up height, period, the number of waves, duration of the sea disturbance, and the extent of flooding. They find mean run-up heights on the Iberian coast of 1-15 m, and wave periods of 10-20 minutes.

Many studies rely on comparison with the magnitude 7.9 M_W earthquake that occurred on 28 February 1969, with its epicentre at the Horseshoe Abyssal Plain (36.01°N/10.57°W). The tsunami generated by this earthquake has been extensively modelled in the hope that a greater understanding of the 1755 earthquake can be achieved. Studies include Heinrich *et al*. (1994), Gjevik *et al*. (1997) and Rabinovich *et al*. (1998). However, the problem of determining the source parameters from tsunami observations appears to be non-unique even for this much more recent event (Gjevik *et al*., 1997).

Section 2.1.1 of this report gives a brief overview of the tectonics of the area between Gibraltar and the Azores. More detailed information can be found in Appendix A. We examine the tectonic features of the source region to determine possible source orientations. Section 2.1.2 gives a brief description of the magnitude 7.9 M_s earthquake of 28 February 1969, which occurred on the Horseshoe Abyssal Plain and also caused a small tsunami. Section 2.1.3 reviews existing literature to determine the most likely source location for this event. We present the arguments both for and against the most widely considered source locations. In Section 2.1.4, we apply published empirical relations to existing earthquake magnitude / moment estimates for the 1755 Lisbon earthquake, and determine a range of fault dimensions and amount of slip. The earthquake mechanisms, fault dimensions and slip are then used to model sea floor displacements.

Once these source models for potential Lisbon events have been derived, this information can be input as initial conditions into numerical models for wave propagation from source to coastline. In Section 2.2, the first stage of numerical

modelling (propagation to nearshore) for the Lisbon events is discussed. The choice of propagation model is discussed in Section 2.2.1 with details of the POL CS3 numerical model provided in Section 2.2.2. Results of the wave propagation from source to nearshore (continental shelf) are presented in Section 2.2.3, which is followed by discussion of results (Section 2.2.4).

Wave data (free-surface elevation and velocities) from Section 2.2 were then input into the TELEMAC model in Section 2.3 for detailed propagation to shoreline. Details of the TELEMAC model including model area, mesh and boundary conditions are given in Sections 2.3.1 – 2.33. Information on simulation runs and results are presented in 2.3.4, followed by comparisons at the UK and Irish coast against observations for the 1755 Lisbon tsunami in Section 2.3.5. Detailed wave elevation levels are presented in Section 2.3.6 for the Cornish coast, the Bristol Channel, the Southern coast of Ireland and the West coast of Ireland.

The second stage of this report (Chapter 3) focussed on a near-field event in the North Sea and the typical impact of such an event on the near coast. The main emphasis related to the tsunami wave inundation, specifically wave height / run-up levels and flow velocities. No specific revision of the source term was required, although a revised estimate is provided in Section 3.1. The source for such an event would be significantly smaller than for a Lisbon-type event, therefore the POL N10 model with a resolution of 3.5km was used. Details of the N10 model set-up are presented in Section 3.2. Nearshore results for the propagating tsunami wave were extracted from the POL N10 model and used in the TELEMAC flow model (Section 3.3) to simulate inundation of typical beach profiles. Typical wave run-up levels and flow velocities on the 1:60 and 1:200 beach slopes are presented in Section 3.4.

The results of Chapters 2 and 3, regarding wave elevation, run-up and flow velocities are placed into context, with regard to hazard, in Chapter 4. Maximum wave elevations for the Lisbon type events, around the Cornish coast and the Bristol Channel are compared against 1:50 and 1:100 year extreme sea levels in Section 4.1.

Water elevations alone may not be sufficient to confirm whether flows are hazardous. In Section 4.2, water depths and flow velocities for the North Sea event are compared against published results for hazardous combinations of flow depths and velocities.

If sufficient time and confidence in recognition of tsunamigenic events is available, the possibility of evacuating individuals from coastal areas is a possibility. Arrival times, for Lisbon type events, at the UK coast are discussed in Section 4.3.

Conclusions of the study are finally drawn together in Chapter 5.

This report has been produced by a large team, comprising of individuals from HR Wallingford, British Geological Survey and the Proudman Oceanographic Laboratory. The project team is listed in Appendix B.

2 Lisbon Event

2.1 Source Terms

2.1.1 Tectonic Overview

The Azores-Gibraltar fault zone (AGFZ) is the westernmost continuation of the boundary between the Africa and Eurasia plates (Figure 2.1). The segment we are particularly concerned with here, in considering a repeat of the 1755 Lisbon earthquake, extends from the Madeira Tore rise in the west to the Straits of Gibraltar in the east (Figure 2.2). Sborshchikov *et al*. (1988) and Sartori *et al*. (1994) give detailed descriptions of this region. Structurally, this area is complex, with bathymetry characterised by a series of ridges and seamounts, such as the Gorringe Bank, separated by significant depressions such as the Horseshoe and Tagus abyssal plains. Neither the location, nor the character of the plate boundary is well understood, but the diffuse distribution of seismicity suggests that there is a wide transpressional zone between the Gorringe Bank and the Tell Atlas mountains (Morel and Meghraoui, 1996). Seismicity on the eastern segment occurs over a broad region (~ 250km) and indicates active WNW-ESE -compression, with crustal shortening accommodated on numerous thrust faults (Buforn *et al*., 1988; Sartori *et al*., 1994). This compression results in earthquakes with significant vertical slip, of a type that can result in tsunami. Earthquake focal mechanisms indicate both right lateral strike-slip and reverse faulting on roughly east - west oriented structures.

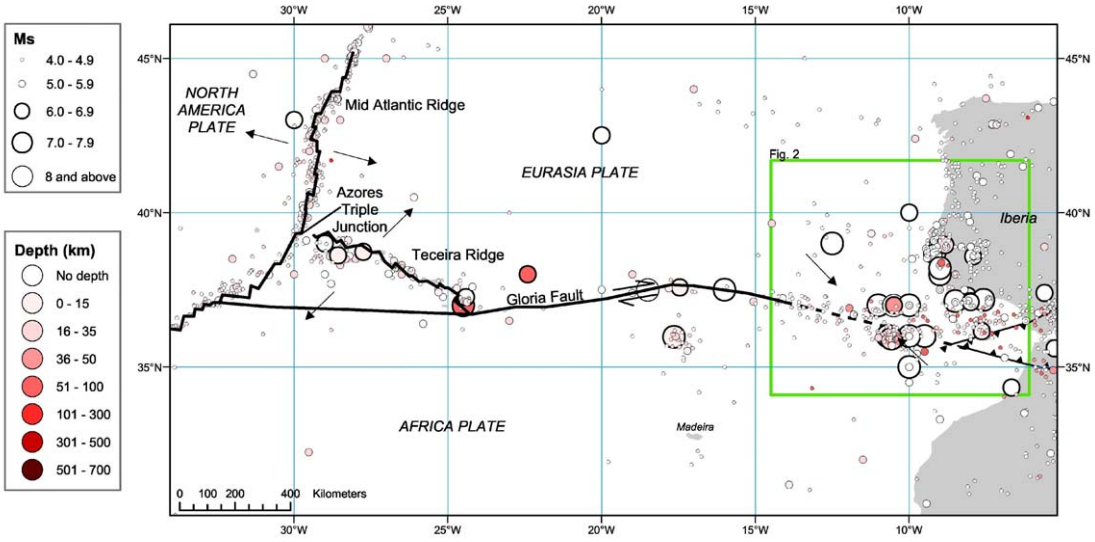

Figure 2.1 Tectonics of the Azores Gibraltar fracture zone region. Plate boundaries after Jiménez-Munt *et al.* (2001). Earthquake data from the BGS World Seismicity Database (Henni *et al.*, 1998).

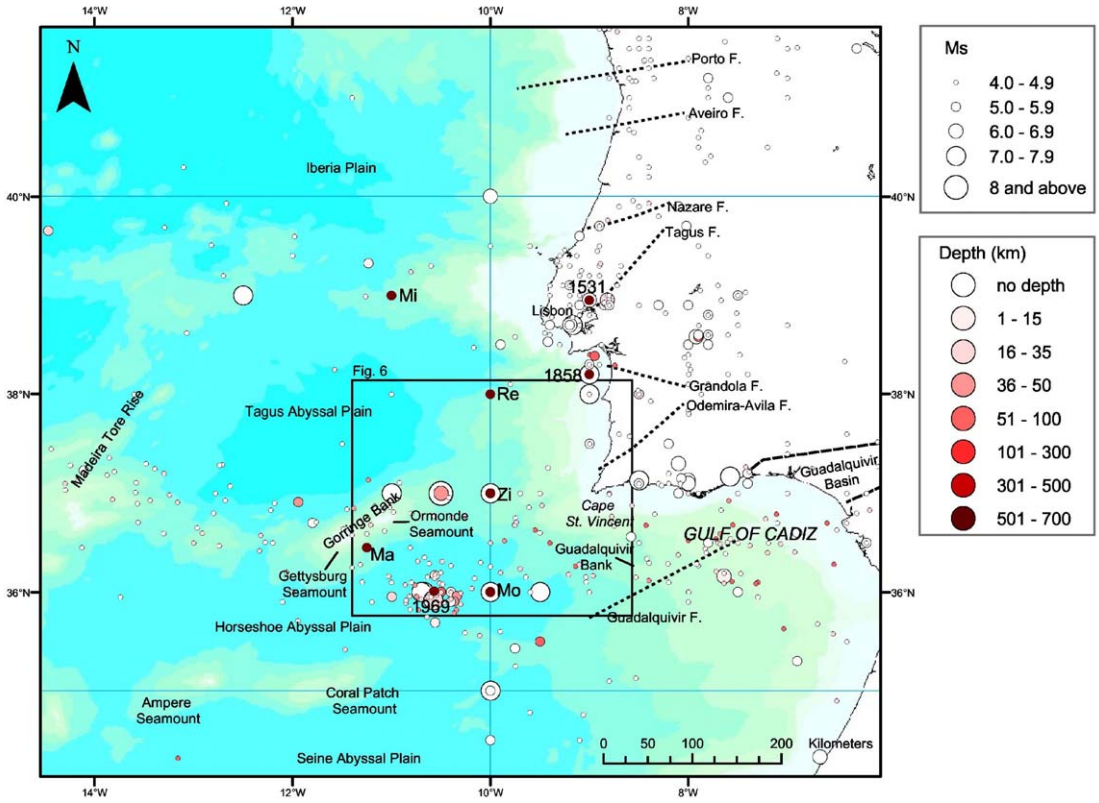

Figure 2.2 **Map of the Azores-Gibraltar fracture zone, east of the Madeira Tore rise. The positions of onshore faults are taken from Alves *et al.* (2003). The position of the Guadalquivir bank is from Baptista *et al.* (2003). Red circles denote earthquake epicentres, including various epicentres proposed for the 1755 earthquake: Ma: Machado (1966); Mi: Milne (cited by Johnston, 1996); Mo: Moreira (1989); Re: Reid (1914); Zi: Zitellini *et al.* (1999). Earthquake epicentres from the BGS World Seismicity Database (Henni *et al.*, 1998) are also plotted. Location of the Guadalquivir fault is from Borges *et al.* (2001). Bathymetry data are taken from the General Bathymetric Chart of the Oceans.**

2.1.2 1969 Earthquake on the Horseshoe Abyssal Plain

On 28 February 1969, a large earthquake (7.9 M_s) occurred in the Horseshoe Abyssal Plain at 36.01ºN, -10.57ºE (Figure 2.2), southeast of the Gorringe Bank (Fukao, 1973). The earthquake generated a small tsunami that was recorded at tidal stations in Portugal, Spain, Morocco, the Azores, and the Canary Islands (e.g. Gjevik *et al*., 1997). The depth of the earthquake (23km) is well constrained (Fukao, 1973). The fault plane solution (derived from both first motion and surface wave data) shown in Figure 2.2 indicates thrust faulting with a small component of left lateral strike slip. Fukao (1973) finds that the aftershock sequence delineates an area extending from the seafloor to a depth of 40-45km that is elongated in the NE-SW direction and dips at approximately the same angle as the north-dipping nodal plane, 52º (Figure 2.3).

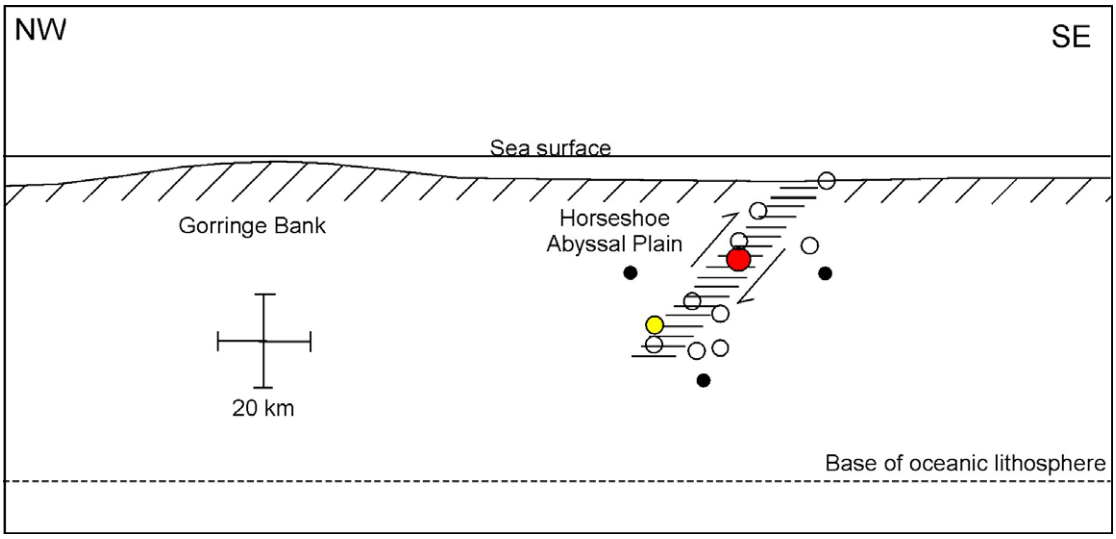

Figure 2.3 Cross section of the aftershock distribution from the 1969 earthquake (after Fukao, 1973).

The tsunami generated by this earthquake has been extensively modelled in the hope that a greater understanding of the 1755 earthquake can be achieved. Studies include Heinrich *et al*. (1994), Gjevik *et al*. (1997) and Rabinovich *et al*. (1998). In their modelling, Gjevik *et al*. (1997) assume that the rupture area measures 80 × 50km and determine a maximum vertical seafloor displacement for the earthquake of ~ 1.8m. Although the resolution of their model is only sufficient for direct comparison with the observed travel time and polarity of the first wave to be made, they find that at six of the thirteen stations used, the model reproduces the data well. However, these stations do not provide a strong constraint on the location of the source, and at Faro and Lagos (Algarve) it is not possible to reproduce the observed travel time for the source configuration. The authors find that it is also impossible to reproduce the observations from Santa Cruz (Tenerife) and Casablanca (Morocco) unless the shape and extent of the source are changed.

Heinrich *et al*. (1994) model the tide gauge observations from the 1969 earthquake. They find that the travel times and wave amplitudes at most of the tide gauges in the region are reproduced reasonably well using the fault plane identified by Fukao (1973). The main discrepancy arises at the Cascais (near Lisbon) tide gauge where the first recorded waves are not reproduced by the modelling. Heinrich *et al*. (1994) suggest that this is either because the tide gauge at Cascais was not very sensitive to the source, or because the local bathymetry is not well known. Their modelling also suggests that tsunami waves in this region are strongly refracted and reflected by the seamounts of the Gorringe Bank, which act as secondary sources.

2.1.3 The 1755 Lisbon Earthquake source

Locating the 1755 earthquake accurately has proved to be somewhat problematic despite the wealth of historical data available. Conflicting information regarding the distribution of intensities, origin time, the timing of strong shaking and tsunami arrivals (Johnston, 1996; Mendes *et al*., 1991), and the diffuse distribution of earthquakes along this part of the AGFZ (Zitellini *et al*., 2001) lead to large uncertainties, and the range of possible epicentres spans around 500km. Modelling of both the tsunami (Baptista *et al*., 1998b) and earthquake intensity (Johnston, 1996) has been used to estimate the location and the size of the source. Detailed geophysical surveying in the eastern section of the AGFZ has been used to identify

possible source structures (Zitellini *et al*. (1999, 2001)). However, different methods and data have led to numerous conclusions. Mendes *et al*. (1999) point out that there are issues concerning how accurately tsunami waves can be modelled and whether seismic source parameters really are compatible with tsunami source parameters.

We have considered a number of possible source models for the 1755 earthquake. The strengths and weaknesses of each model and where possible, its consistency with the historical dataset are discussed in Appendix C. These models fall into the following four categories:

1. Gorringe Bank models; a single large thrust fault source distant from the Portuguese coast (Johnston 1996).
2. Thrust faulting on western Iberian margin; for example the Marques de Pombal fault, or the Horseshoe Fault (Baptista *et al* 2003).
3. Composite source models involving triggered rupture on two separate fault systems. For example, an earthquake local to Lisbon, along the Lower Tagus Valley Fault, triggered by a more distant event, e.g. on the Gorringe Bank (Vilanova *et al* 2003).
4. Cadiz subduction models; an earthquake on a small subduction front in the Gulf of Cadiz (Gutscher *et al* 2002).

2.1.4 Realistic source models

As described in the previous section, a large number of source models for the 1755 Lisbon earthquake have been proposed. The problem of determining hypocentre location, source mechanism and rupture dimensions appears to be underdetermined and a large number of models can be found that partially match the macroseismic and tsunami observations. At the same time, most of these models contradict some of the observations. This is summarised in Table 2.1. It was pointed out by Gjevik *et al*. (1997) that even for the 1969 event the problem of determining the source parameters from tsunami observations was non-unique.

In this section we derive source dimensions and average slip based on realistic assumptions of the earthquake magnitude and empirical relationships for the source scaling of intraplate earthquakes. We then combine this information with possible earthquake source mechanisms. We have rejected the subduction model of Gutscher (2004) on the basis that there is a significant amount of evidence against subduction, for example Stich *et al*. (2005). We also exclude any of the composite source models, such as Vilanova *et al*. (2003), on the basis that these models include rather complicated features that are not relevant to modelling the tsunami risk to the UK and Ireland.

Table 2.1 A summary of the previously proposed source models for the 1755 earthquake, and the fit they provide to existing data.

	Gorringe Bank	Iberian Margin	Composite Source	Subduction Source
Fits macroseismic data	Yes	Yes	Yes	No
Fits tsunami data	No	Yes	Partially	Partially
Observed seismicity	Yes	Some	Yes	Yes
Realistic tectonic explanation	Several large structures exist that could have caused the earthquake	Series of smaller structures exist, but possibly too small to cause a tsunamigenic earthquake	Seems unlikely and involves only small structures	No, model controversial

EARTHQUAKE SIZE

Estimates of the magnitude of the 1755 earthquake generally vary between 8.5 and 9.0. Abe (1979) determines a tsunami magnitude for the earthquake (defined as the logarithm of the maximum amplitude of far-field tsunami waves measured on tide gauges, or their equivalent) between 8.5 - 8.75, with a best fit of $M_t = M_W = 8.6$. Johnston (1996) uses isoseismals to determine moment magnitude (M_W) for the Lisbon earthquake, finding a best-fit magnitude of 8.7 ± 0.39. However, some authors, for example Frankel (1994), argue that felt area does not scale linearly with magnitude at high magnitudes.

In this study we choose a source magnitude of $M_W = 8.5 \pm 0.2$, based on the magnitude of Abe (1979). This gives lower and upper estimates of earthquake magnitude of 8.3 and 8.7 M_W, respectively. We have excluded extreme estimates of magnitude of 9.0 and above, such as that given by Mader (2001), since earthquakes of this size are only likely to occur in subduction zones.
The moment magnitude is linked to the seismic Moment M_0 through

$$M_W = \frac{\log M_0}{1.5} - 10.73 \quad , M_0 \text{ in dyn-cm}$$

The seismic moment is defined as

$$M_0 = \mu A D$$

where μ is the shear modulus, which characterizes a medium's resistance to shearing. A is the fault area ($A = WL$, width W and length L) and D is the average slip. For oceanic lithosphere, $\mu = 6.5 \times 10^{11}$ dyn/cm^2 (Johnston, 1996). Heinrich (1994) assumes $\mu = 4 \times 10^{11}$ dyn/cm^2.

TECTONIC REGIME AND EARTHQUAKE SCALING

Source scaling relationships are different for intraplate earthquakes (within a tectonic plate) compared to interplate earthquakes (on the interface between tectonic plates) (Scholz *et al*., 1986). From earthquake observations it is seen that average fault slip scales linearly with fault length (Scholz, 1982) (as long as the length of the fault is not more than ten times the width)

$D = \alpha L$

with $\alpha = 6.5 \times 10^{-5}$ for intraplate earthquakes (Scholz, 2002), although it could be as large as $\alpha = 10^{-4}$ (Scholz *et al*., 1986). For interplate earthquakes, $\alpha = 1.5 \times 10^{-5}$ (Scholz, 2002). This linear relationship between D and L implies that the moment scales as L^2W.

For the 1755 and 1969 earthquakes it seems more realistic to assume an intraplate tectonic setting, which is plate boundary related, as there is no clear evidence that the earthquakes were of interplate origin as they would be if the source was in a subduction zone.

SEISMOGENIC ZONE

The seismogenic zone (where earthquake rupture occurs) near the Gorringe Bank is about 60km thick (Stich *et al*., 2005). We assume that the 1755 earthquake ruptured the entire seismogenic zone (between 60km depth and the surface). With a fault dip of about 50° (Fukao, 1973), this means that a realistic fault width is about 75km.

PHYSICAL DIMENSIONS

Fault length and average slip are derived as follows

$$M_0 = \mu\alpha W L^2 \Rightarrow L^2 = \frac{M_0}{\mu\alpha W}$$

Assuming a range of moment magnitude we obtain a range for the length and average slip, which together with slip and fault orientation are required as input for the computation of seafloor displacement (Table 2.2). Although the parameters W, μ and α have uncertainties attached as well, we only use a best estimate. This is done to keep the number of models to a manageable size as the total number will be given by the number of dimension models times the number of source orientation/location models.

Table 2.2 Models of physical source dimensions.

	Model 1	Model 2
M_W	8.3	8.7
M_0 (dyn-cm)	3.5×10^{28}	1.4×10^{29}
μ (dyn/cm2) ($\pm 2 \times 10^{11}$)	6.5×10^{11}	6.5×10^{11}
W (km) ($\pm$15)	75	75
α ($\pm 3 \times 10^{-5}$)	6.5×10^{-5}	6.5×10^{-5}
L (km)	105	210
D (m)	6.8	13.6
$\Delta\sigma$ (bars)	50	70

FAULT ORIENTATION AND LOCATION

As discussed previously, the exact source of the 1755 earthquake remains unknown. This means that we cannot simply model a single source. We propose three possible fault orientations and locations, shown in Figure 2.4, combined with the source dimensions discussed above:

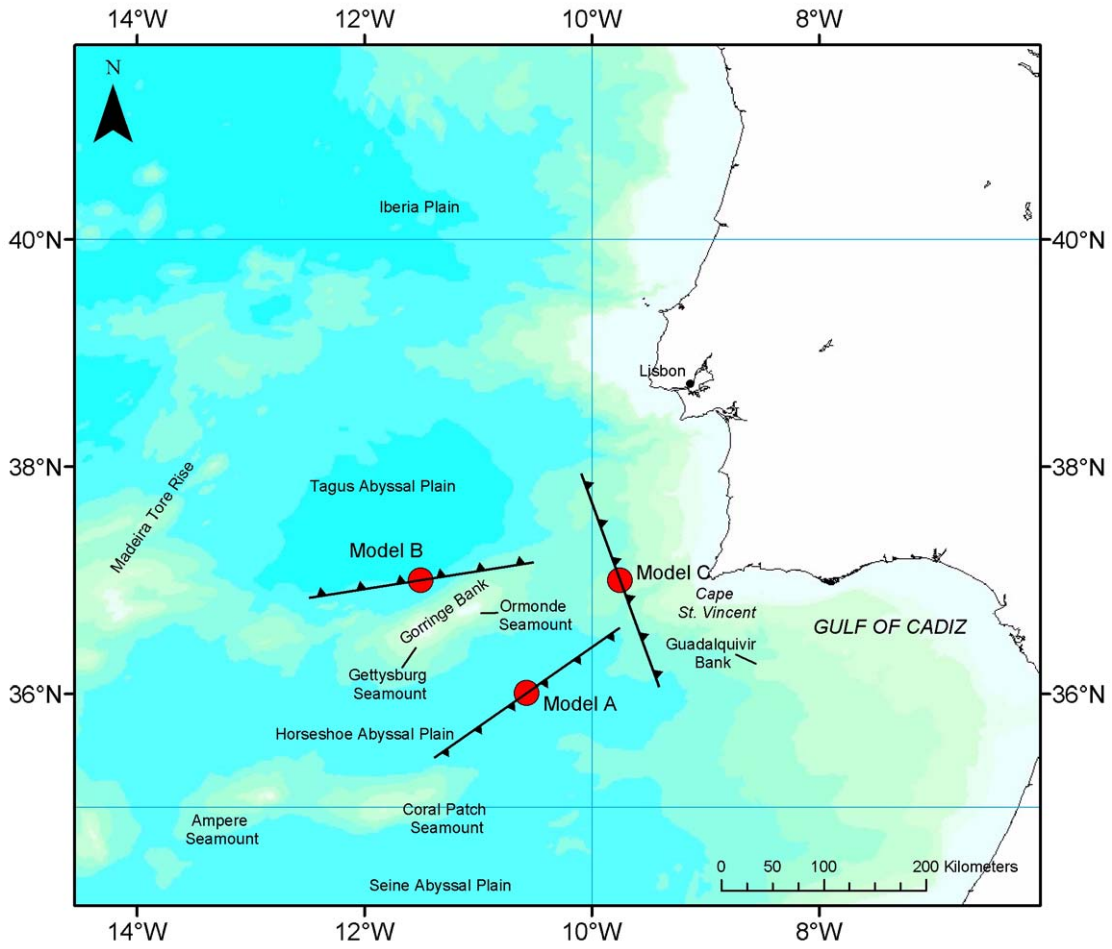

Figure 2.4 The three source models proposed for further investigation in this study.

Model A: An earthquake with the same epicentre as the 1969 earthquake in the Horseshoe Abyssal Plain to the southeast of the Gorringe Bank as described by Fukao (1973). The earthquake has a thrust mechanism on a fault plane that dips to the north and is related to the tectonic uplift of the Gorringe Bank. The fault orientation is favourable to compression in northwest-southeast direction. The origin of the 1969 earthquake, which was of significant size and did cause a tsunami, is reasonably well understood and, therefore, can be used as a realistic source for tsunamis affecting the UK. This model provides a good fit for the macroseismic data, the Horseshoe Fault is an active tectonic feature and there is significant seismic activity in this area. However, Baptista *et al*. (1998b) suggest that sources analogous to the 1969 earthquake do not reproduce the observed distribution of wave heights and travel times along the Iberian coast.

Model B: An earthquake north of the Gorringe Bank as suggested by Johnston (1996), occurring on a thrust fault that dips to the south and is related to the tectonic uplift of the Gorringe Bank. Such a fault orientation is favourable to compression in northwest-southeast direction. As a fault plane solution we use the south-dipping auxiliary plane of the Fukao (1973) model for the 1969 event. The model is also similar to the top hat model of Gjevik *et al*. (1997), which assumes uplift of the Gorringe Bank ridge as a source. The Gorringe Bank certainly appears to be a large structure, but some evidence, for example Zitellini *et al*. (2005), suggests that it is inactive. However, comparison of Models A and B will allow us to examine the effect that structural highs such as the Gorringe Bank, have on tsunami waves propagating towards the UK.

Model C: This model is equivalent to the N160 model of Baptista *et al*. (1998b) shown in Figure B2. The source location is offshore/southwest of Lisbon, closer to the Iberian shore than Models A and B, between the Gorringe Bank and the edge of the continental shelf west of C San Vicente. The earthquake occurs on a thrust fault dipping to the northeast. Baptista *et al* (1998b) find that this model produces tsunami arrival times that are a better match to those observed on the Iberian Peninsula, than models A and B. However, the underlying tectonics of such a model are less well-defined. This model will also allow us to examine the effect of source orientation on tsunami waves reaching the UK and Irish coasts.

The two different earthquake magnitudes (8.3 and 8.7 M_W) were used as inputs for each of the three of the models discussed above to derive the width, *W*, length, *L*, and average slip, *D*. These parameters, along with the location of the source are given in Table 2.3.

Table 2.3 Models of fault location and orientation, combined with physical source dimensions (Table 2.2)

	Model A		Model B		Model C	
Fault plane Strike/dip/rake	235/52/73		81/41/110		340/45/90	
Fault centre Lat/Lon	36.01°N/10.57°W (Southeast of Gorringe Bank)		37.0°N/11.5°W (North of Gorringe Bank)		37.0°/9.75°W (Southwest of Lisbon)	
	A1	A2	B1	B2	C1	C2
L (km)	105	210	105	210	105	210
W (km)	75	75	75	75	75	75
D (m)	6.8	13.6	6.8	13.6	6.8	13.6

2.1.5 Seafloor displacement

The analytical expressions of Okada (1985) are used to model the surface displacements due to an inclined, finite rectangular fault buried in a half-space. Surface displacement is calculated as a function of fault length and width, the dip, strike and rake of the fault, the slip dislocation and Lamè's constants λ and μ. Here, we assume that material is a Poisson solid, i.e. $\sigma = 0.25$, therefore $\lambda = \mu$.

The numerical results from our implementation of this method have been checked in two ways. Firstly by comparison with Chinnery's (1961) calculations of ground displacement on the surface of a half-space for slip on a vertical strike slip fault, with a length equal to down-dip width (Figure 2.5). Secondly, by comparison with

the vertical displacements computed by Heinrich (1994) for the magnitude 7.9 M_s earthquake of 1969, south of the Gorringe Bank. Fukao (1973) determines the fault parameters for this event as follows: dip 52°, strike 235°, rake 73° and maximum slip 4m. The fault length and width, determined from the distribution of aftershocks are 80km and 50km respectively. In both cases the agreement between our calculations and the previously published result is good.

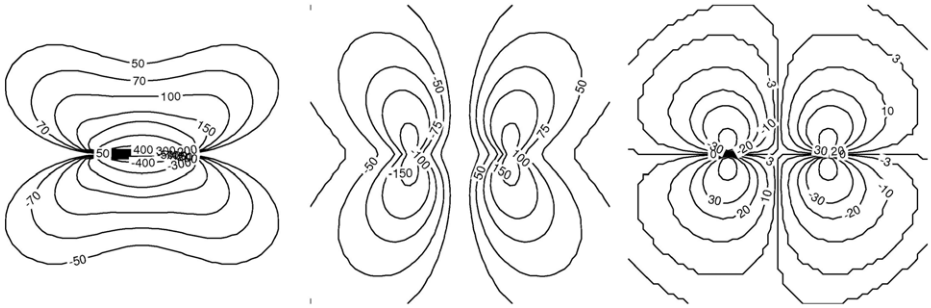

Figure 2.5 Ground displacement on the surface of a half-space computed for slip on a vertical strike slip fault, with a length equal to down-dip width (after Chinnery, 1961).

The surface displacements for each of the six models described in Table 2.3 are shown in Figure 2.6. The displacements are calculated for regular rectangular grids of points, whose origins correspond to the location epicentres, also given in Table 2.3. The X- and Y- axes of the grids correspond to East and North, respectively, the cell spacing is 5km, and the vertical displacements are given in metres. In all cases, we see significant areas of uplift on the hanging wall/down-dip side of the fault and corresponding subsidence on the up-dip side. A magnitude of 8.7 M_W gives a maximum vertical uplift of 7 - 8m in a narrow zone close to the fault. The zone of deformation is approximately 200km long by 400km wide. A magnitude of 8.3 M_W gives a maximum vertical uplift of approximately 3m and a zone of deformation that is 100km long by 250km wide.

2.1.6 Discussion

Notwithstanding the uncertainties in source location and magnitude, there are a number of other parameters used in our modelling that can strongly influence the seafloor deformation and the tsunami wave that is generated. The scaling parameter α is important because it relates the fault length and the amount of slip on the fault. This dependence is shown in Figure 2.7. Fault length decreases with increasing α, while fault slip increases. An important implication of this is that an intraplate earthquake requires a smaller fault size than an interplate earthquake with the same seismic moment. This is compensated for by the larger slip in intraplate earthquakes.

The width of the fault is constrained by thickness of the seismogenic zone and the dip and rake (direction of slip) of the fault itself. For large earthquakes, it is reasonable to assume that the earthquake ruptures the entire lithosphere. Given the composition and age of oceanic lithosphere in the eastern AGFZ, brittle behaviour will occur to depths of about 60km, as constrained by the 600°C isotherm (Abercrombie and Ekstrom, 2001). This agrees reasonably well with the

observed depths of earthquakes in the region, so this parameter is well constrained.

The shallower the dip of the fault plane, the greater the fault width. The fault plane solution for the 1969 earthquake determined by Fukao (1973) gives a fault dip of about 50°, resulting in a fault width of 75 km. Moment tensor focal mechanisms for the region given by Stich *et al* (2005) show a mixture of strike slip and thrust faulting. Earthquakes with significant thrust components typically show fault dips of 30° to 70° with an average of 50°. The compressional tectonics of the region and the fact that a tsunami was generated, means that a thrust mechanism can be assigned to the 1755 earthquake with relatively high confidence. Figure 2.8 shows both the dependence of fault width on fault dip for a fixed seismogenic thickness of 60 km, and also how this translates to fault length for a number of different values of α. Increasing the fault dip from 30º to 70º reduces the width from 120 to 60km.

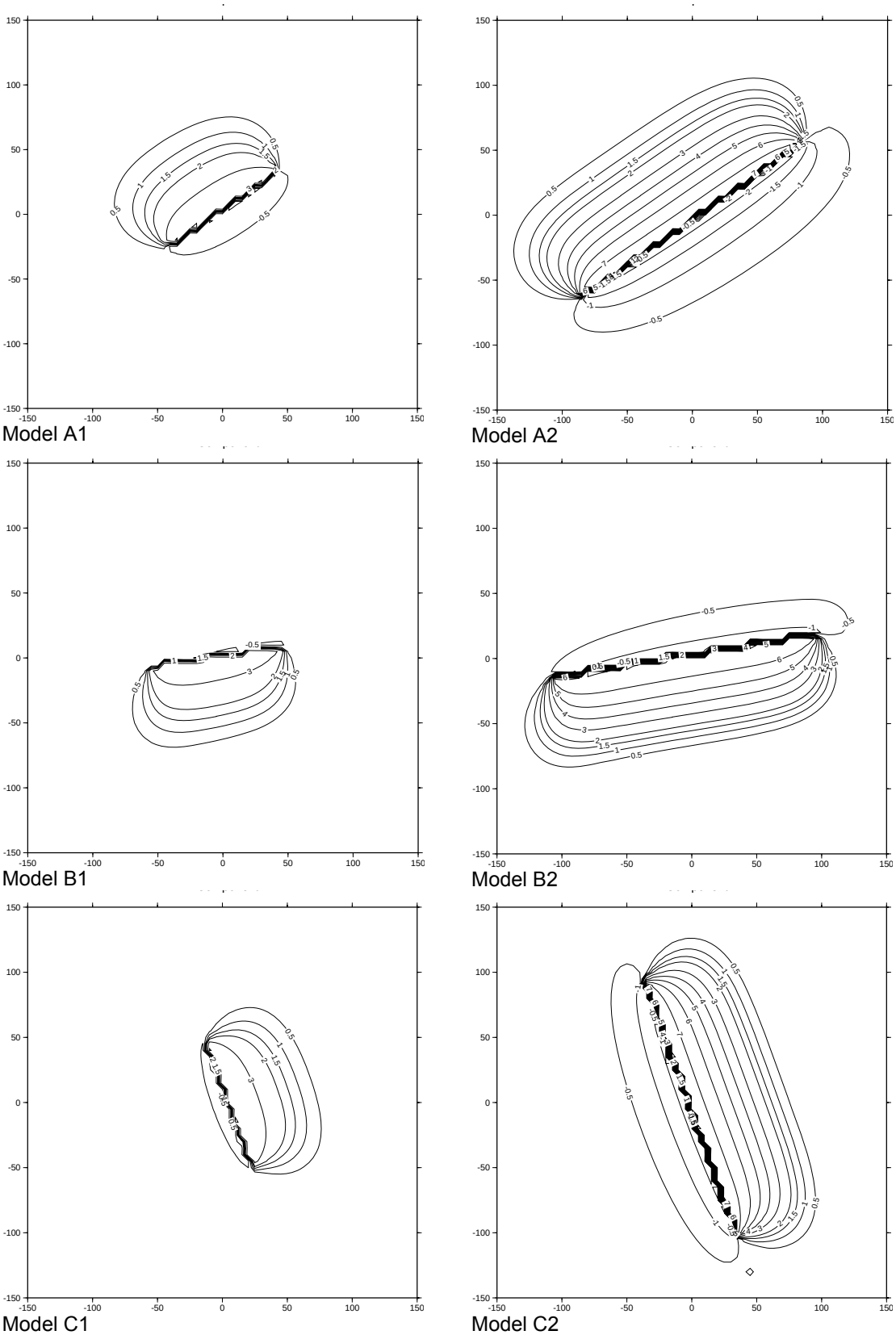

Figure 2.6 **Surface displacements using Okada's (1985) method, for the six source models described in Table 3.**

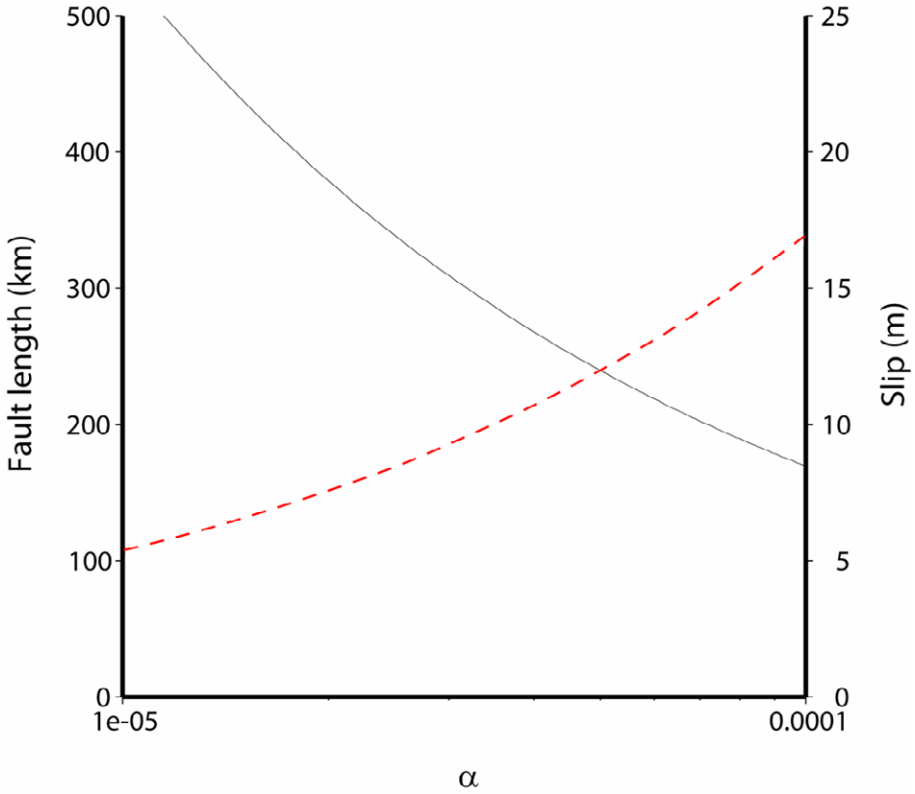

Figure 2.7 **The dependence of fault length (black) and slip (red) on the scaling parameter α for a fixed seismic moment, M_0, of $1.4x10^{29}$ dyn-cm, 8.7 M_w. Values of α vary between $6.5x10^{-5}$ for intraplate earthquakes to $1.5x10^{-5}$ for interplate earthquakes. Assuming an intraplate value of α results in a shorter fault, but greater slip for the same seismic moment.**

A wider fault will result in a wider zone of surface deformation, increasing the wavelength and period of the generated tsunami wave. We estimate that a dip of 50º will result in a tsunami wavelength of 200km (Figure 2.9). Applying the shallow water equation, with a water depth of 4000m gives a wave velocity of 200km/s. The initial wave period is then 15 minutes. This value shows good agreement with the observations of the tsunami wave period on the Iberian coast of 10-20 minutes noted by Baptista *et al*. (1998a).

A magnitude of 8.7 M_W would make the 1755 earthquake one of the largest intraplate earthquakes, and, according to Johnston (1996,) the largest observed oceanic lithosphere earthquake. This is significantly greater than other large intraplate earthquakes, for example, New Madrid 1812, magnitude 8.1 M_W, Assam 1897, magnitude 8.1 M_W, and Gujarat 2001 magnitude 7.9 M_W. However, it is important to distinguish between earthquakes that occur in stable continental regions, such as New Madrid and Assam, and those in diffuse plate boundary environments, such as Lisbon, 1755. Scholz *et al*. (1986) suggest three categories of earthquake: earthquakes that occur in mid-plate regions, far from any plate boundary; earthquakes that occur on clearly defined plate boundaries; and, earthquakes that occur either in a diffuse zone surrounding a plate boundary and which contribute to the deformation associated with the plate boundary. Earthquakes such as New Madrid, 1812, and Assam, 1897, clearly belong to the first category. The Lisbon 1755 earthquake falls into the last category, since seismicity along this part of AGFZ is diffuse and the plate boundary itself is poorly

defined. A positive aspect of this is that the recurrence period for intraplate earthquakes is much larger due to slower strain accumulation than for interplate settings. The typical recurrence period for Lisbon style intraplate earthquakes (plate boundary related) is in the range 1,000-10,000 years (Scholz *et al*., 1986).

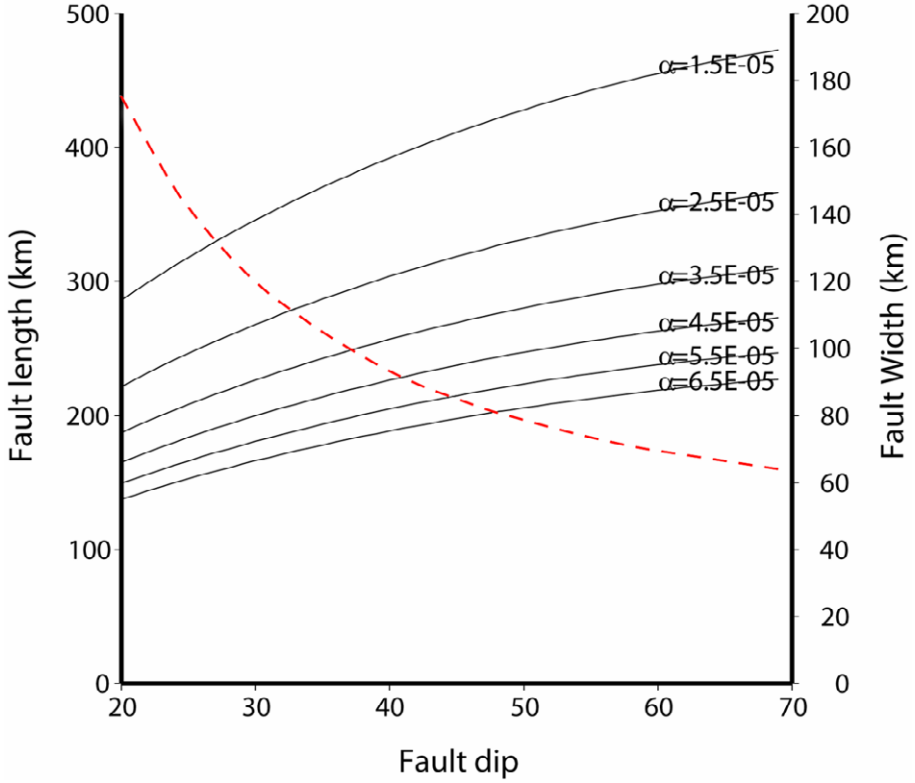

Figure 2.8 **The relationship between fault length (black) and width (red) on fault dip, given a seismogenic thickness of 60 km and a fixed seismic moment, M_0, of 1.4×10^{29} dyn-cm, 8.7 M_w . Fault lengths are shown for five different values of α from 6.5×10^{-5} for intraplate earthquakes to 1.5×10^{-5} for interplate. Smaller values of α show greater dependence.**

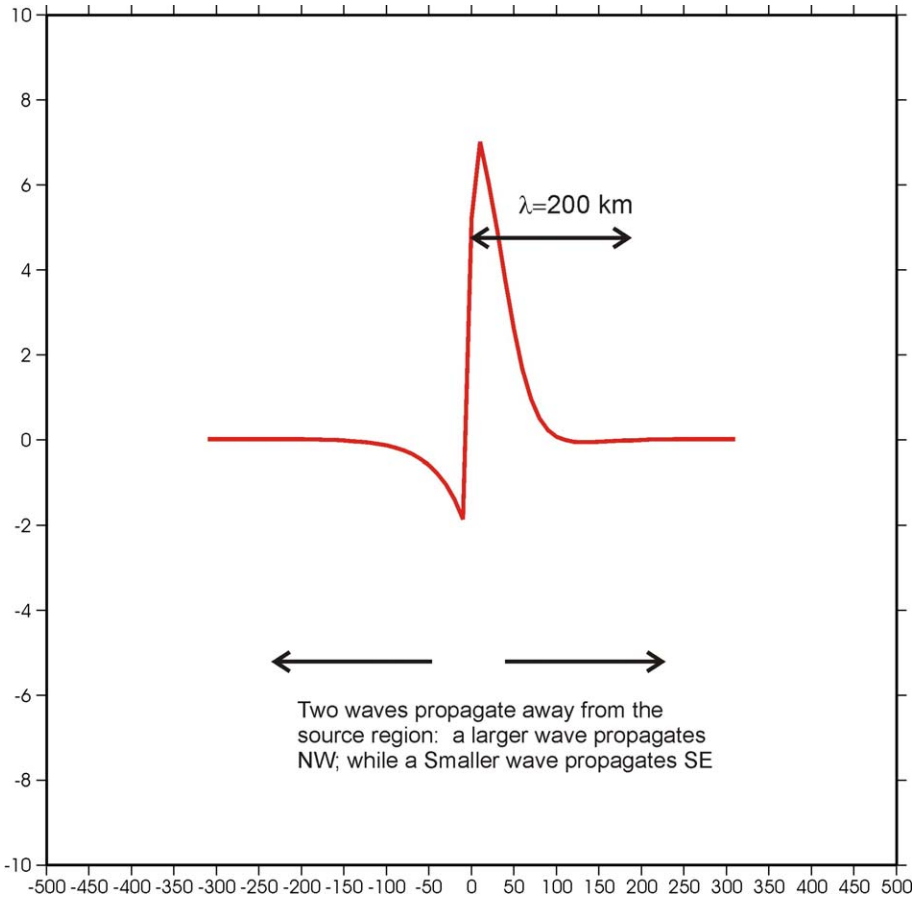

Figure 2.9 **A cross-section of the vertical seafloor displacement for Model A2. The maximum vertical displacement is almost 8 m. The shallow water equations give wave speed *c* as $c=\sqrt{gh}$., where *g* is gravity and *h* is the water depth. Applying this gives *c*=200m/s for a depths of 4000m. For *λ*=200 km, the wave period is then T= 1000 s ≈ 15 minutes. This is consistent with the observations of period published in Baptista *et al.* (1998b), and also with observations in Gibraltar and the UK.**

2.2 Propagation to Nearshore

2.2.1 Introduction

The model described here solves the non-linear shallow water (NLSW) equations, which are a suitable choice for modelling tsunami propagation away from the immediate source. It is well known (Marchuk *et al*, 1983) that large earthquakes produce tsunamis whose periods are a broadly a function of source width (corresponding to the scale of the fault) which could be of the order one hour. For smaller sources (e.g. landslides, volcanic explosions) the generated tsunami will possibly only have a period of as little as several minutes. This simplification led to the assumption of relatively large spatial scale for the disturbances modelled in the initial Defra study (Kerridge, 2005). The refined source terms, provided in Section 2.1, allow an improved estimate for the size of the event and the propagation of the wave towards the UK and Irish coastlines.

The modelling protocol chosen was to nest models of appropriate resolution so that the (relatively short period) primary tsunami wave was always well discretised. In order to best represent the tsunamis originating from the west of Iberia the choice of numerical model was changed from the original POL North East Atlantic (NEA) model, with a grid resolution of approximately 35km, to the POL CS3 12km operational storm surge model (Flather, 2000). The CS3 model was extended from its normal domain of the European shelf southwards to 34°N and westwards to 14°W. This extension was required to accommodate the initial sea surface disturbances provided as source parameters. The improved seismic sources gave rise to tsunamis with periods of approximately 15 - 20 minutes, originating in 4000-5000m of water; implying wavelengths of approximately 200km, which is consistent with the deformation fields shown previously in Figure 2.6. The 12km horizontal grid of the CS3 model, as previously mentioned, resolves the tsunami wave over 16 discrete cells, which is sufficient for effective discretisation and avoidance of numerical dispersion (e.g. Kowalik, 2001). Recent comparisons in Japan of model predictions with reliable coastal observations (Choi *et al*., 2003) show that nested finite-difference NLSW models produced accurate simulations of coastal inundation and run-up. The study by Choi *et al* used an extremely fine (30m) coastal grid to maintain resolution as the tsunami wavelength shortens with reduced depth. The 200km wavelength used in this study reduces to 24km in a depth of 20m, demanding horizontal resolution of the order 1km. Therefore, an unstructured finite element model (TELEMAC) uses the CS3 model data to propagate the wave inshore. Finite element models have recently been used successfully for tsunami modelling (e.g. Walters, 2005) and for many aspects of coastal oceanography finite element and finite difference models are interchangeable (Walters, 2002).

Here, the sea surface elevation resulting from the uplift or subsidence of the sea floor (induced by an earthquake) is estimated from analytical relationships that predict surface deformation from a range of fault parameters (Okada, 1985). In a modelling study by Gjevik *et al*. (1997), this formulation provided acceptable agreement with observations along the Iberian coastline of the well-documented tsunami event of February 1969. Although both vertical and horizontal movements can be accounted for in the governing equations of hydrodynamic models, tsunamis can be effectively modelled by neglecting any horizontal momentum and assuming impulsive deformation (e.g. Bundgaard *et al*. 1991). This was confirmed within this study: the tsunamis caused by the larger of the two earthquake magnitudes (8.7 M_W) were each modelled with (a) the perturbation introduced at a

single time-step (i.e. instantaneously) and (b) sea surface deformation introduced over four time-steps (120s); the results were indistinguishable. Whether the actual sea floor uplift over the affected region occurs in a temporally uniform way can have an impact on the magnitude of any tsunami generated. Slowly spreading uplift of the sea bed can be shown to influence tsunami amplitude by an order of magnitude due to wave focussing and source directivity (Hayir, 2004). We have mapped the sea floor deformation resulting from Okada (1985) directly onto the sea surface. There are deficiencies in this assumption as pointed out by Gjevik *et al*. (1997) who employed an idealised non-hydrostatic model to show that the maximum surface elevation can be 30% less than the displacement at the sea bed. Neither can the surface deformation contain the discontinuity that is present at the sea bed at the precise line of a fault. In practice, our modelling scheme smoothes the sea surface deformation resulting from the application of Okada (1985) by introducing the deformation fields (Figure 2.6) into the model via a near neighbour contouring package. A similar approach was adopted by Gjevik *et al*. (1997).

2.2.2 CS3 model

The model used solves the two-dimensional non-linear shallow water equations in finite difference form in Earth coordinates. A quadratic formulation for stress at the sea bed and radiation conditions at the open lateral boundaries allows any disturbances generated within the domain to propagate freely outwards. The model provides sea surface elevation and horizontal currents at all points in the domain; these values were later used as input parameters to model propagation to shoreline (Section 2.3). A full description of the model is given by Flather (2000). The same model is in routine use for storm surge warning as part of the Storm Tide Forecasting System (STFS). The standard operational grid is shown in Figure 2.10.

This model formulation was chosen to correctly resolve the six initial sea surface disturbances. To facilitate this, this computational domain was extended as shown in Figure 2.11. Tidal boundary forcing for the extended CS3 model was extracted from a larger scale North Atlantic Model. It is necessary to include tidal dynamics in the model runs because of possible dynamical interactions between the tidal wave and the tsunami. Furthermore as the tsunami enters the shelf, friction becomes important and friction in shallow water is effectively controlled by tidal motions. Consequently all simulations shown here were run twice: firstly with tides only and secondly with tides plus the tsunami. To assist clear presentation, the tides were then subtracted from the tsunami run so that the propagation and impact of the modelled tsunami can be seen clearly.

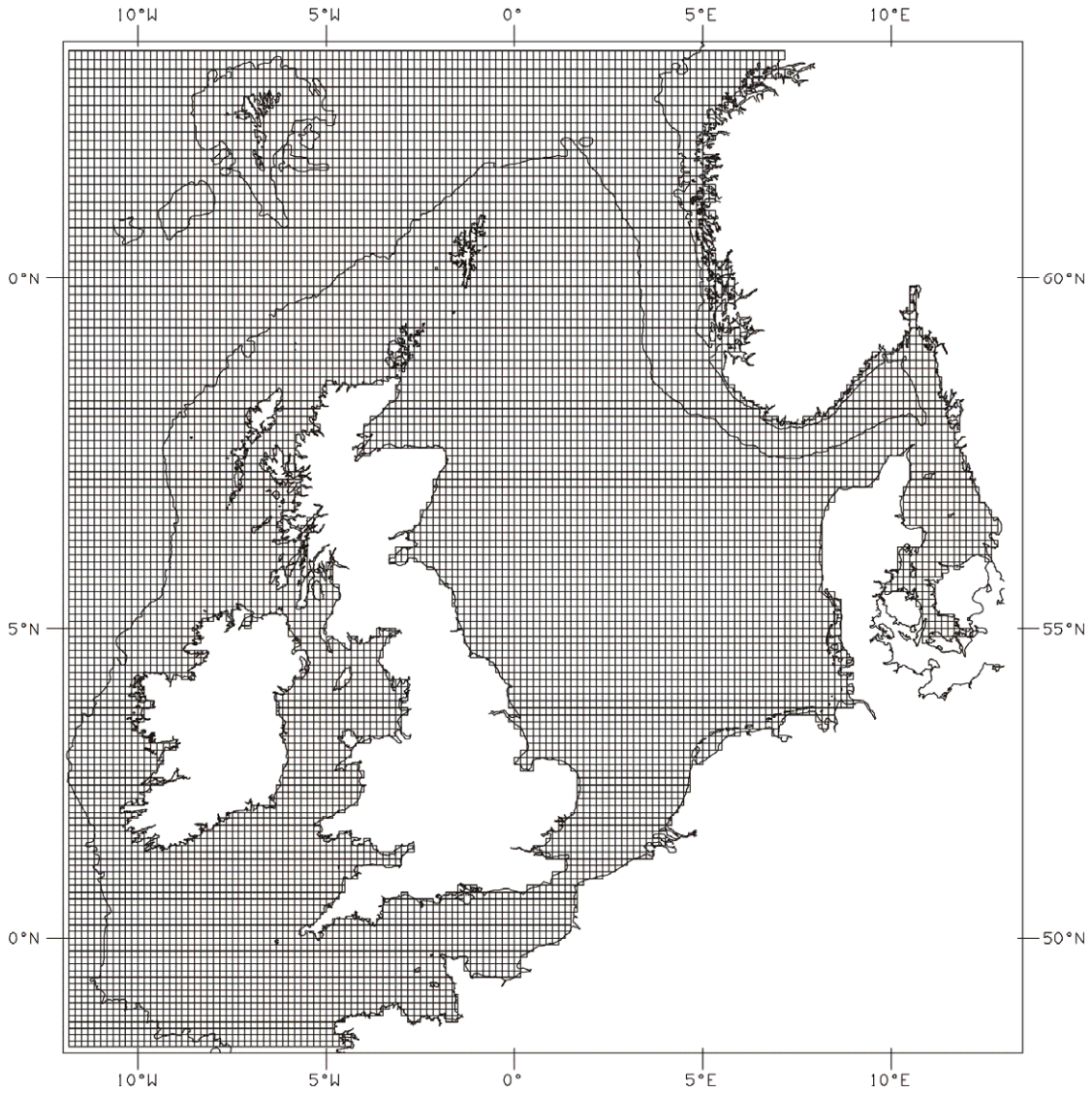

Figure 2.10 Standard operational computational grid of the POL CS3 model with 12km resolution. The solid line is the 1000m bathymetric contour.

The results of the six model runs (A1, A2, B1, B2, C1, C2) which correspond to the source terms proposed in Table 2.3 are described in the following section. The influence of the state of the tide was tested for run A2. Figure 2.12 shows the sea level disturbance for this run where the tsunami is introduced at three different states of the tide. The image is from 5 minutes after the tsunami was introduced and the tidal state is advanced by three hours in each case: Figure 2.12a is the original run, Figure 2.12b has the tsunami introduced with the tide advanced by 3 hours and Figure 2.12c advances the tide by six hours.

It is clear from Figure 2.12 that the state of the tide at the source has no significant impact on the generation, or immediate propagation of any disturbance. This avoids a multiplicity of model runs for each seismic scenario. Of course, the state of the tide at the destination (i.e. the UK coast) may be a significant factor in determining the total water level when a tsunami arrives.

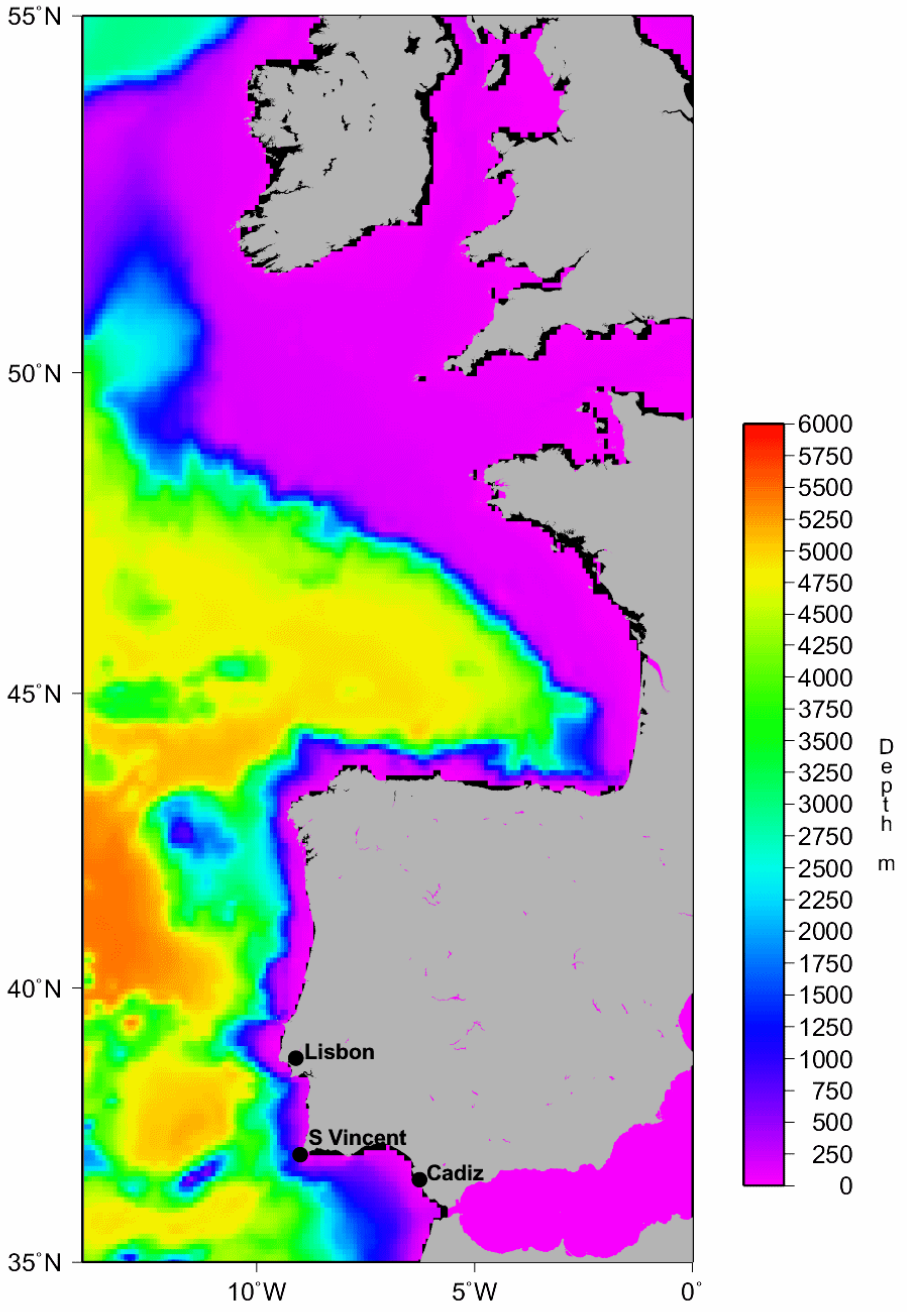

Figure 2.11 Bathymetry and domain of extended CS3 model with 12 km resolution.

In the results that follow our model can be used to analyse the behaviour of the leading wave train, and subsequent waves in deep water. However, as noted previously, a spatial resolution significantly smaller than the 12km used in the CS3 model is needed to correctly model the tsunami in very shallow water, as it approaches the coastline. Direct comparisons of wave interactions around Spain and Portugal after 1 hour are not possible because of local reflections and resonant effects, not captured by our 12km model.

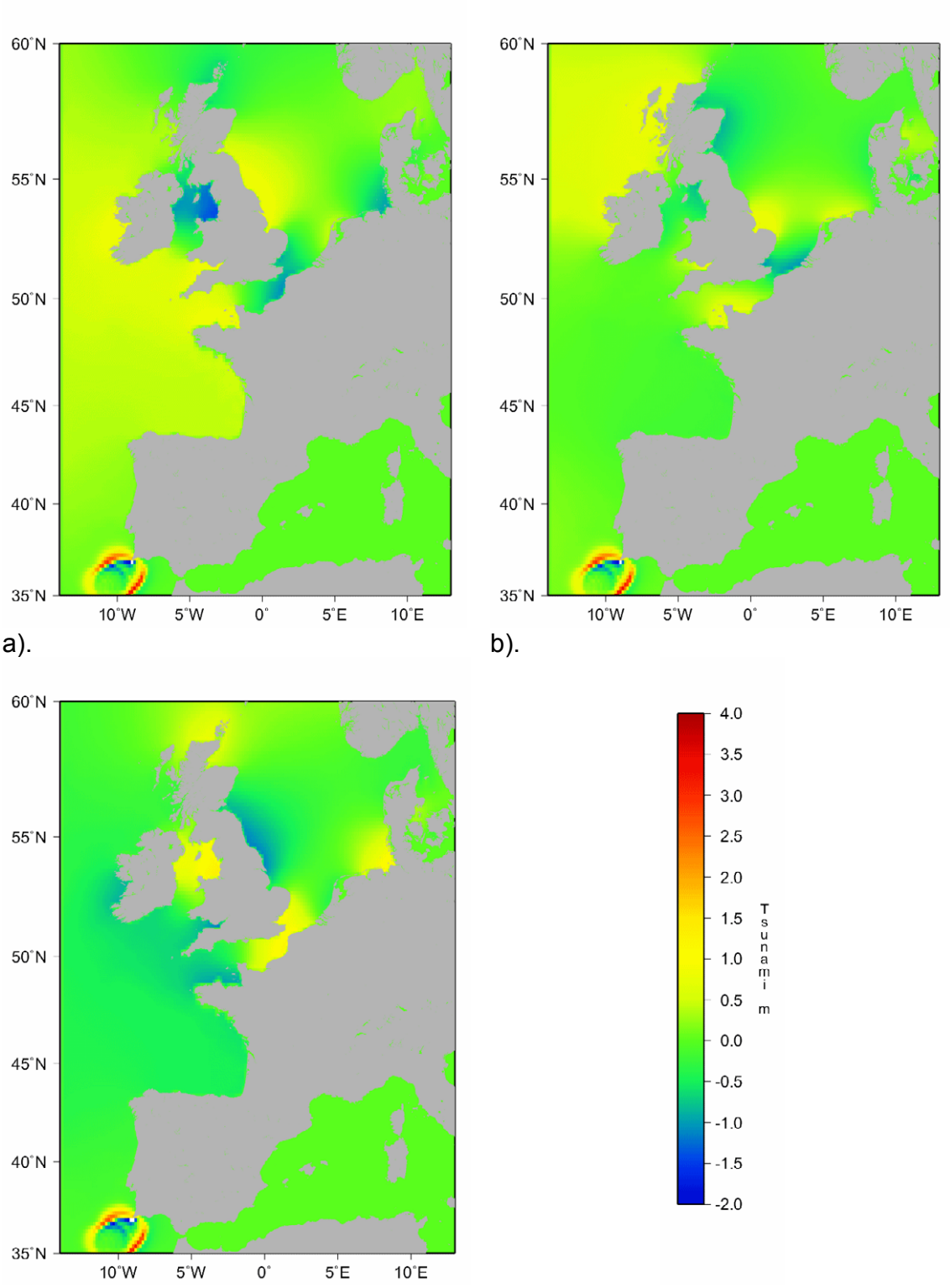

Figure 2.12 Model A2 tsunami with tide (a) actual conditions, (b) advanced by 3 hours, (c) advanced by 6 hours.

2.2.3 Results

The results of each individual source (A1 – C2) are now described and results presented in Figures 2.13 – 2.18.

The results of model A1 are shown in Figure 2.13. This source corresponds to the epicentre of the 1969 earthquake in the Horseshoe Abyssal Plain (Fukao, 1973) but with moment magnitude 8.3. Initial sea surface disturbances of 2m persist within a few 100km of the source region, but lateral spreading of the wave results in wave amplitudes of approximately 0.1m by the time the tsunami reaches the continental shelf break, to the southwest of the Celtic Sea. Even so, there is evidence of considerable refraction of the wave as it reaches the northwest tip of Spain and the Bay of Biscay.

The pattern of wave propagation for run A2, shown in Figure 2.14, is of course similar to that of Figure 2.13 although with larger wave amplitudes. The wave amplitudes reaching the shelf break are now 0.3 – 0.4m. In terms of its local effects the initial waves, in excess of 2m reach Cape St Vincent between 10 and 20 minutes after the tsunami is initialised in the model. This is consistent with the most reliable travel time value of 16 minutes reported by Baptista *et al*. (1998a). Our model is in excellent agreement with that of Gjevik *et al*. (1997) for the wave propagation towards the Portuguese coastline with identical wave shapes (although not amplitude – the 1969 tsunami was a much smaller event) after 20 minutes. Observations of the February 1969 tsunami reported the first peak arrival at Cascais (at the mouth of the river Tagus) after 37 minutes, and the corresponding time series from model run A2 is shown in Figure 2.19 for the neighbouring town of Oeiras. The good agreement provides confidence in both the source term and hydrodynamic modelling of model A.

Model Runs B1 (Figure 2.15) and B2 (Figure 2.16) examine the source location north of the Gorringe Bank proposed by Johnston (1996). Again, the 8.3 M_W event resulted in wave amplitudes of only 0.10 – 0.15m at the shelf break, whereas the 8.7 M_W event gave rise to tsunami amplitudes approaching the UK shelf of approximately 0.5m. This source model has a more east-west orientation of the fault and the resulting tsunami undergoes less refraction (and therefore energy loss) as it propagates towards the shelf break. The arrival time of the primary wave at Cape St Vincent is approximately 20 minutes, and arrival at Lisbon is 30 - 40 minutes after generation (see Figure 2.20). Again, these timings are consistent with our best interpretation of literature surrounding the 1755 event (Baptista *et al*., 1988a).

Runs C1 (Figure 2.17) and C2 (Figure 2.18) use a source equivalent to a rotation of the 1969 event, and equivalent to the N160 model of Baptista *et al*. (1988b). For model C, the majority of the wave energy is directed immediately towards the Portuguese coast (and westwards, out of our model domain). This scenario causes the most rapid arrival of the wave at both Lisbon and Cape St Vincent but has the weakest effect on wave propagation towards northern European coasts. The energy has either travelled into the deep Atlantic or dissipated against the Iberian coastline. Model run C2, Figure 2.18, propagates a tsunami wave of amplitude 0.1 – 0.2m towards the UK shelf, despite the source elevations being equivalent to model run A2. Clearly the source orientation is an important factor with regard to tsunami levels at specific coasts. This aspect of historical tsunami analysis, where several source orientations are appealed to in order to reconcile apparently

contradictory observations, is quite common (e.g. Zahibo *et al*., 2003). The same is true of attempts to reproduce descriptions of the 1755 Lisbon tsunami, with Baptista *et al*. (1988b) introducing a compound source to explain the coeval accounts.

In addition to the free-surface elevation near Oeiras (Figure 2.19 – 2.21), time series elevations are also provided at Cadiz in Figures 2.22 – 2.24. These time series are recorded at the nearest cell in the computational domain.

Whilst we do not attempt to model travel times for all of the locations at which reports of the 1755 tsunami exist, the model runs performed here allow some comparison with Baptista *et al*. (1988b). Our run C2 agrees well with their N160 source, which it should, and provides the best agreements with travel time at Oeiras (25±10 minutes) and Cadiz (78±15 minutes). The historical compilation of Baptista *et al* (1988a) suggested a period of 10 minutes at Oeiras with more than three distinct waves, this makes our model B the least likely source term. Run B2 produces the largest incident tsunami at the UK continental shelf break although it is the least plausible for a repeat of the tsunami that occurred in 1755. Allowing for run-up effects in very shallow water (not produced in the CS3 model), the amplification of the 2.5m wave, seen in Figure 2.19, to reported values of approximately 6m is well within empirical factors for run-up. It is well known that most tsunamis will undertake a form of breaking, developing into turbulent bores with run-up of between 2-5 times the wave height as it crosses the initial shoreline. At Cadiz, our arrival times again agree well with the reported values, but it is less credible that the approach wave amplitudes could increase from 0.5m to the 15m cited by Baptista *et al*. (1988a). However, even with their compound earthquake Baptista *et al*. (1988b) could only attain run-up values of 7m for Cadiz.

2.2.4 Discussion

Clearly, from the modelling undertaken so far, it appears that, none of the 8.3 M_W models are likely to produce waves with any considerable consequence for flooding around the UK and Irish coastline. Even allowing for local amplification, the modest wave amplitudes of approximately 0.1m approaching the shelf break are an order of magnitude smaller than storm surges. This is also smaller in magnitude than climatic long period swell in the Celtic Sea.

The larger amplitude seismic events (8.7 M_W) all models produce similar wave at the UK continental shelf break, approximately 2-3 hours after the initial disturbance. The largest tsunami was generated by model run B2, with amplitudes of about 0.5m reaching the shelf break. Smaller amplitudes (0.1 - 0.2m) were obtained from model A2. Variation in wave amplitude along the crest has implications for the detail of local amplification. Run C2 results in the lowest tsunami amplitudes at the shelf break due to orientation, yet this model is the most comparable, of our model scenarios, with previous efforts to reproduce the 1755 Lisbon tsunami.

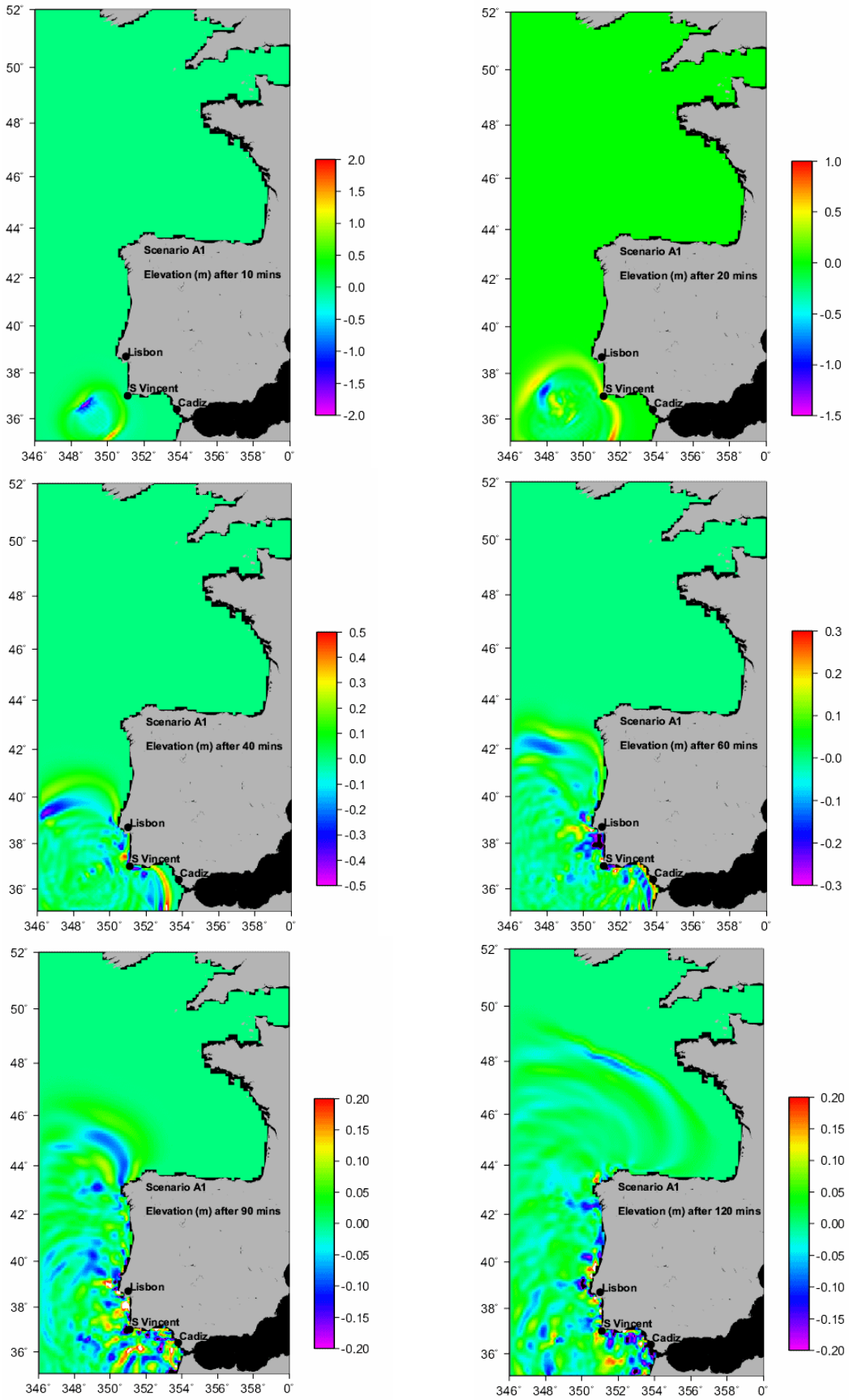

Figure 2.13 Surface elevation (m) resulting from Scenario A1 (Note: colour scale differs between plots)

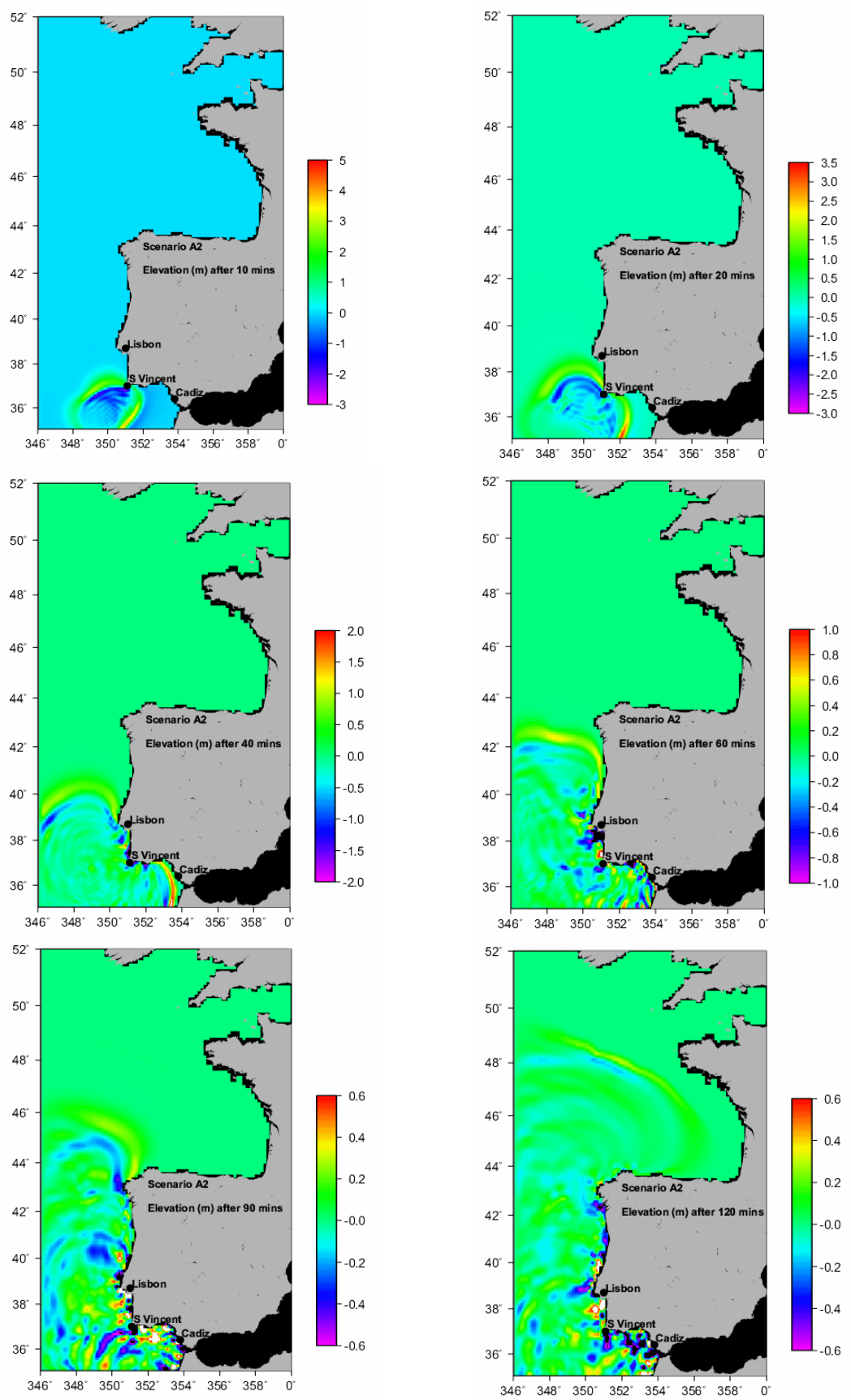

Figure 2.14 Surface elevation (m) resulting from Scenario A2 (Note: colour scale differs between plots)

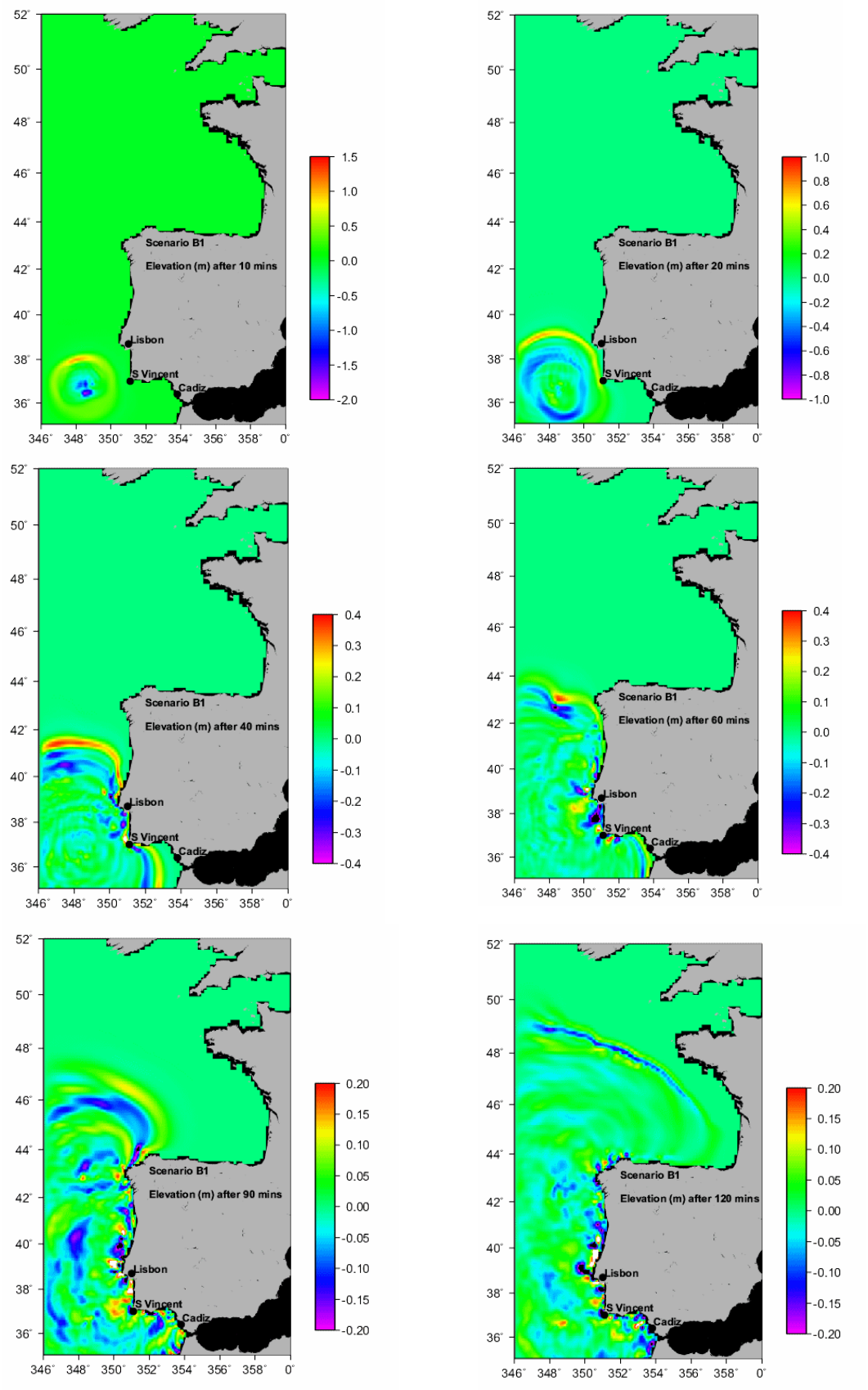

Figure 2.15 Surface elevation (m) resulting from Scenario B1 (Note: colour scale differs between plots)

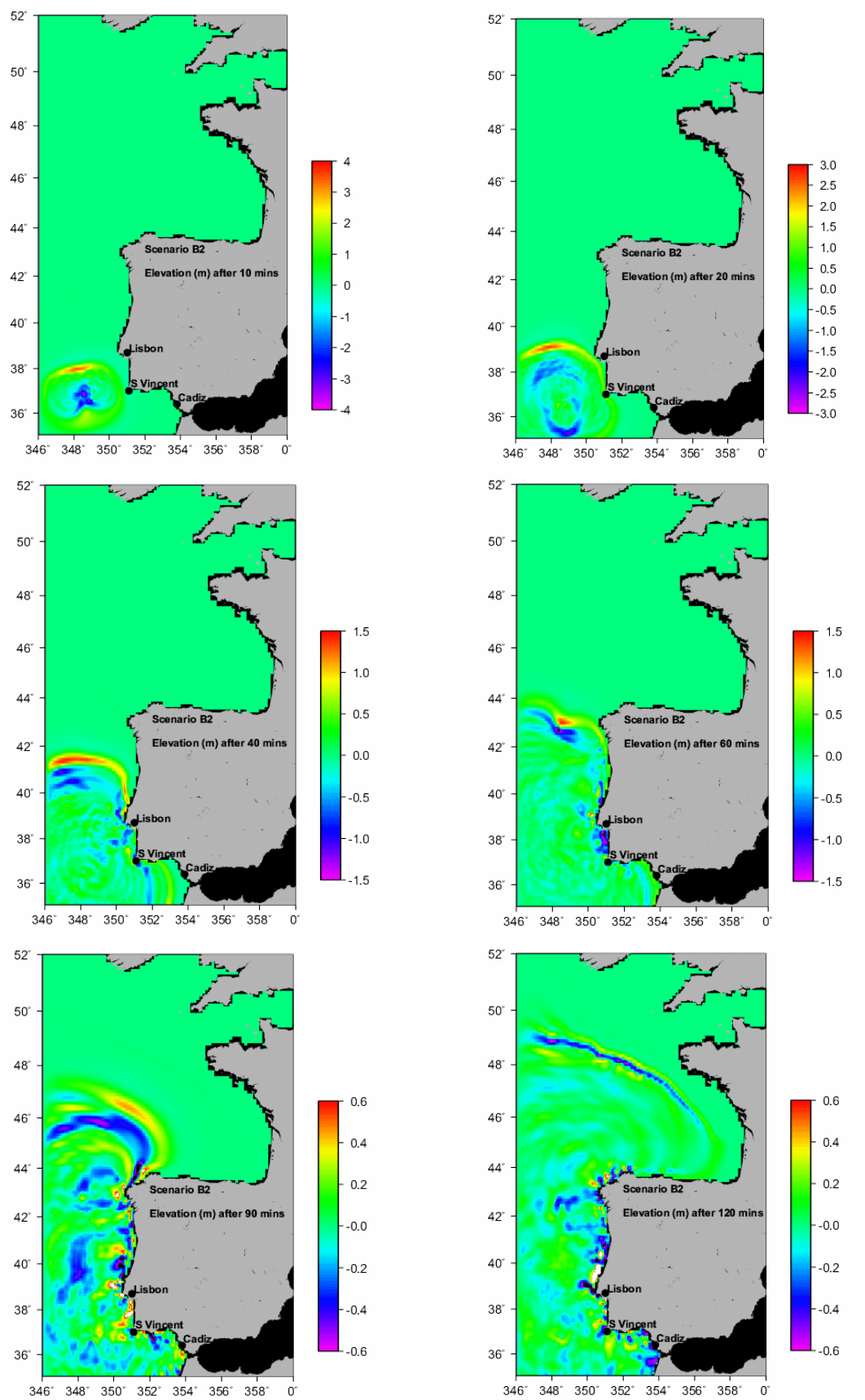

Figure 2.16 Surface elevation (m) resulting from Scenario B2 (Note: colour scale differs between plots)

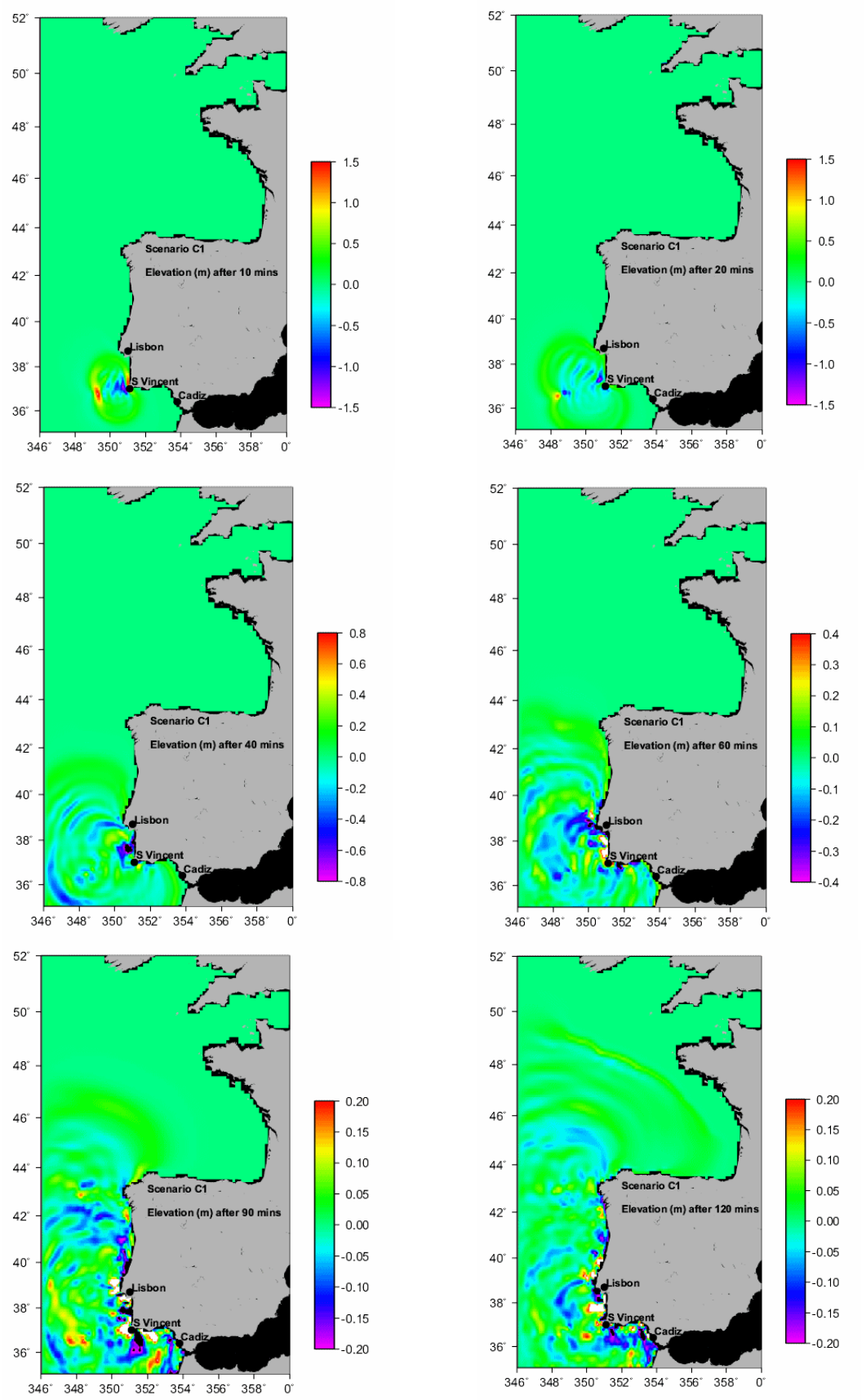

Figure 2.17 Surface elevation (m) resulting from Scenario C1 (Note: colour scale differs between plots)

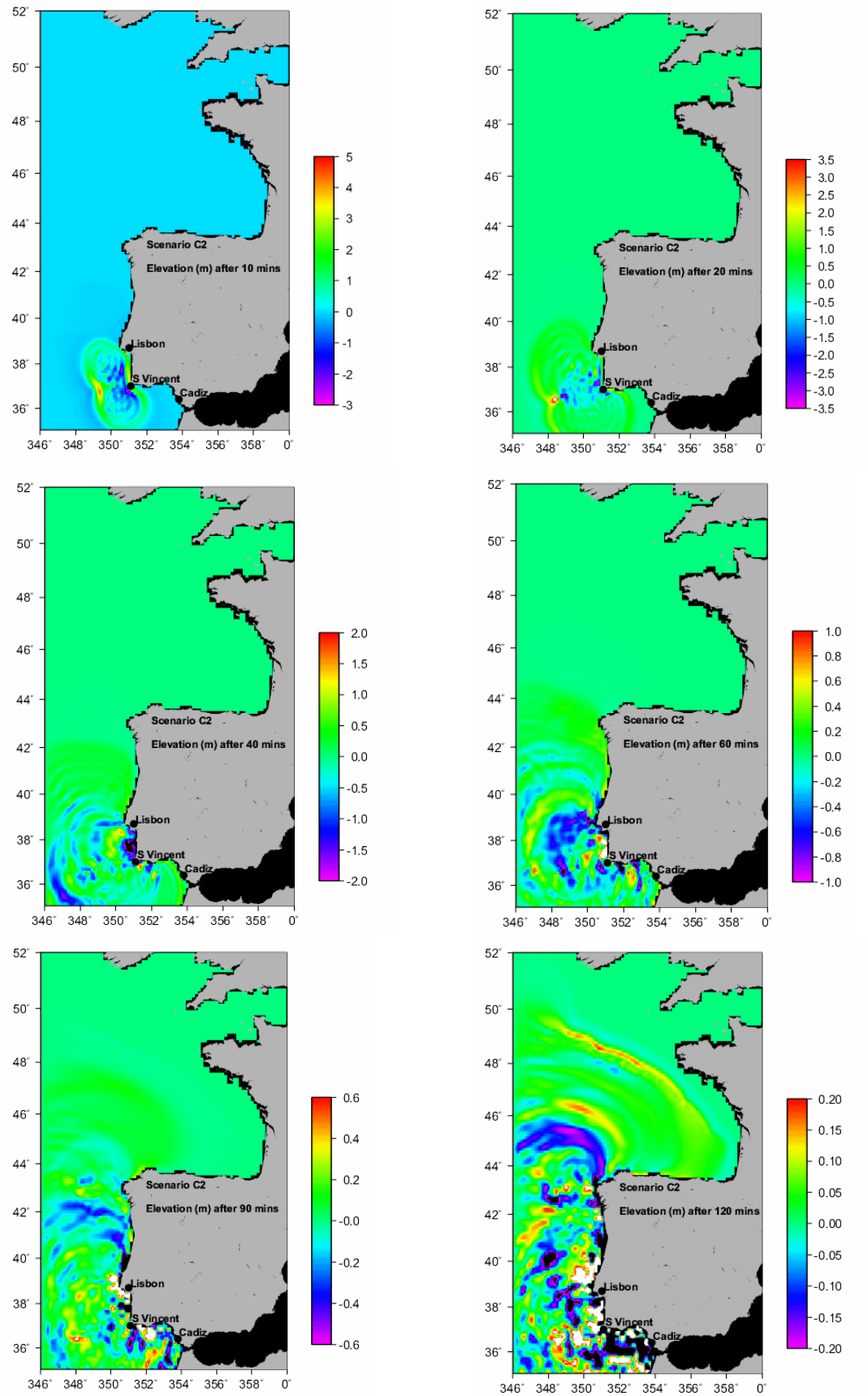

Figure 2.18 Surface elevation (m) resulting from Scenario C2 (Note: colour scale differs between plots)

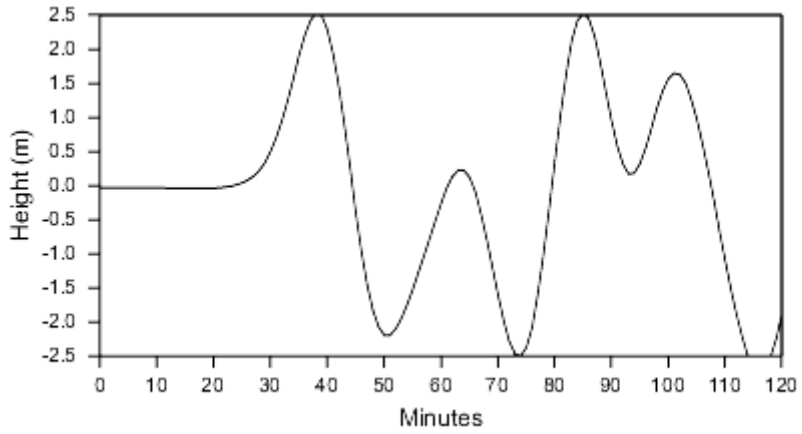

Figure 2.19 Time series of elevation at model point nearest Oeiras (38.67°N, 9.32°W) for scenario A2 (M_w 8.7)

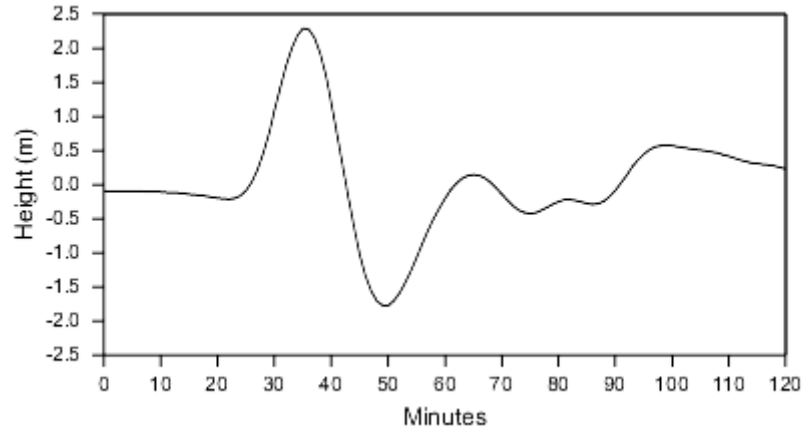

Figure 2.20 Time series of elevation at model point nearest Oeiras (38.67°N, 9.32°W) for scenario B2 (M_w 8.7)

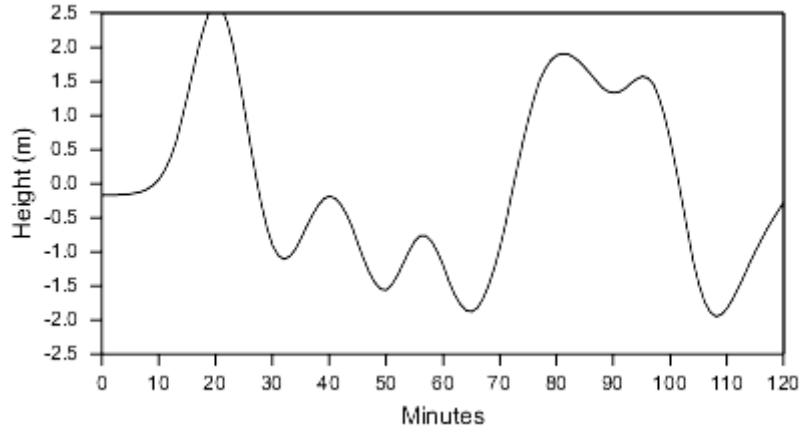

Figure 2.21 Time series of elevation at model point nearest Oeiras (38.67°N, 9.32°W) for scenario C2 (M_w 8.7)

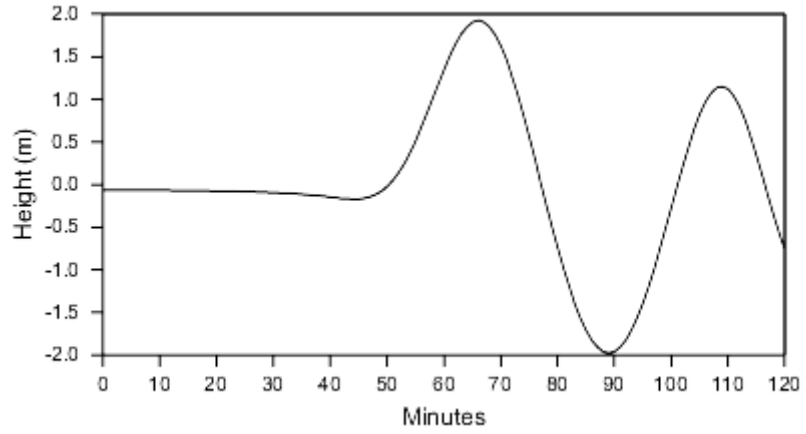

Figure 2.22 Time series of elevation at model point nearest Cadiz (36.5°N, 6.3°W) for scenario A2 (M_w 8.7)

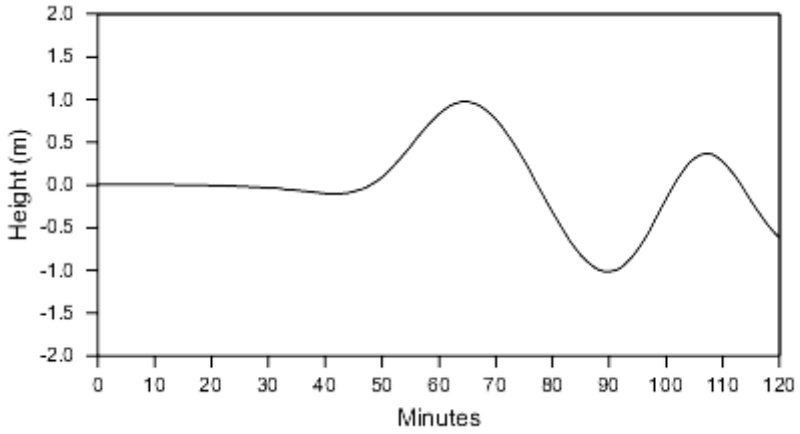

Figure 2.23 Time series of elevation at model point nearest Cadiz (36.5°N, 6.3°W) for scenario B2 (M_w 8.7)

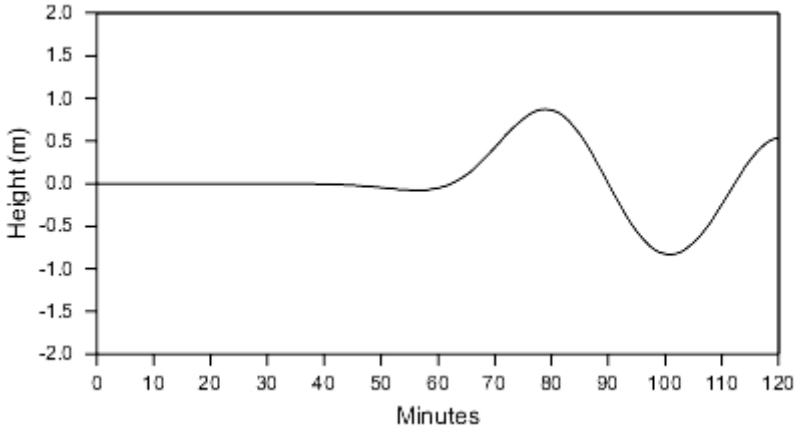

Figure 2.24 Time series of elevation at model point nearest Cadiz (36.5°N, 6.3°W) for scenario C2 (M_w 8.7)

2.3 Propagation to shoreline

2.3.1 Introduction

In order to simulate tsunami propagation to the shoreline, caused by events such as the Lisbon earthquake of 1755, it is necessary to have a fine grid model of the UK and Irish coasts. For this reason a TELEMAC-2D flow model has been developed, which used relevant wave data (free-surface elevation and depth-averaged velocities), produced by the POL CS3 extended 12km grid model, as a boundary condition. The input tsunami wave is then transformed up the continental shelf and refraction and diffraction effects are modelled as the wave approaches the coast. The simulated tsunamis have a typical wave period in UK and Irish coastal waters of approximately 20 minutes. Even though the wave period of the tsunami is maintained, shallow water theory states that the wave length varies proportionally to depth. It is therefore beneficial in the modelling of tsunami waves in shallow waters to use a variable grid model, allowing the number of cells per wavelength to remain approximately constant. Such a variable mesh was generated by the modelling software and used in the hydrodynamic model TELEMAC-2D.

2.3.2 Model area

For this part of the study the tsunami waves were simulated in the English Channel (up to the Isle of Wight), in the Bristol Channel, on the South and West coasts of Ireland. The model area used is identified in Figure 2.25.

In order to simulate how the tsunami wave transforms from deep ocean waters up to the continental shelf, it was decided to place the model's boundary as far as possible seaward of the shelf. Therefore the computational domain's southern boundary was placed entirely seaward of the shelf, except close to the continental coast (Figure 2.26). The western coast of France was not modelled; here an absorbing boundary was placed adjacent to the model's southern boundary.

The model's western boundary was located approximately in accordance with that of the POL CS3 extended model. Almost all the boundary was located in very deep water beyond the Continental Shelf. A small section of boundary, midway up the west coast of Ireland, was in less deepwater.

In order to maintain compatibility between the POL CS3 model and the TELEMAC model, the TELEMAC runs were performed using the same bathymetric data set as used in the POL model. Elevations for this bathymetry are presented in Figure 2.26.

For computational efficiency, a minimum water depth of 5m was imposed in the computational model therefore avoiding wetting and drying at the coast (i.e. on the beach areas).

Figure 2.25 Computational domain for the TELEMAC model (boundary conditions identified)

2.3.3 Model mesh and boundary conditions

The model mesh was set up using the spherical co-ordinates option of the TELEMAC model system. The model mesh size is flexible and was set up to be approximately 12km at the offshore southern boundaries, comparable with the cells size of the POL model. As previously described, in shallower waters the mesh size is required to be finer and was therefore defined as proportional to the square root of the water depth, allowing a constant number of cells per wavelength to be achieved. This allowed the number of cells per wavelength to be approximately 10 for the 20 minute tsunami wave period modelled here. Near to the UK and Irish coast the mesh size was approximately 1km, as shown in Figure 2.27. The mesh, shown in Figure 2.27, contains 46,000 nodes and 88,000 elements.

The various boundary conditions used in the model were previously depicted in Figure 2.25. Radiating boundaries conditions were imposed on all boundaries except the south boundary, where the tsunami was imposed from the POL 12km flow model.

In model runs 1-4, see Table 2.4, the boundary conditions were directly imposed from the POL CS3 extended model (run tidally but with the tide subtracted out to give only the tsunami elevation). In model run 5, the A2 tsunami source input conditions was used again, although with the use of the TELEMAC incident wave boundary condition which allowed the absorption of reflected waves. No significant difference can be seen for the propagation of the incoming wave, as shown in Figure 2.32.

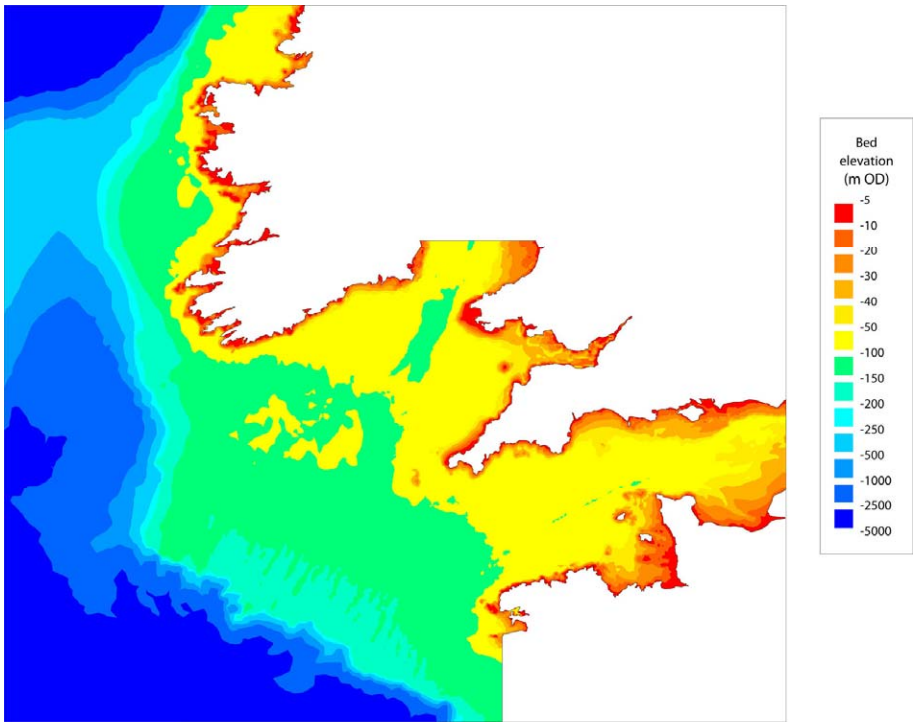

Figure 2.26 Bathymetry levels in the TELEMAC model

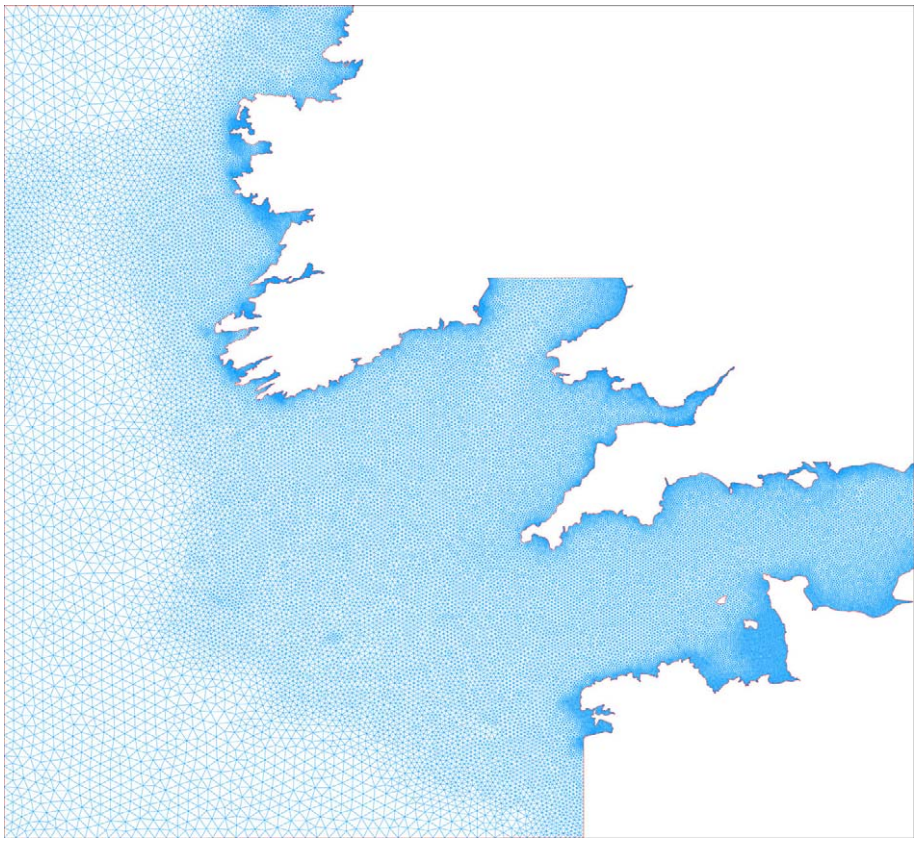

Figure 2.27 Computational mesh for TELEMAC

2.3.4 Model runs

The output from the CS3 model simulations indicated that the larger magnitude events (8.7 M_W) were of more interest as the tsunami wave approached the UK and Irish coast. Input from the model runs A2, B2 and C2 were used as input for the TELEMAC runs. For sensitivity analysis the A1 wave parameters were also used at the wave generation boundary. The model simulation runs are defined in Table 2.4.

Table 2.4 Definition of TELEMAC model runs

Run number	Tsunami source	Additional information
1	A2	-
2	B2	-
3	C2	-
4	A1	-
5	A2	Sensitivity test using incident wave boundary for tsunami wave
6	B2	+2.55m above mean sea level, corresponding to approximately high water at the Cornish coast.
7	B2	-2.55m below mean sea level, corresponding to approximately low water at the Cornish coast.

Runs 1 - 5 were performed without including any effect of the tide (the water level was set to a mean sea level and the only motions were those driven by the tsunami event). Runs 6 and 7 reviewed the effect of the tide on the incoming tsunami waves; the sea level was increased and decreased by 2.55m, corresponding to a mean high and low water spring tides at Cornwall.

The model runs simulated up to 12 hours of wave propagation after the earthquake at Lisbon. During these runs bed friction was represented in the model as a Nikuradse roughness length of 0.01m.

Results of model runs 1 – 7 are presented in Figure 2.28 – 2.34 respectively. These figures indicate that scenario B2 has the largest tsunami approaching the UK and Irish coasts. Further information regarding maximum free-surface elevation around the coast for Runs 1 – 4 are provided in Figures 2.35 – 2.38. It can clearly be seen that the maximum free-surface elevation around the coasts is significantly larger from the B2 tsunami source, in comparison to the other source conditions.

For all models, the south coast of Ireland, specifically near Ross Carbery, Kinsale and south of Dingle Bay recorded water surface elevations in excess of 1m. For Run 2 (tsunami scenario B2) the majority of the south coast of Ireland, near Clifden on the west coast and a large majority of the Cornish coast (between Kingsbridge and Bude) recorded water surface elevations in excess of 1m. Exact free-surface elevations are given in detail in Section 2.3.6.

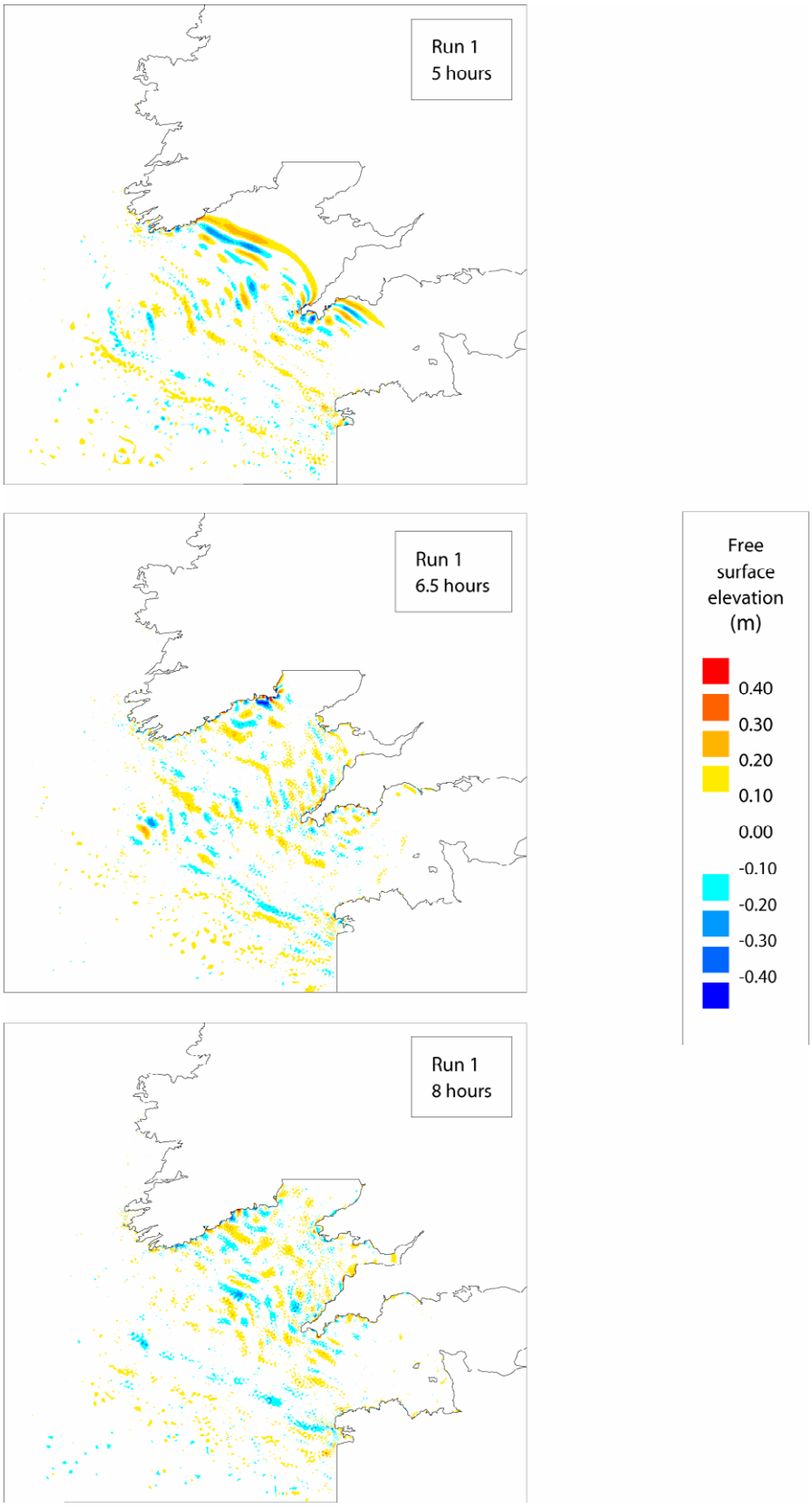

Figure 2.28 Free surface elevation at 5, 6.5 and 8 hours after the earthquake, TELEMAC model run 1 (Tsunami scenario A2)

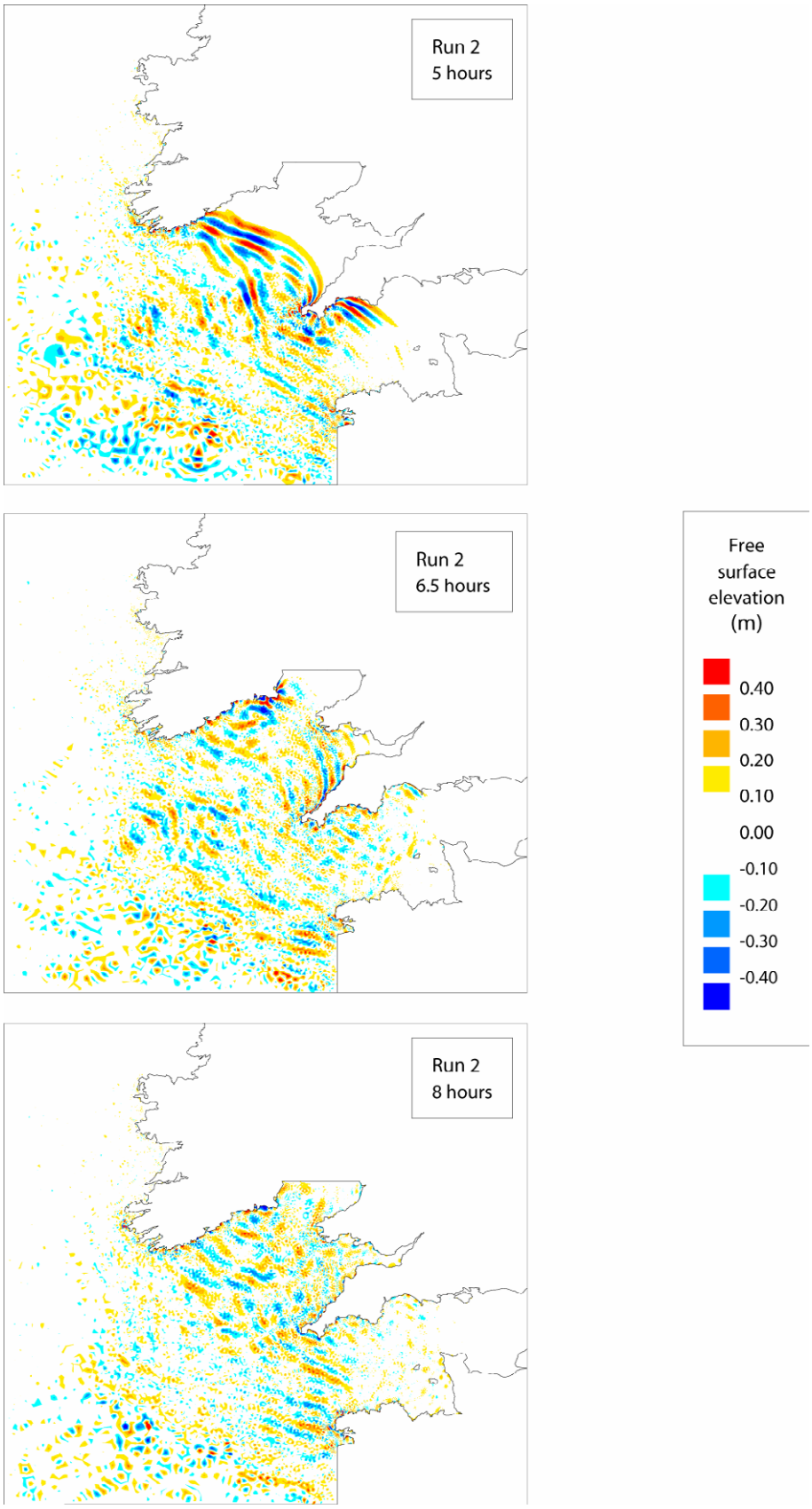

Figure 2.29 Free surface elevation at 5, 6.5 and 8 hours after the earthquake, TELEMAC model run 2 (Tsunami scenario B2)

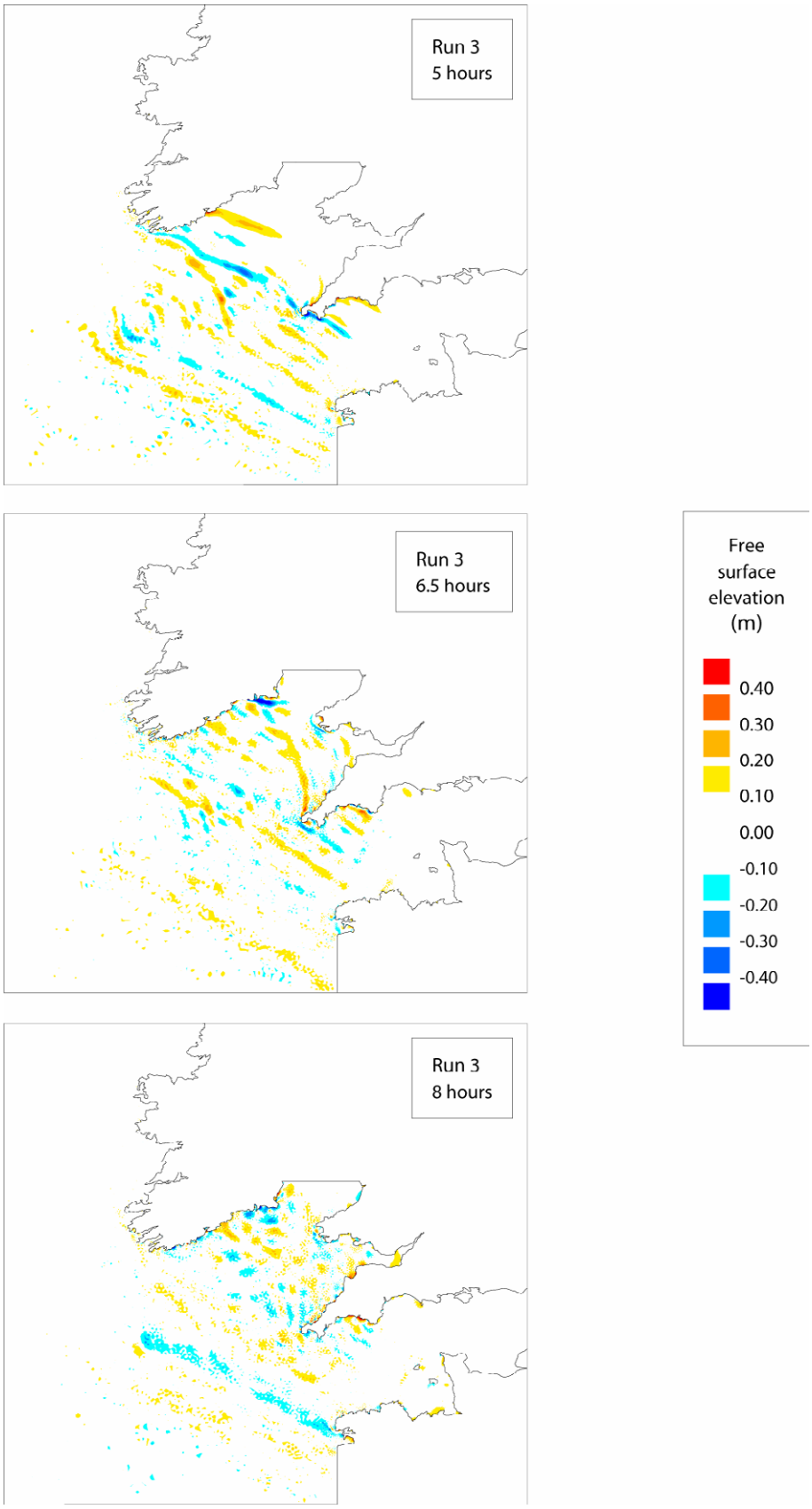

Figure 2.30 Free surface elevation at 5, 6.5 and 8 hours after the earthquake, TELEMAC model run 3 (Tsunami scenario C2)

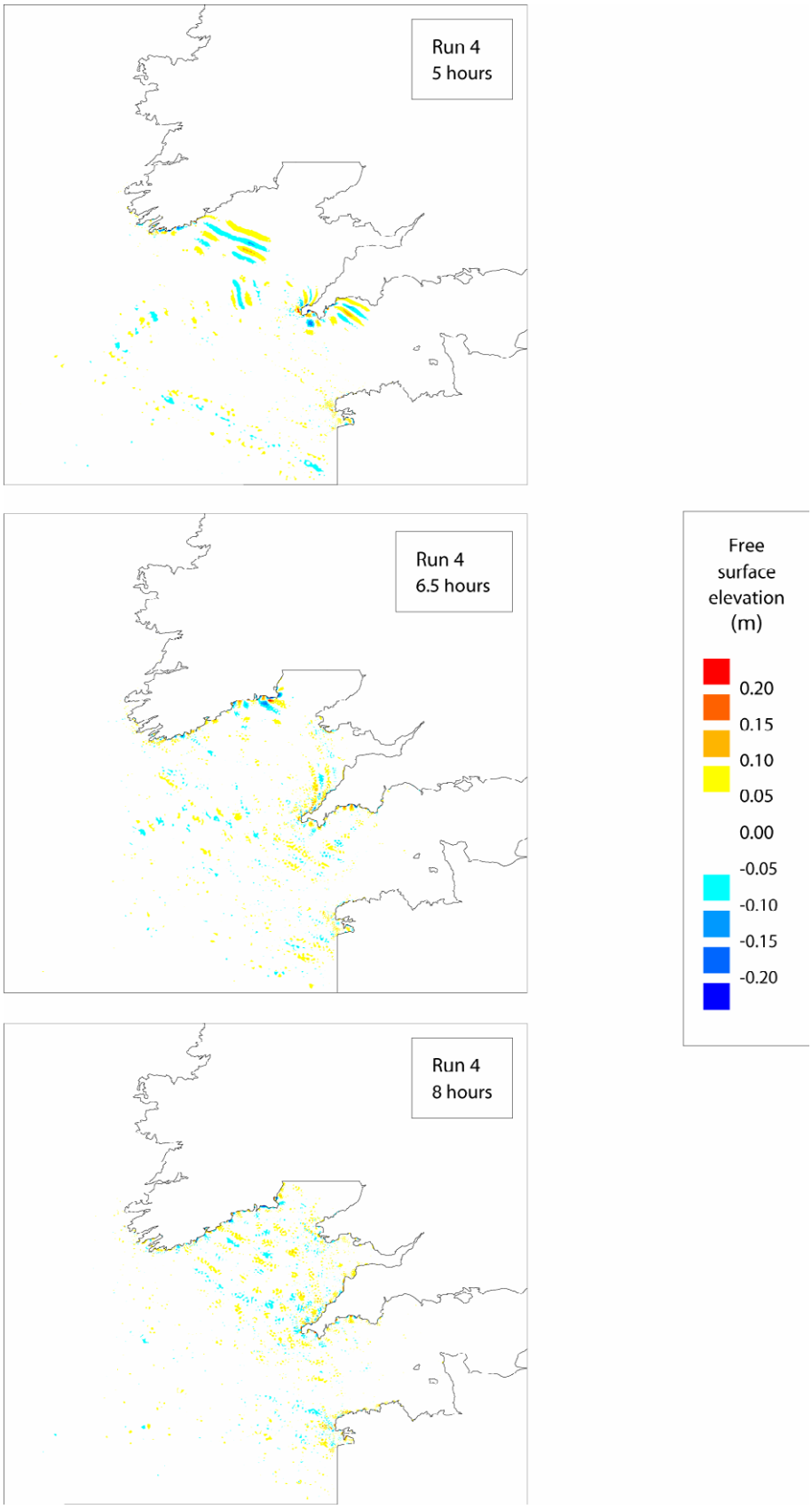

Figure 2.31 **Free surface elevation at 5, 6.5 and 8 hours after the earthquake, TELEMAC model run 4 (Tsunami scenario A1)**

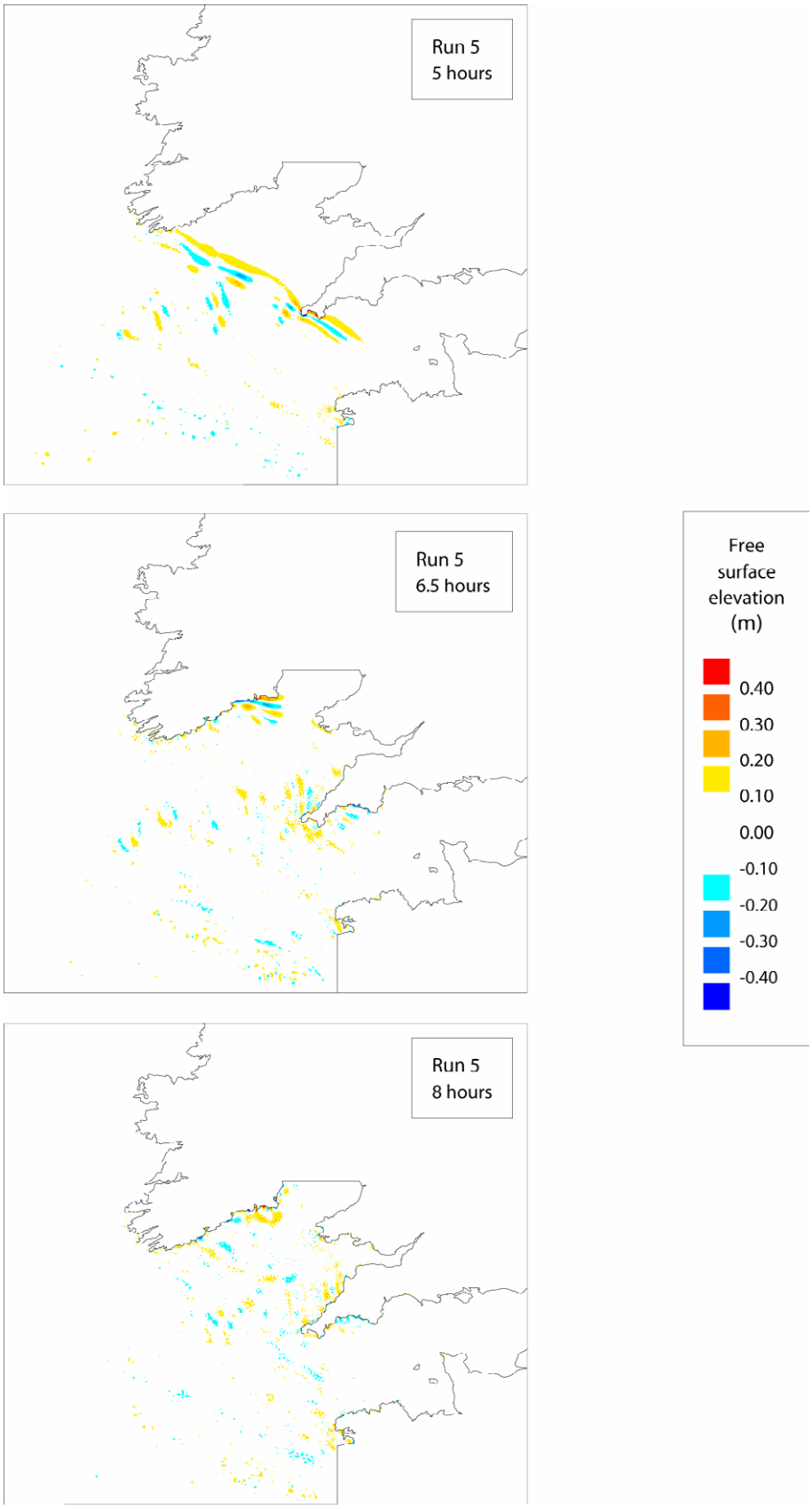

Figure 2.32 Free surface elevation at 5, 6.5 and 8 hours after the earthquake, TELEMAC model run 5 (Tsunami scenario A2)

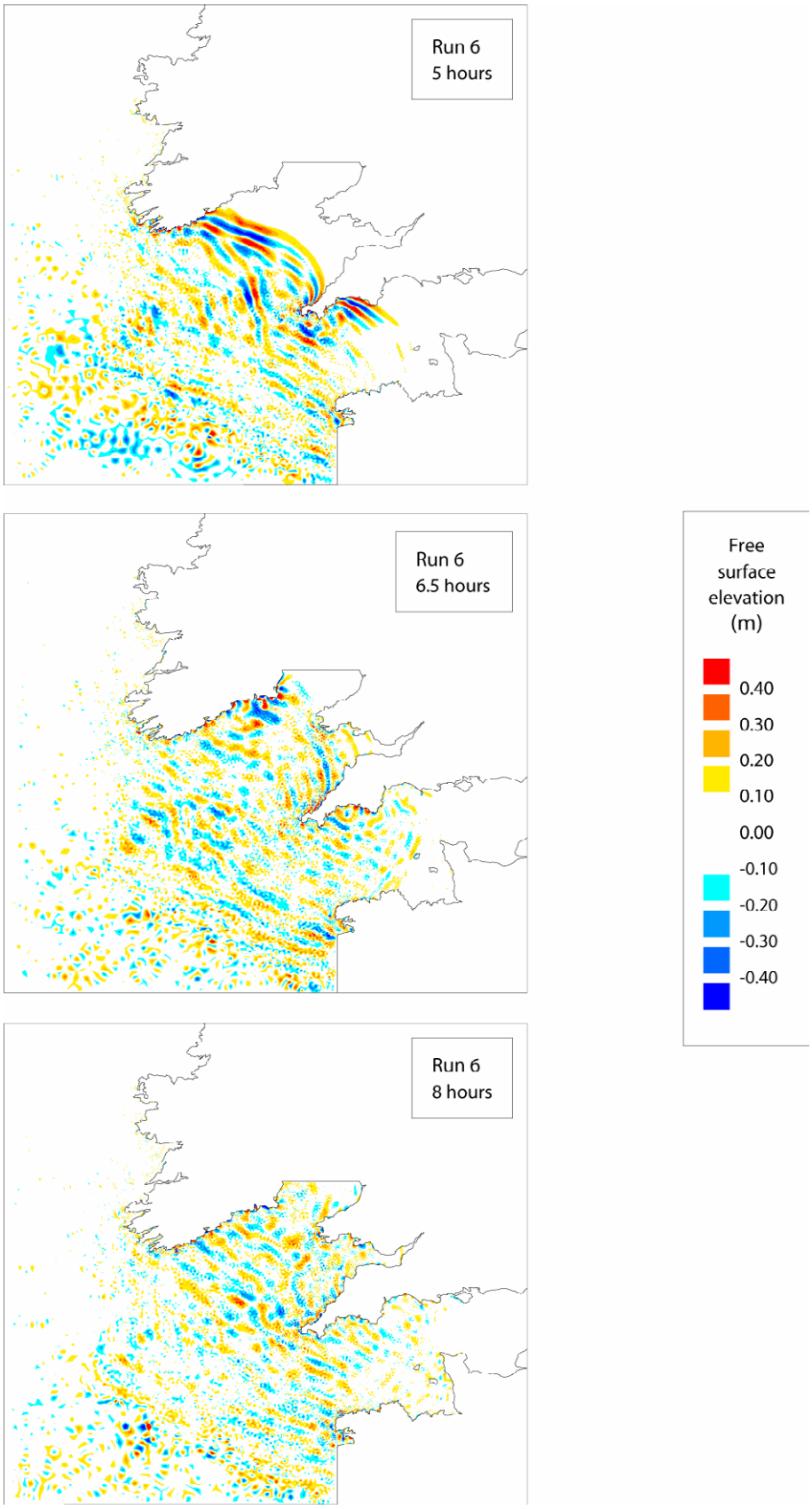

Figure 2.33 Free surface elevation at 5, 6.5 and 8 hours after the earthquake, TELEMAC model run 6 (Tsunami scenario B2)

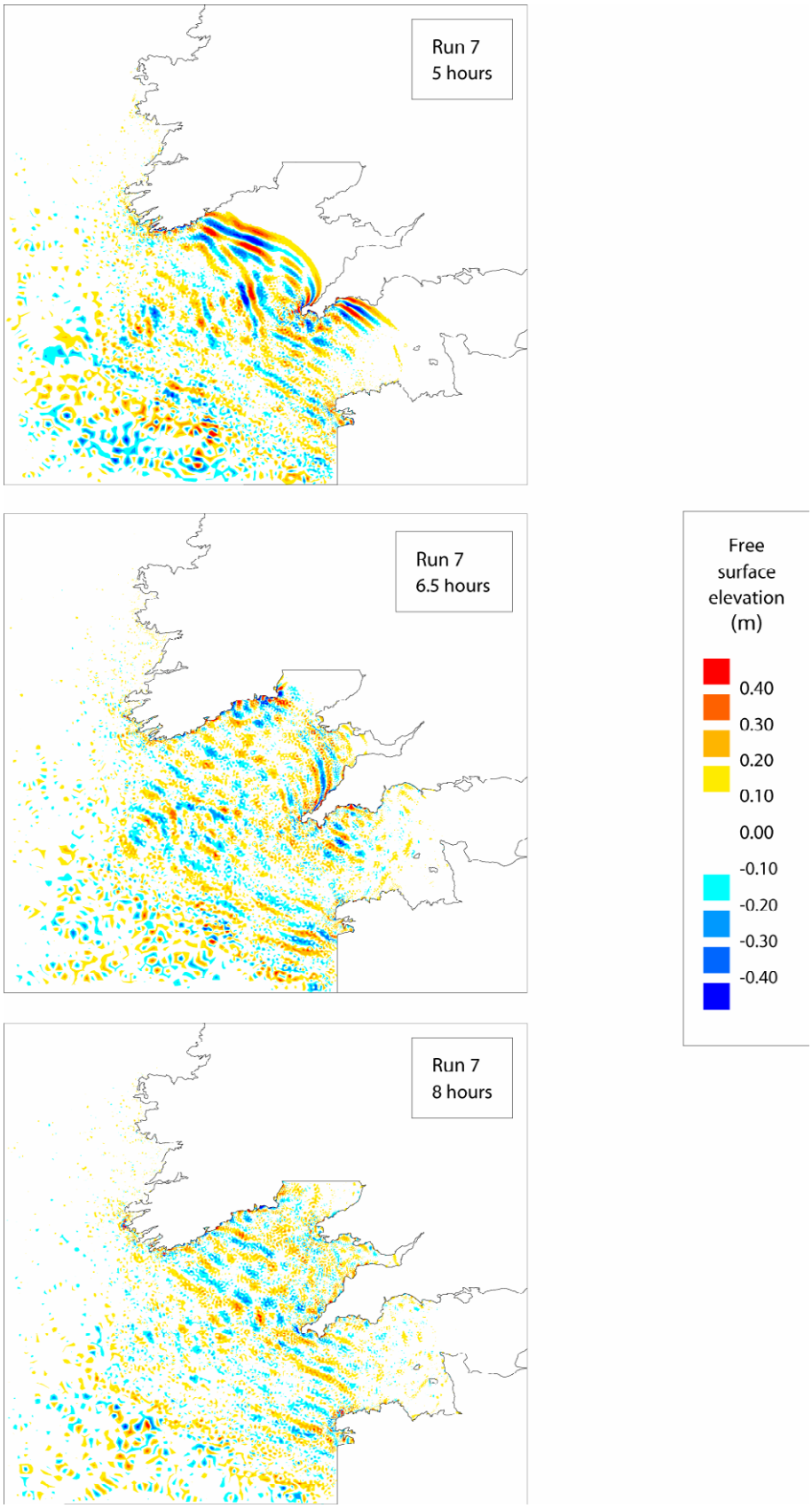

Figure 2.34 Free surface elevation at 5, 6.5 and 8 hours after the earthquake, TELEMAC model run 7 (Tsunami scenario B2).

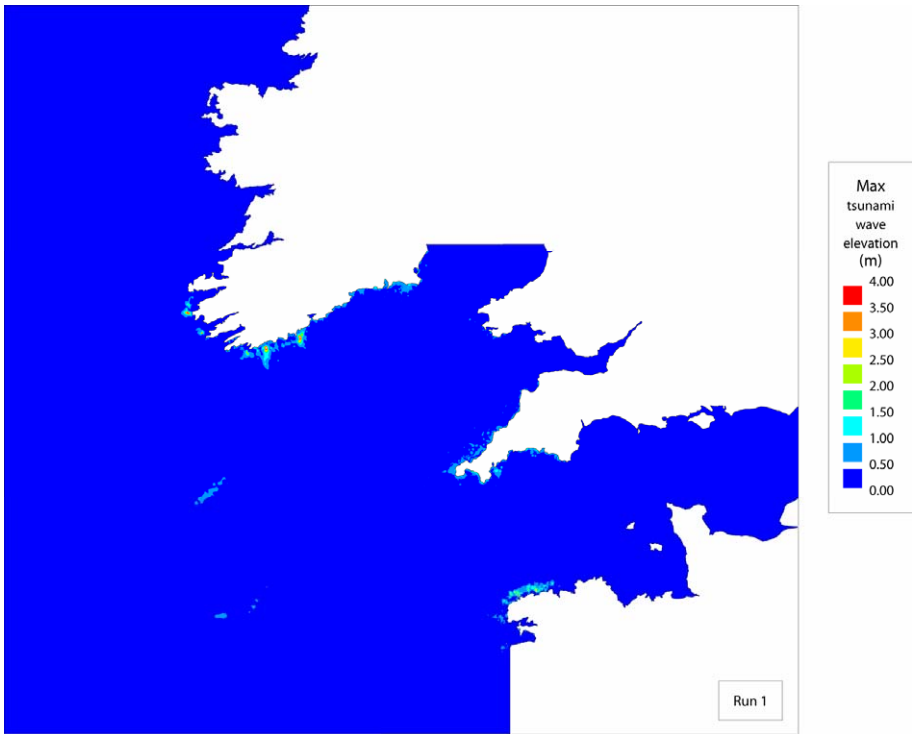

Figure 2.35 Maximum free surface elevation, TELEMAC model run 1 (Tsunami scenario A2)

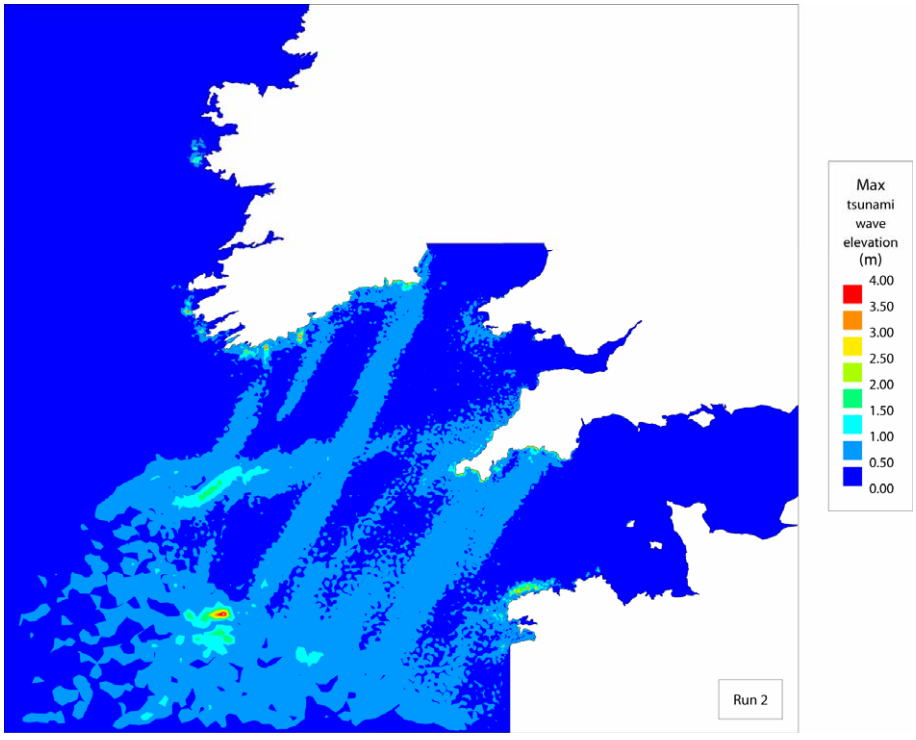

Figure 2.36 Maximum free surface elevation, TELEMAC model run 2 (Tsunami scenario B2)

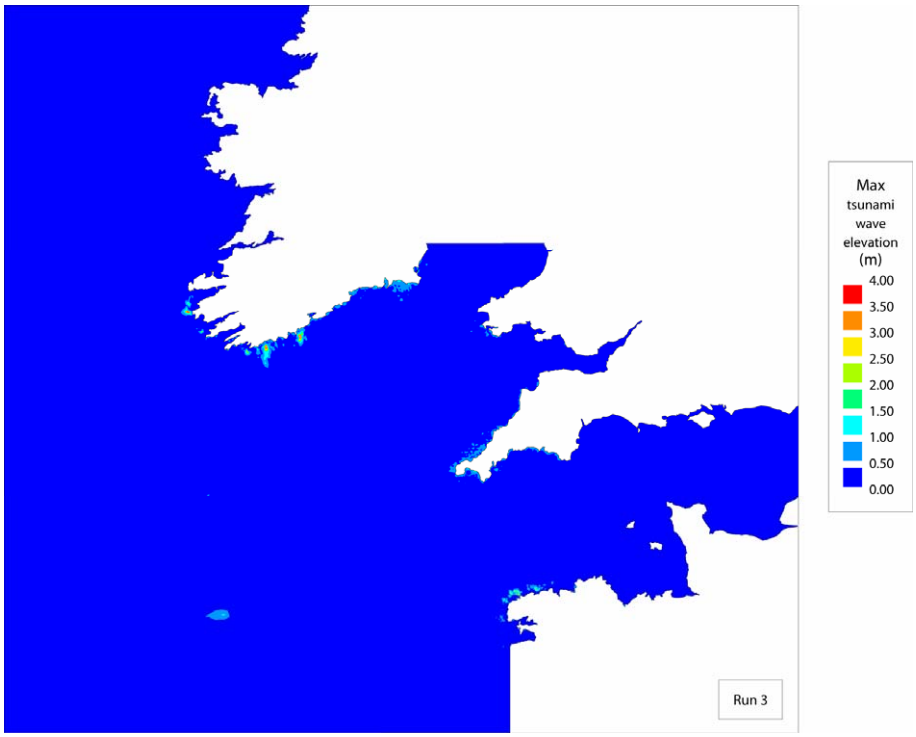

Figure 2.37 Maximum free surface elevation, TELEMAC model run 3 (Tsunami scenario C2)

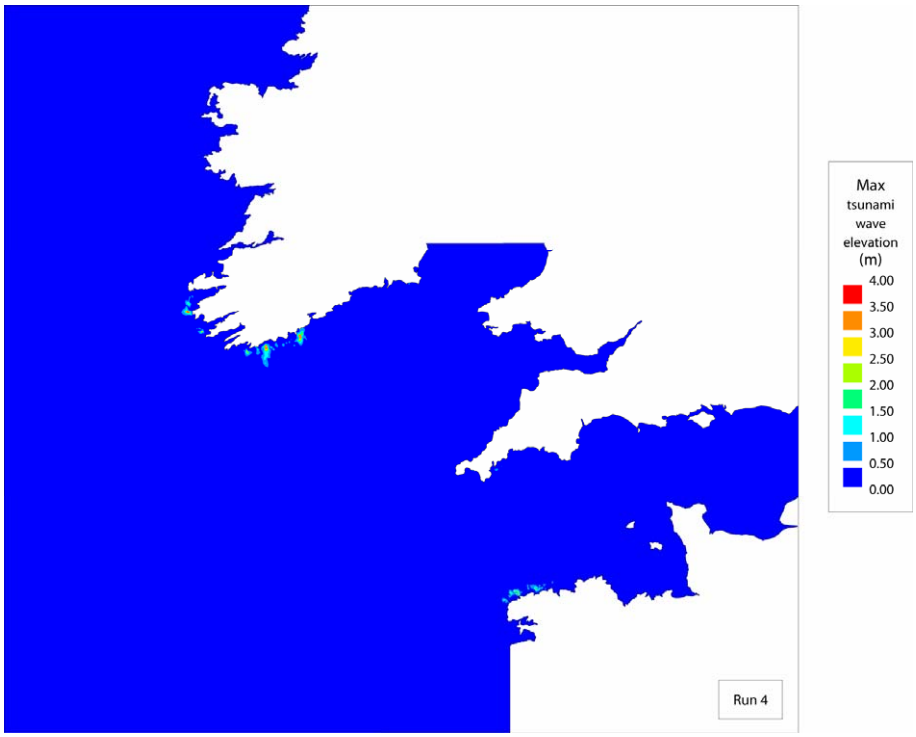

Figure 2.38 Maximum free surface elevation, TELEMAC model run 4 (Tsunami scenario A1)

2.3.5 Comparisons against UK observations of 1755 tsunami.

The work of Baptista *et al* (2003) puts forward information from observations made in Cornwall on the day of the Lisbon 1755 tsunami. These include the travel time of the tsunami wave from Lisbon to Penzance and Plymouth of 315 and 390 minutes, respectively. These observations are considered to represent the time to the first peak of the tsunami wave reaching the coast. They also include the most reliable information regarding wave height, an observation of 2.1m (maximum) at Penzance.

The results from the model runs 1 - 4 for the maximum elevation at Penzance and travel times to Penzance and Plymouth are given in Table 2.5. It can be seen that the travel times are in relative agreement with the simulation of Baptista which gave the times as 268 and 332 minutes, respectively. The model result closest to the maximum wave observation is run 4 (B2).

Table 2.5 TELEMAC model result for travel time and maximum free-surface elevation at Penzance and Plymouth

Tsunami Source	Penzance		Plymouth	
	Travel time	Max. elevation	Travel time	Max. elevation
A2	274	0.8	324	0.8
B2	264	1.7	312	1.7
C2	262	0.8	312	0.7
A1	272	0.3	320	0.2

The time history of the water level at Penzance and Plymouth for runs 1 - 4 are shown in Figures 2.39 – 2.42. For several of the runs the first wave is not the largest, which is in agreement with the observations of Borlase (1755, 1758). He described the arrival of the tsunami in Mounts Bay, Cornwall, noting

'*... the first and second refluxes were not so violent as the 3rd and 4th (tsunami waves) at which time the sea was as rapid as that of a mill-stream descending to an undershot wheel and the rebounds of the sea continued in their full-fury for fully 2 hours... alternatively rising and falling, each retreat and advance nearly of the space of 10 minutes until five and a half hours after it began*'.

The wave period in the model is approximately 20 minutes, which appears to be consistent with the comments of Borlase (10 minutes each for advance and retreat).

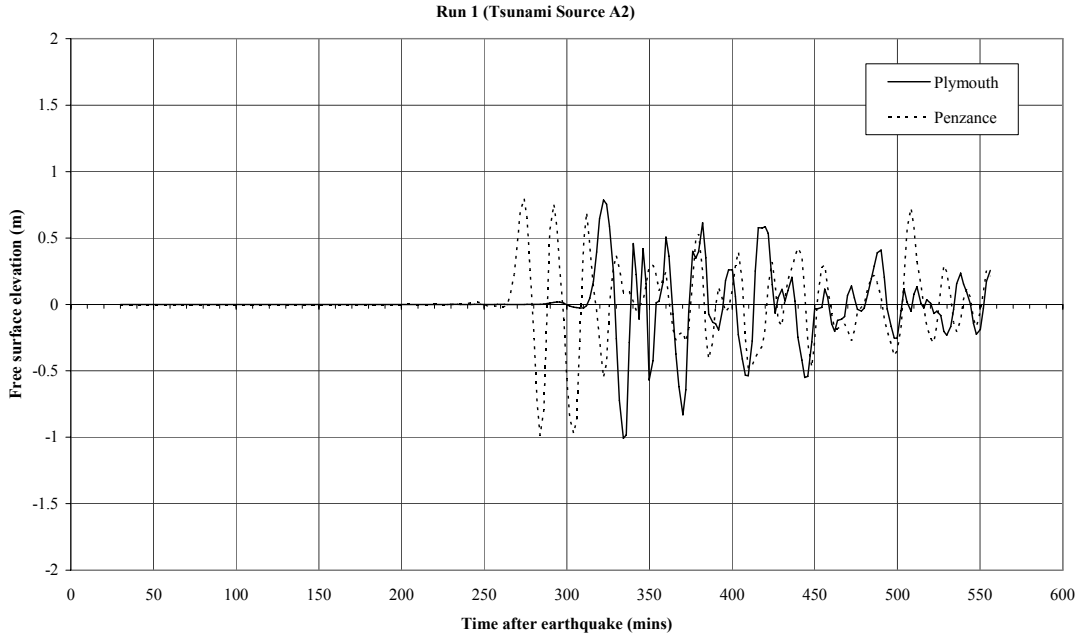

Figure 2.39 Time history of free surface elevation at Penzance and Plymouth, Run 1 (Tsunami source A2)

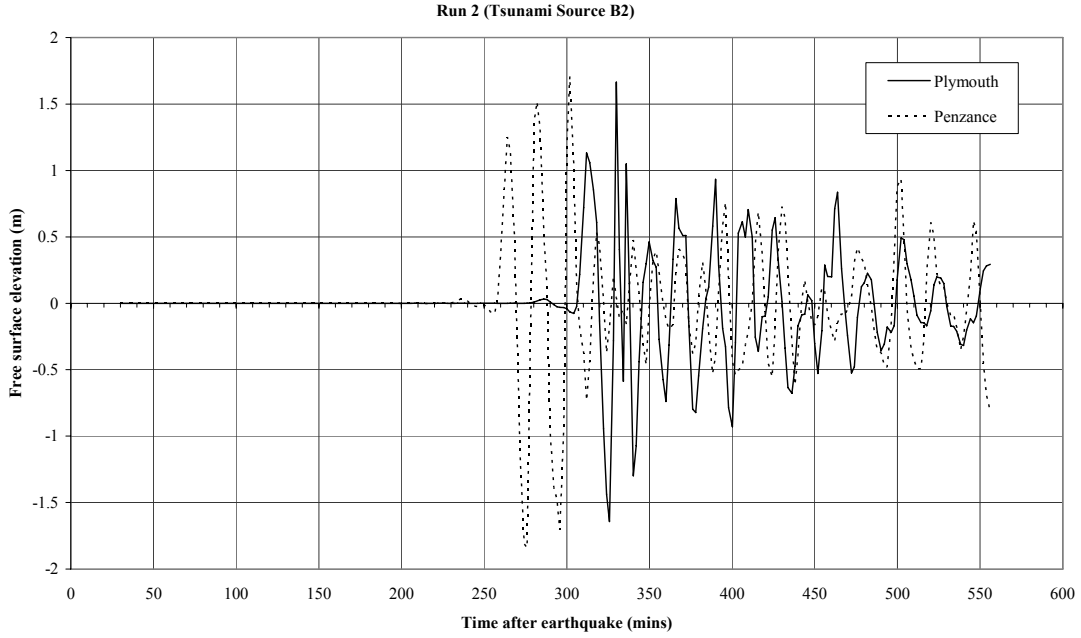

Figure 2.40 Time history of free surface elevation at Penzance and Plymouth, Run 2 (Tsunami source B2)

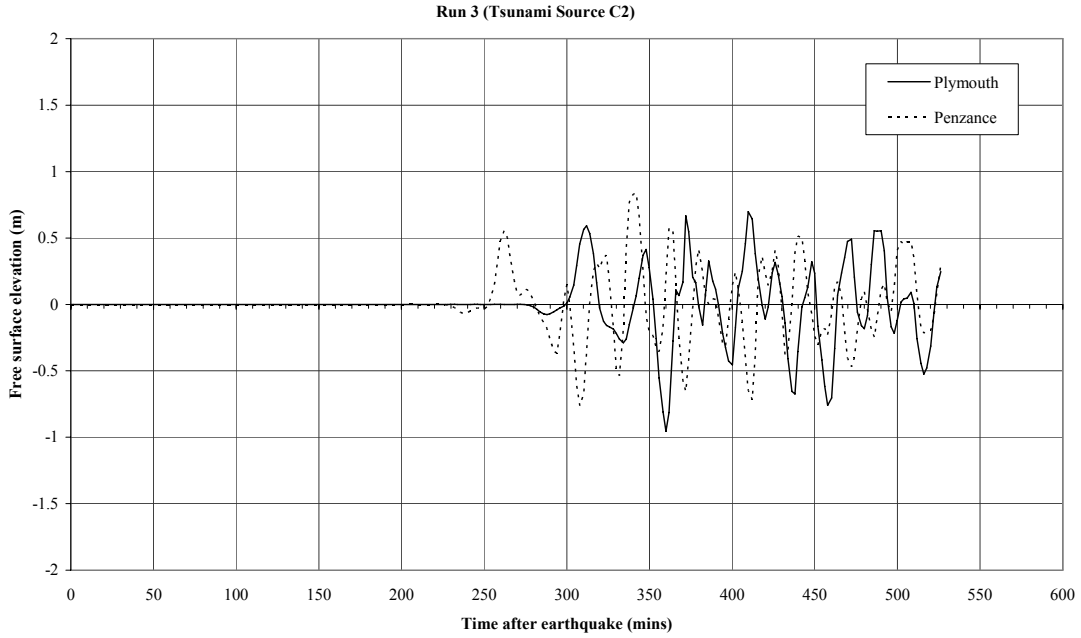

Figure 2.41 Time history of free surface elevation at Penzance and Plymouth, Run 3 (Tsunami source C2)

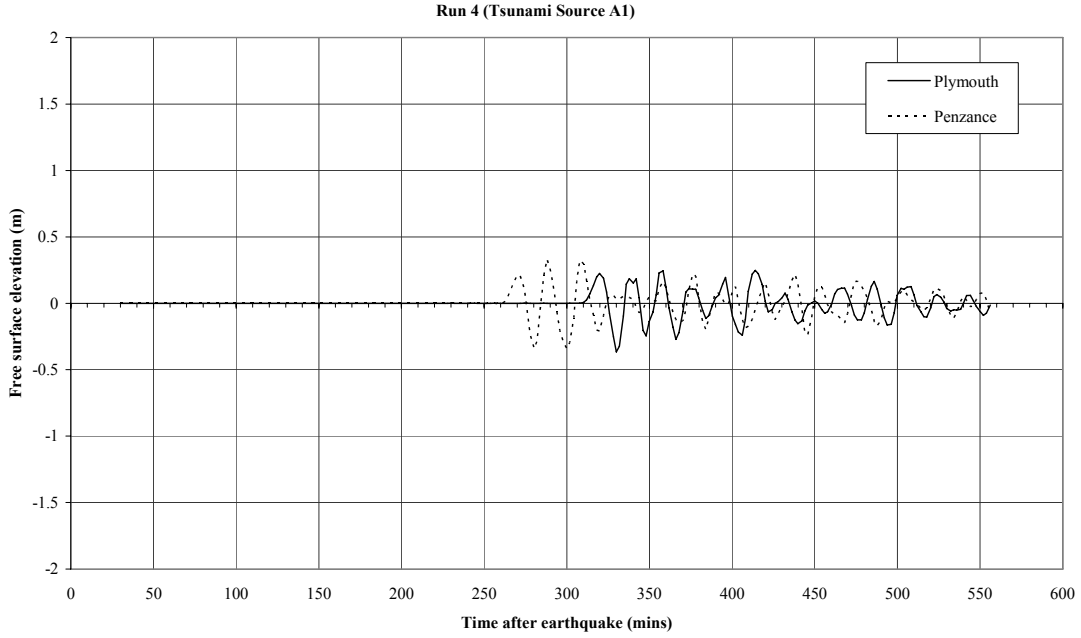

Figure 2.42 Time history of free surface elevation at Penzance and Plymouth, Run 4 (Tsunami source A1)

The TELEMAC model runs gave many high values at the coastline for the maximum elevation in Mount's Bay, as shown in Figure 2.46 for Run 2. Several of the wave heights are greater than 2m.

The reason for the high wave heights in Mount's Bay are as follows:

1. focussing of the wave heights from offshore towards this part of Cornwall (Figure 2.32);
2. wave height increase as the wave travels up the Continental Shelf slope. The wave front is in shallower water and travels slower than the back of the wave, therefore reducing the wave length (i.e. the wave appears to get squashed) and the height increases;
3. local wave resonance in Mount's Bay (maximum levels all greater than 1m in the Bay, Figure 4.1);
4. at the coastline the reflections double the wave height.

These factors appear to be the important ones in creating shoreline maximum levels of 2m and above at some locations.

Note that the English Channel does not receive much diffracted energy, this is related to the short wavelength (of the order of 20km). This is consistent with the absence of historic observations of the tsunami wave eastward of Plymouth.

Also, the Bristol Channel does not receive much wave energy, largely because of bathymetry driven refraction pushing waves towards the north coast of Cornwall.

2.3.6 Height of simulated wave at UK and Irish coasts

As noted previously model Run 2, tsunami source B2, created the largest free-surface elevations around the UK and Irish coastline. These maximum water levels are presented graphically here over four segments of coastline (Cornish, Bristol Channel, southern Irish and western Irish), shown in Figures 2.43 – 2.46. The corresponding maximum elevations, for each of the coastline segments, are presented in Figures 2.47 - 2.52.

The effect of tide on the tsunami elevation at the coastline was reviewed in Runs 6 and 7. Figures 2.51 and 2.52 indicate that the maximum wave elevation is relatively consistent along the coast for both the low and high tidal conditions. Local maxima between Penzance and Lizard Point, varied slightly in magnitude and location, although maximum water elevation remained approximately 4m. It should be noted that the mesh resolution at the coast is approximately 1km, so any further localised effects will not be resolved in the model.

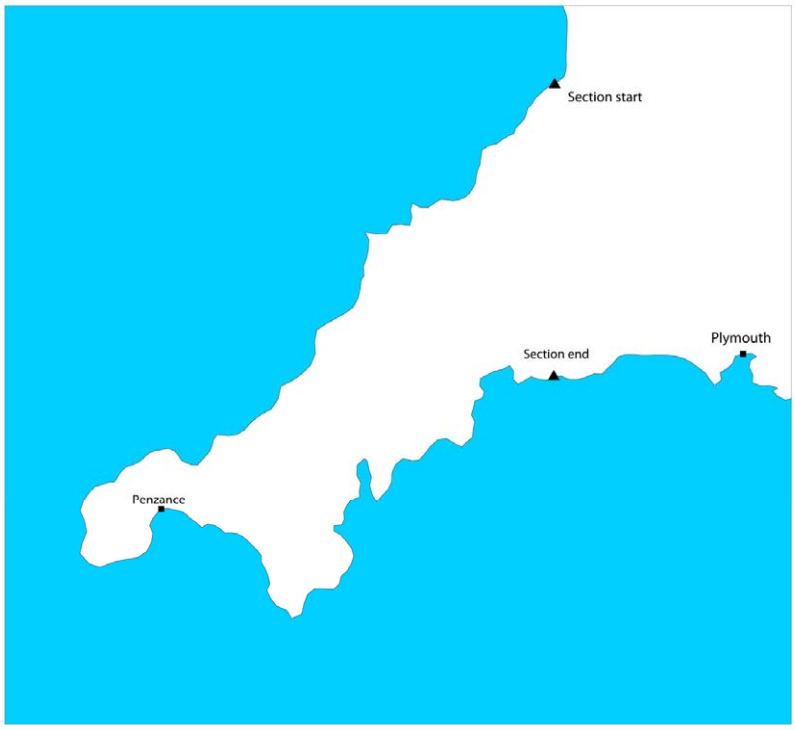

Figure 2.43 Cornish segments of coastline for recorded maximum free surface elevation

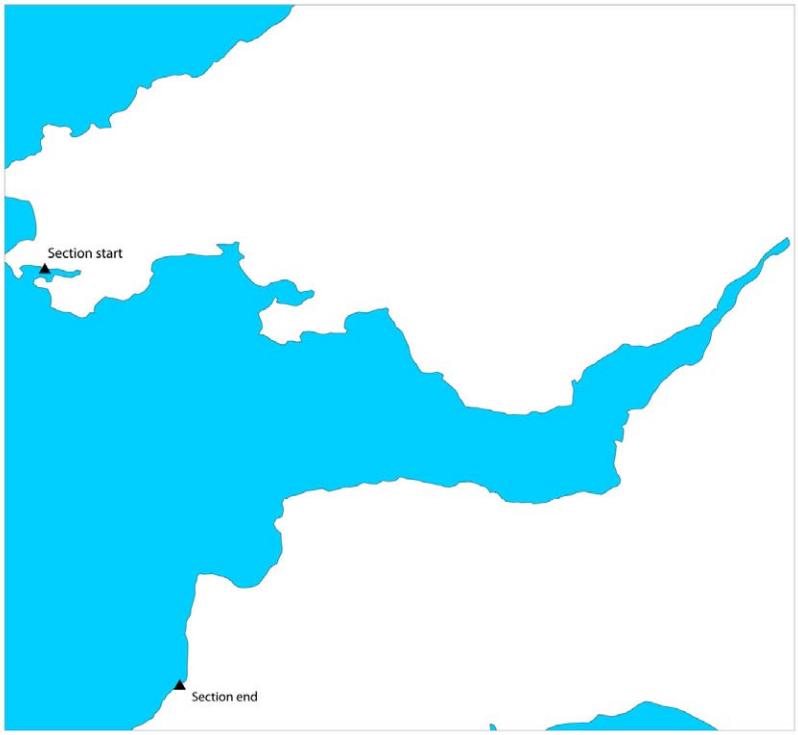

Figure 2.44 Bristol Channel segment of coastline for recorded maximum free surface elevation

Figure 2.45 Western Ireland segment of coastline for recorded maximum free surface elevation

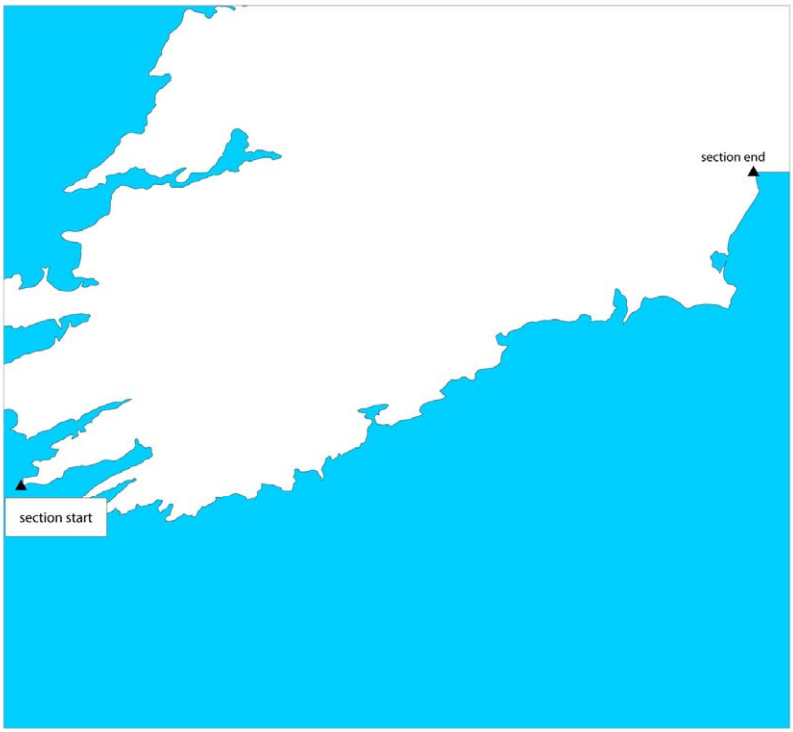

Figure 2.46 Southern Ireland segment of coastline for recorded maximum free surface elevation

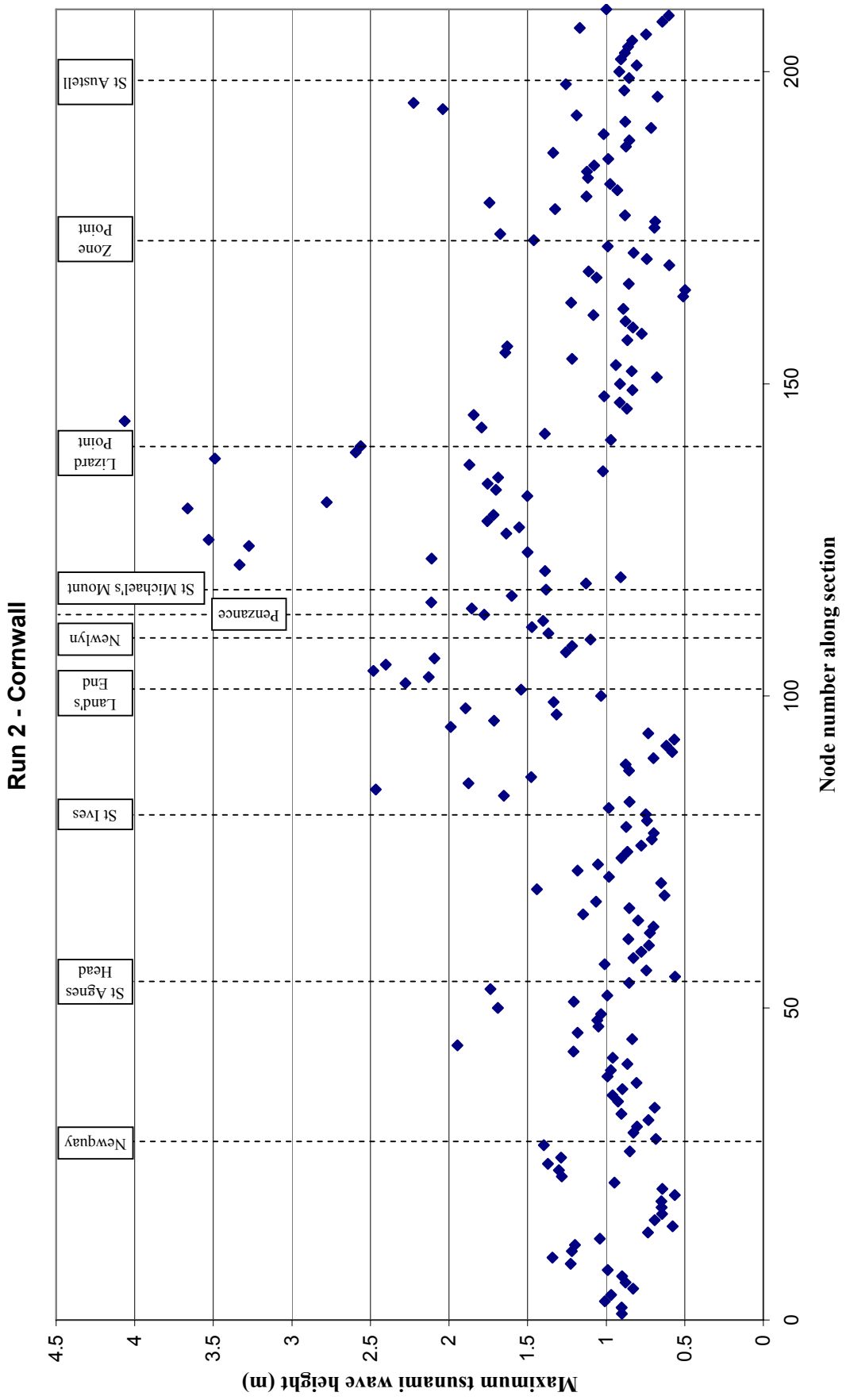

Figure 2.47 Maximum free surface elevations along the Cornish Coast (TELEMAC Run 2)

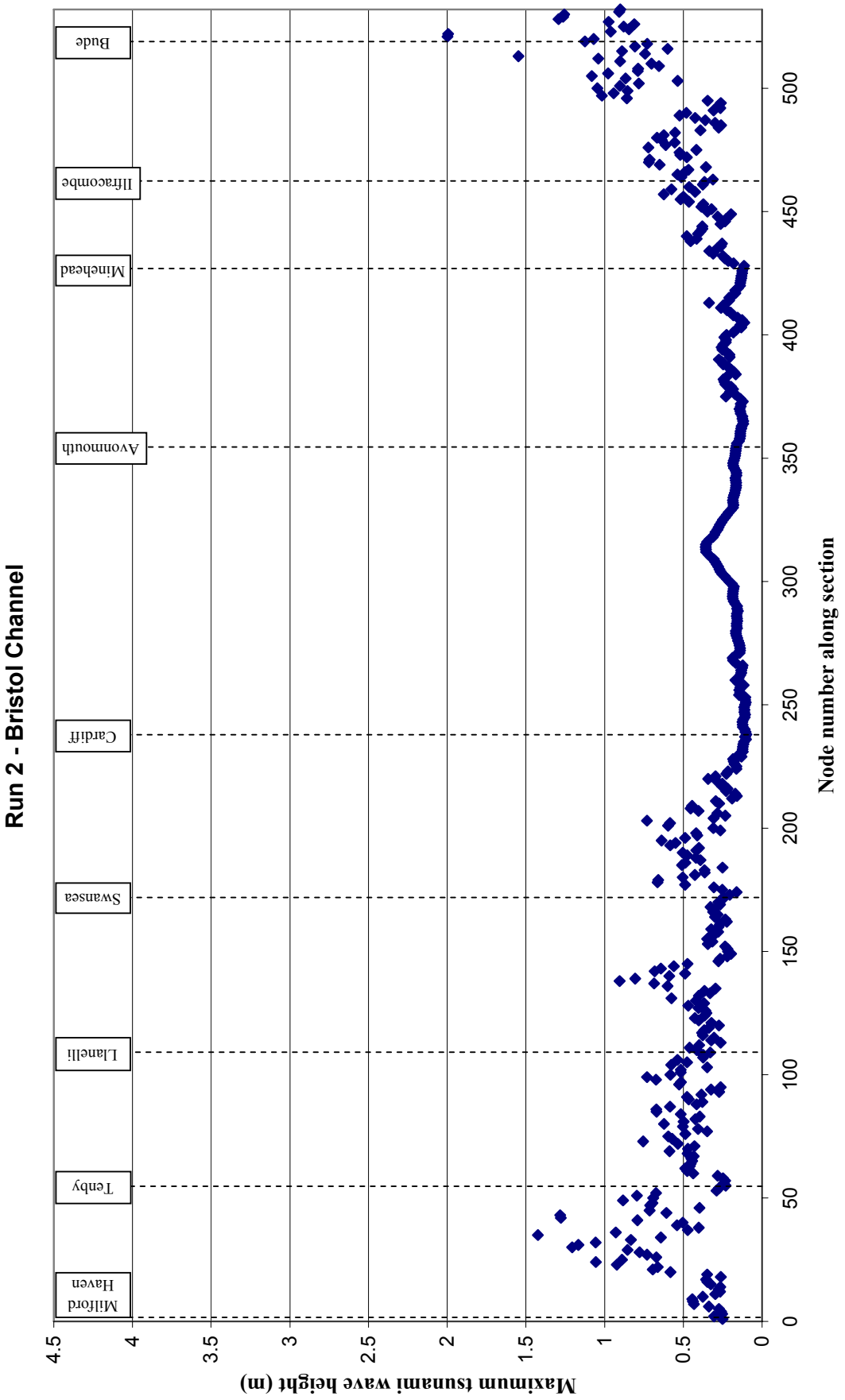

Figure 2.48 Maximum free surface elevations along the Bristol Channel (TELEMAC Run 2)

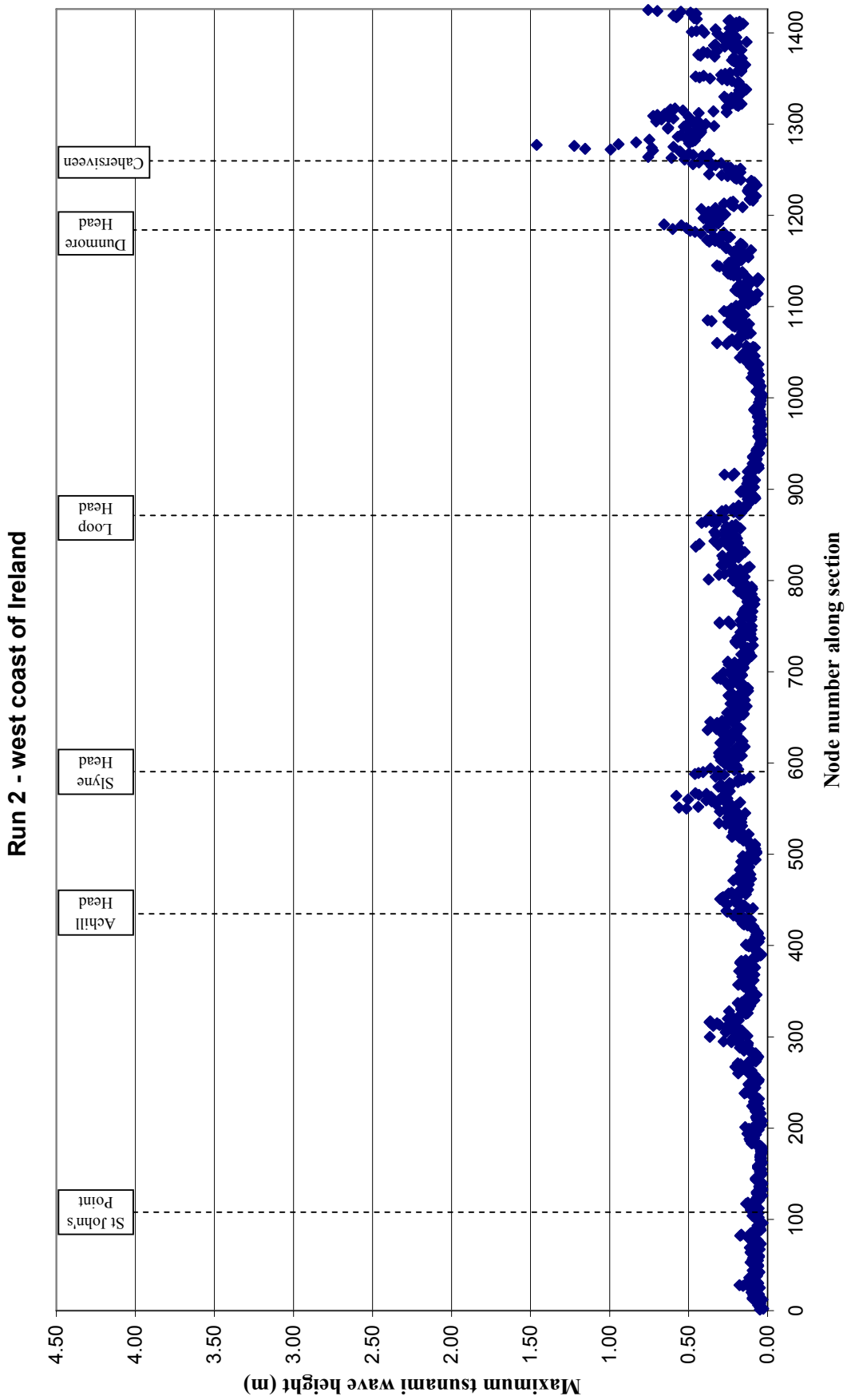

Figure 2.49 Maximum free surface elevation along the west Irish coast (TELEMAC Run 2)

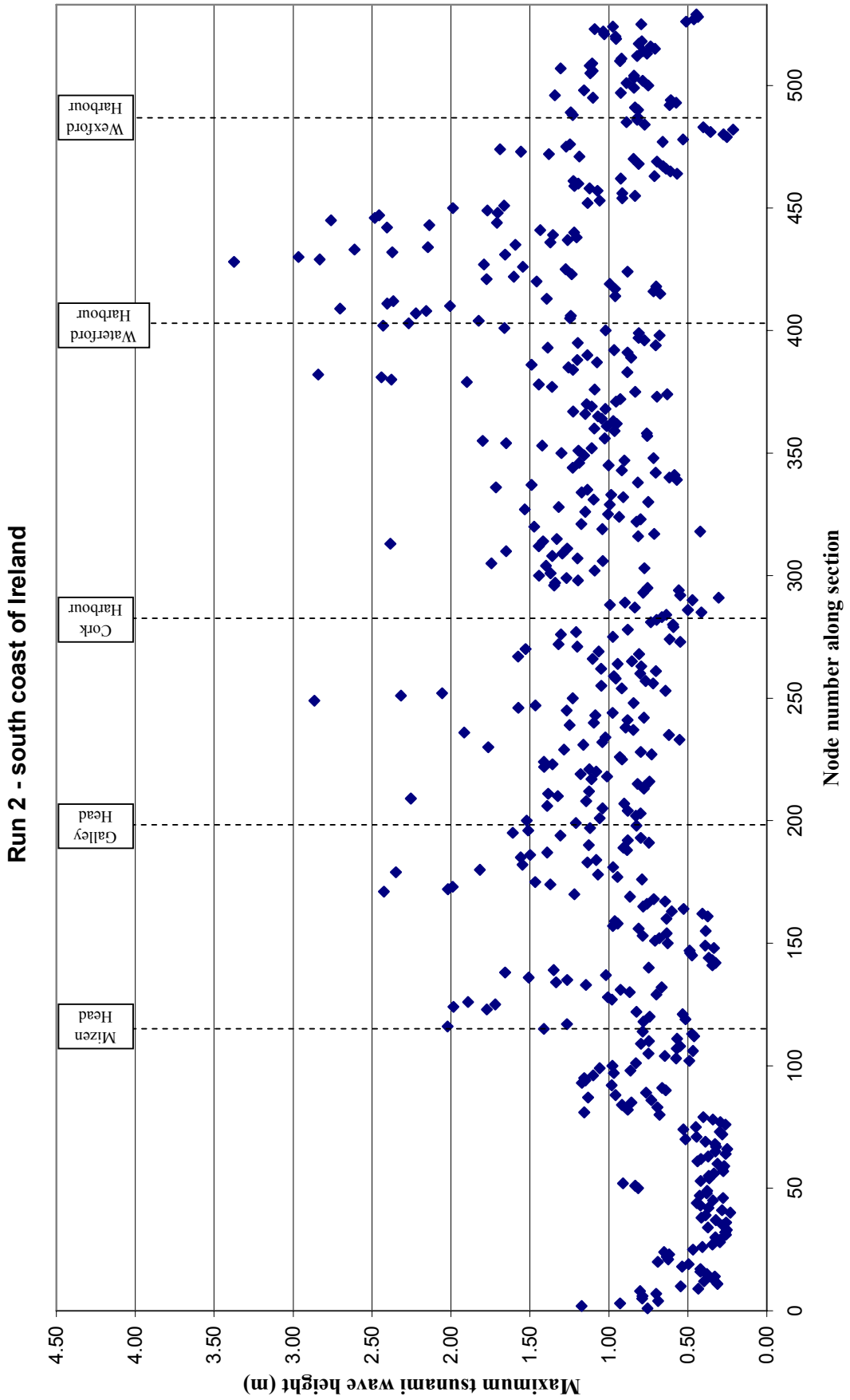

Figure 2.50 Maximum free surface elevation along the south Irish coast (TELEMAC Run 2)

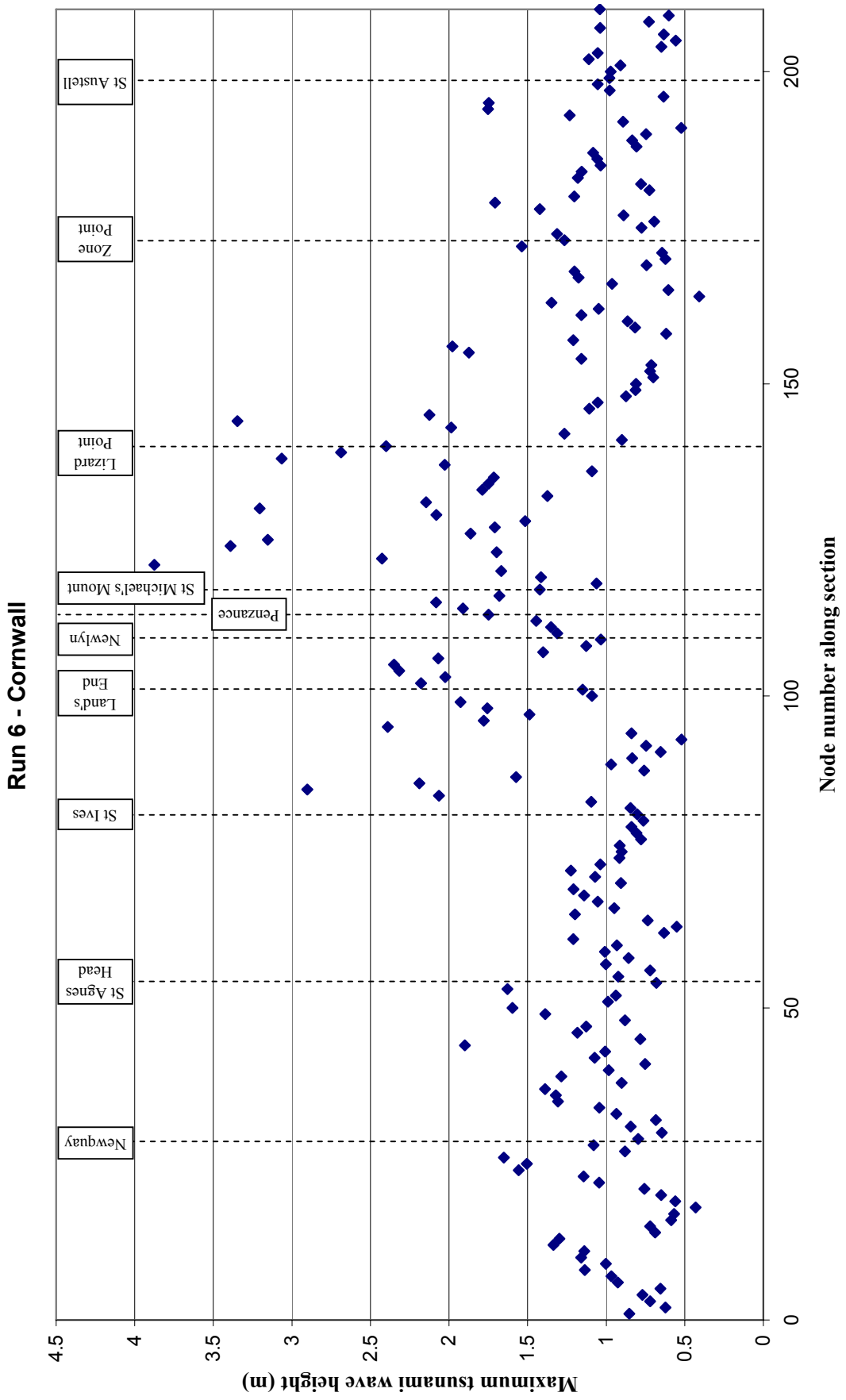

Figure 2.51 Maximum free surface elevation along the Cornish coast (TELEMAC Run 6)

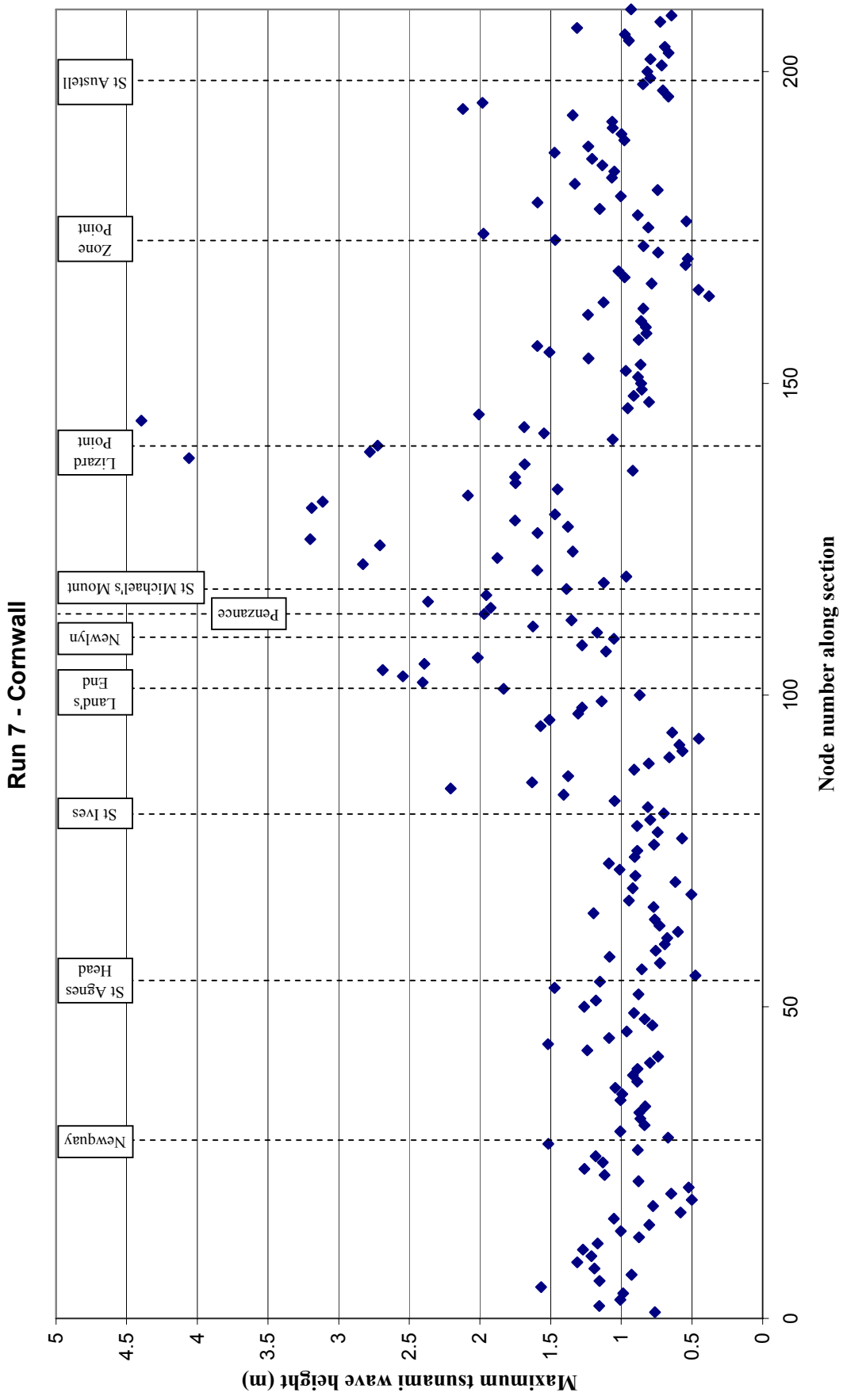

Figure 2.52 Maximum free surface elevation along the Cornish coast (TELEMAC Run 7)

3 North Sea Event

3.1 Introduction

In the previous Defra study (Kerridge, 2005) a near field event in the North Sea was investigated. It was noted in this report that there is no historical evidence for earthquakes larger than 5.4 ML (local magnitude) onshore or in the Irish Sea. However offshore seismicity, especially in the North Sea, is prone to larger events.

The previous modelling study assumed the source was located at the position of the 1931 earthquake. The free-surface displacement was assumed to be 1m in elevation and axisymmetric, with a period of between 20 and 30 minutes.

As part of this study the source of the tsunami was amended and the new configuration input into numerical models. These computational runs were undertaken to simulate the transformation of the tsunami as it came onshore and the subsequent inundation.

The location of the 1931 earthquake, as well as faults and seismicity for the Flamborough Head – Sole Pit region are shown in Figure 3.1. The 1931 earthquake was approximately 5.7 M_W and we have based our North Sea event reviewed here on a 6.0 M_W event.

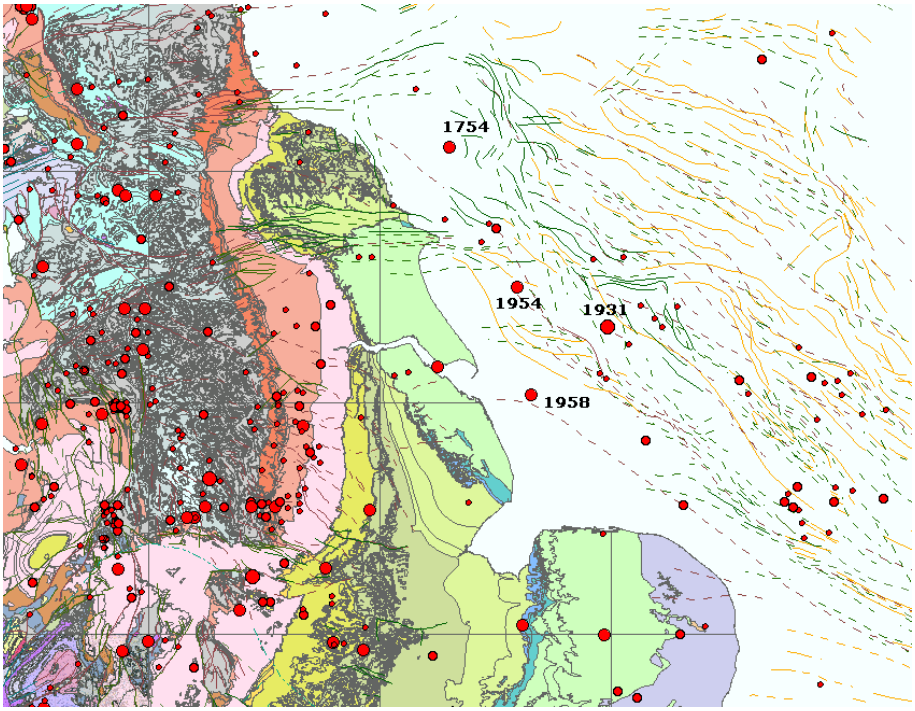

Figure 3.1 Faults and seismicity for Flamborough Head – Sole Pit region

Using the assumption of a 6.0 M_W then the predicted surface rupture length would be 8km (at least between 5-13km), with a maximum displacement of 0.3m and an average displacement of 0.2m. The fault orientation was northwest – southeast, located at the 1931 earthquake, as shown by the fault lines depicted in Figure 3.1.

3.2 Propagation from source

The source parameters defined above were used as input for the free-surface displacement at source and the POL 3.5 km resolution N10 model used to propagate the resulting waves from source. The N10 model area and grid is shown in Figure 3.1.

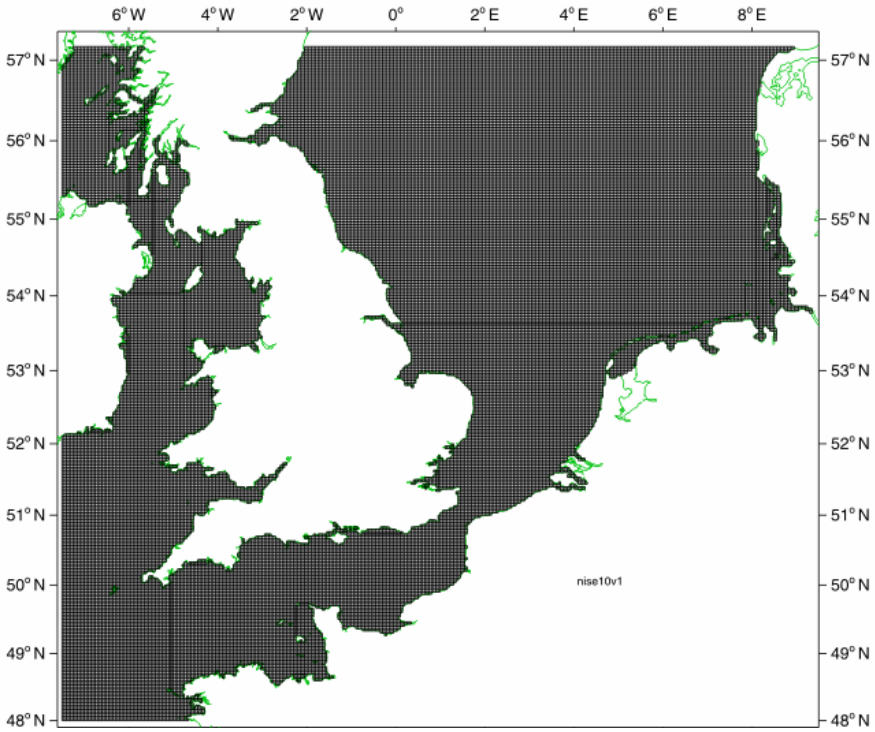

Figure 3.2 Computational grid of the POL N10 model with 3.5 km resolution

The initial tsunami wave reaches the Yorkshire coastline after approximately 30 minutes (Figure 3.2), a similar time to previous simulations of North Sea events (Kerridge, 2005). The alternative source parameters, used here, have reduced the inshore wave elevation from approximately 1m in the previous Defra study to less than 0.3m.

3.3 Propagation inshore

A TELEMAC model was used to model the wave propagation from offshore to the shoreline and consequent inundation of the beach. As the purpose of this stage of the study was essentially to assess the inundation capacity of tsunamis more generally, the three-dimensionality of the original source was neglected and the simulation performed using a one-dimensional profile model. As the actual event is spreading out laterally, it is best for the travel distance to be as close to the shoreline as possible. Wave data approximately 10km offshore with a bed elevation of -17.4m was extracted from the POL N10 model. This was used as input to the tsunami profile model.

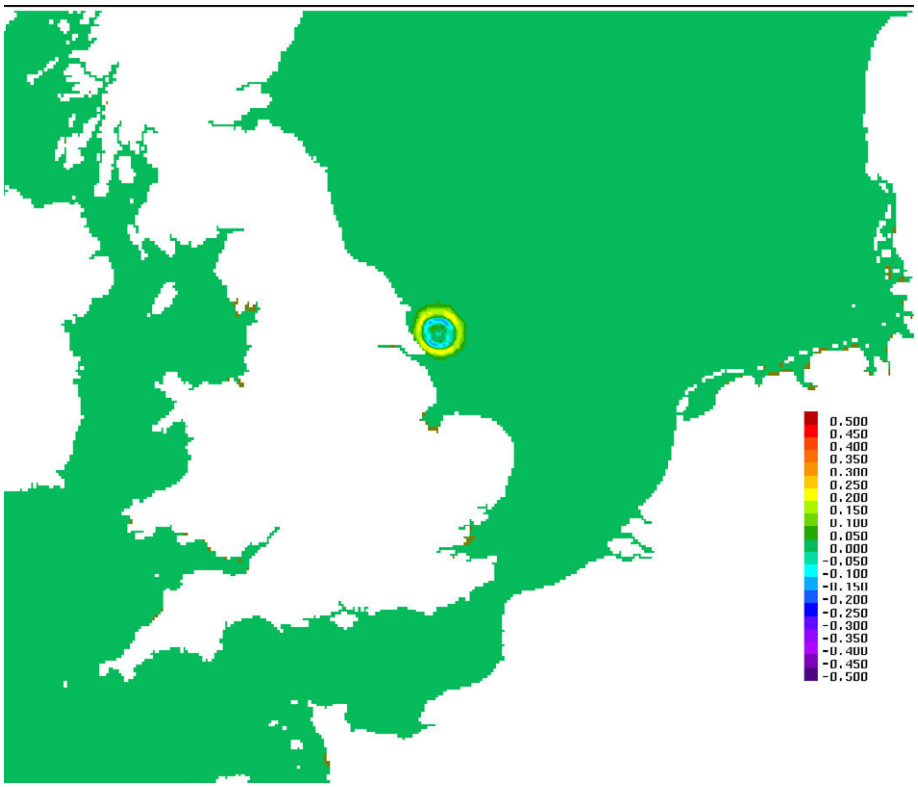

Figure 3.3 Tsunami waves reaches Yorkshire coastline after approximately 30 minutes

TELEMAC is essentially a two-dimensional numerical model, but in this case it was run as a one-dimensional model. To perform the simulation in this way a small number of elements were used across the domain.

3.3.1 Model method

The model was run using a finite volume solver for the non-linear shallow water equations. The benefit, over the usual finite element method, is that the finite volume method is shock capturing, allowing bores, hydraulic jumps or breaking wave to be modelled in the solution. In a finite element method shocks are not captured and oscillations occur in the solution, normally over a number of elements. This finite volume method has also been found to be effective where initially dry areas of the domain are flooded, for example when carrying out dam break studies. In addition some runs were carried out using the finite element as used for the work described in Chapter 2.

The model runs were carried out without bed friction or turbulent viscosity in order to produce the greatest feasible inundation.

3.3.2 Model bathymetry

The profile of the bed from the input boundary to the shoreline (a distance of 10km) was taken from Admiralty Chart 121 of Flamborough Head to Withernsea. The resulting profile of the bed and beach is shown in Figure 3.4. The beach (above the initial still water level) is taken as a continuation of the bed slope (1:60). As a change in profile was of interest, the model was also set up with a very shallow beach slope of 1:200, from the initial mean sea level.

3.3.3 Model mesh

The model mesh includes the 10km of travel from point 2 to the coast and 1000m of beach area. The model was set up as a strip of width 500m with the intention to make a one dimensional profile model.

The mesh size varied from 100m to 10m in the region of the lower beach close to the still water location. For a water depth of the order of 10m offshore the wavelength of a tsunami wave of 1000s period is about 10km. This means that the model has in the outer part about 100 cells per wavelength and accurate solutions are expected.

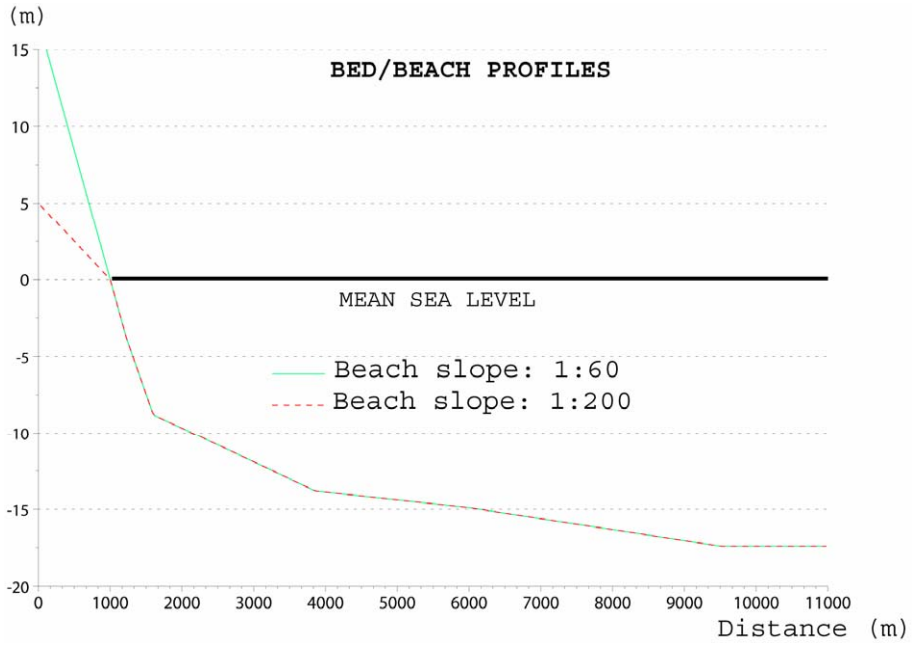

Figure 3.4 Bed profile between Flamborough Head and Withernsea

3.3.4 Boundary conditions

The model covers a distance from the wave-generating boundary to the beach of about the tsunami wavelength and therefore it was recognised that the results from the POL N10 model would be very soon affected by wave reflections off the beach. For this reason approximations to the incident and reflected wave were computed from the free surface elevations and depth average current data supplied. The result is shown in Figure 3.4, which depicts the free surface, elevation supplied by the POL N10 model and the separated incident and reflected waves. Clearly the initial wave is incident only but the next wave is affected by the wave interaction which has a larger reflected component than incident wave.

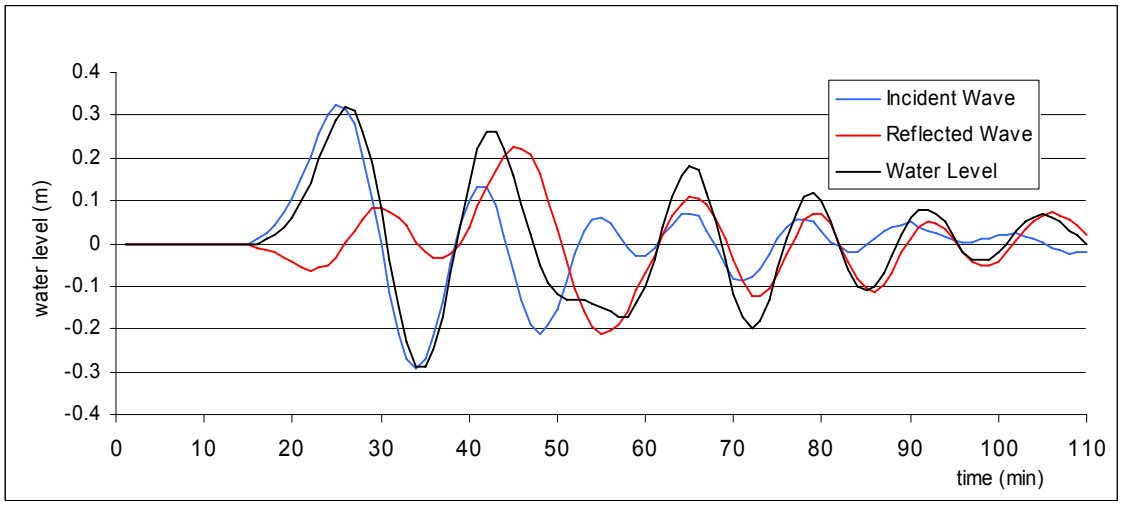

Figure 3.5 Free surface elevation of North Sea event (incident and reflected waves)

3.4 Model results

The TELEMAC model simulations were run using the POL N10 data, with the resulting maximum free surface elevation and wave run-up computed as shown in Figure 3.5. The water level at several times (100s increments from 800s) is shown as well as the maximum elevation over a period of one hour. It can be seen that the offshore wave has an initial elevation of approximately 0.32m. There is very little increase in the maximum free surface level until it reaches a depth of 3.5m, about 3000m from the shoreline. The wave then grows and inundates the beach to a maximum elevation about 0.76m, which is about 2.4 times the height of the incoming wave. This means that the wave would have inundated about 46m of the beach. Although 46m is not an insignificant distance, the event does not appreciably inundate the coast with a 1:60 beach slope.

The test was repeated using the finite element form of the TELEMAC flow model and results shown in Figure 3.6. This test run was undertaken because the Lisbon-type event modelled in Section 2 used the finite element solver within TELEMAC-2D. The use of a finite-element solver, when discontinuities in the solution may occur, is not normally implemented due to the potential for spurious numerical oscillations occurring within the solution. Some small oscillations were noted in the resulting simulation, although the results are similar to those obtained for the finite volume method presented previously (Figure 3.5). The finite element method does well in this case as the wave height is small and there is no formation of a bore or “wall of water” on the beach.

The inshore beach slope was now changed from the 1:60 to 1:200 and the simulation re-run using the finite volume method. The maximum elevation was of the order of 0.85m, this time inundating inshore a distance of about 170m of beach, see Figure 3.7. The run up level is about 2.7 times the size of the incident wave approaching the beach.

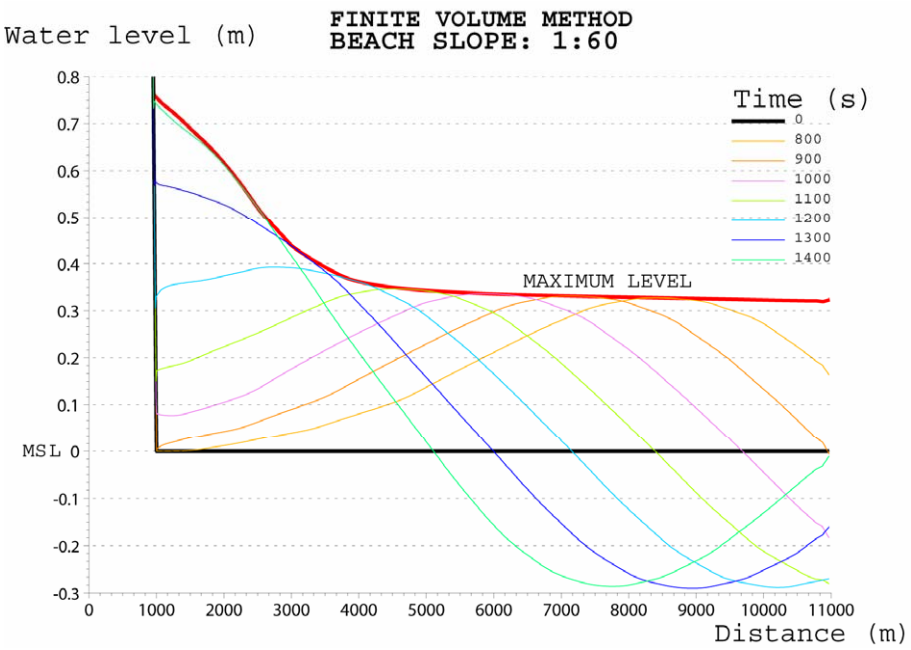

Figure 3.6 **Wave inundation of the 1:60 beach slope (finite volume method)**

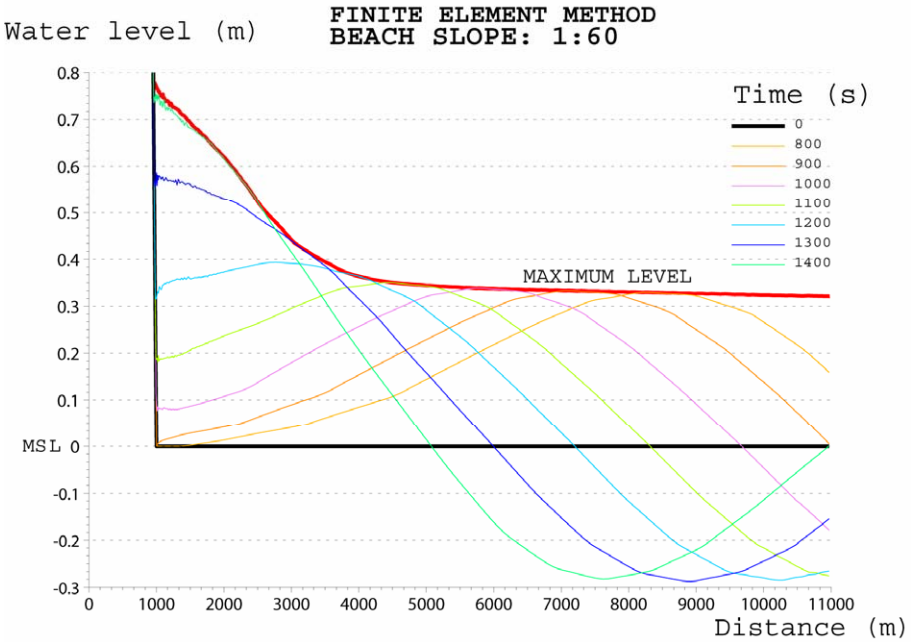

Figure 3.7 **Wave inundation of the 1:60 beach slope (finite element method)**

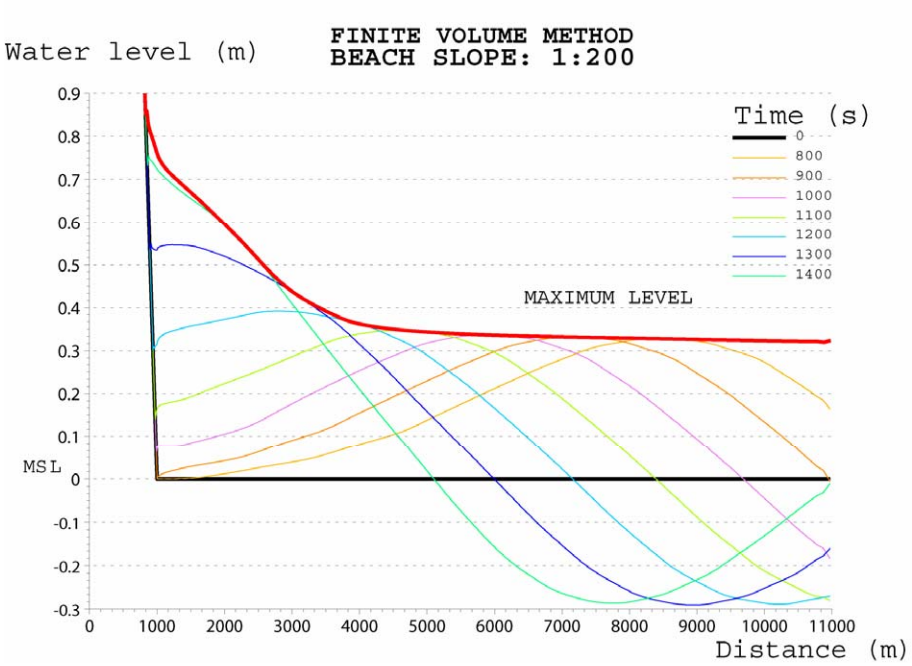

Figure 3.8 Wave inundation of the 1:200 beach (finite volume method)

The results obtained for these inundation simulations, for relatively flat beach slopes, produced similar run-up levels in the region of 2.5 – 3.0 times the incoming wave elevation.

4 Assessment of Hazard

To assess the hazard of a tsunami at the coast line, the maximum free surface elevation predicted using the described numerical models was compared against the extreme sea levels presented in Dixon and Tawn (1997) “Estimates of extreme sea conditions – Final Report: Spatial Analysis for the UK Coast”.

4.1 Water elevation at coast

Results presented in Section 2.3 indicate that the most exposed coasts around the UK and Ireland for a Lisbon type event are the Cornish coast and Southern Ireland. The study undertaken by Dixon and Tawn covered only the coastlines of England, Scotland and Wales. Therefore extreme sea levels for Ireland are not available from this report. Estimates of the 1:50 year extreme sea levels for Southern Ireland have been derived from Admiralty Tide Tables and 1:50 year surge elevations predicted by numerical modelling (Flather *et al*, 1998)

The most severe scenario, of those modelled, was from source B2. This source was for an 8.7 M_W tsunami positioned north of the Gorringe Bank with the fault lying virtually east west. Maximum water surface elevations east of Lizard Point reached in excess of 4m above still water level. The maximum water surface elevation, above still water level, around the Cornish coast, the Bristol Channel and Southern Ireland are shown in Figures 4.1 and 4.3, respectively.

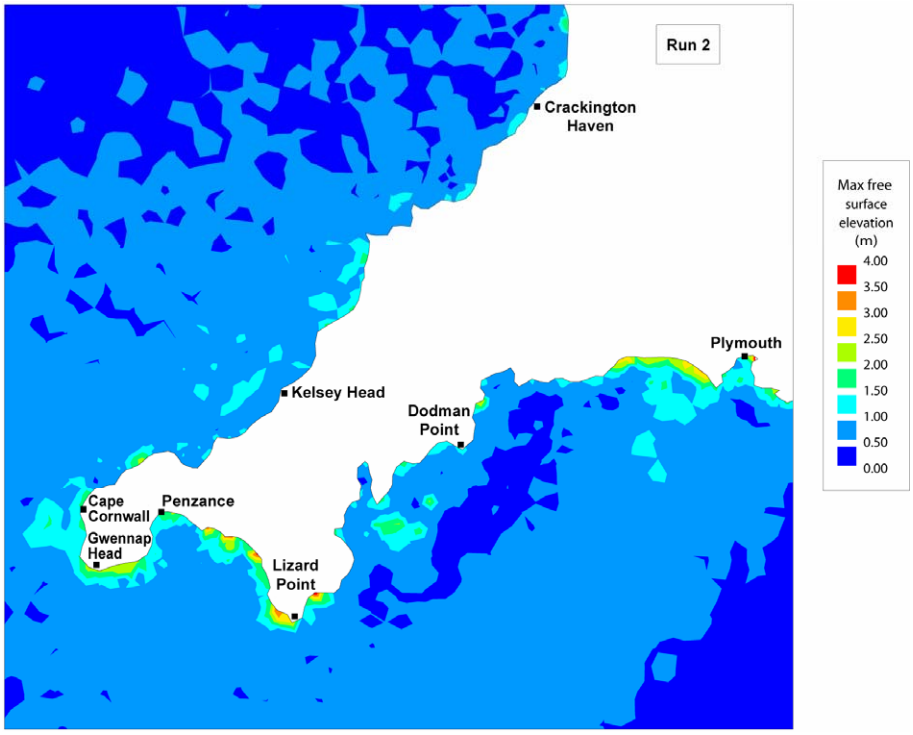

Figure 4.1 Maximum water elevation around the Cornish coast above still water level (Tsunami source B2)

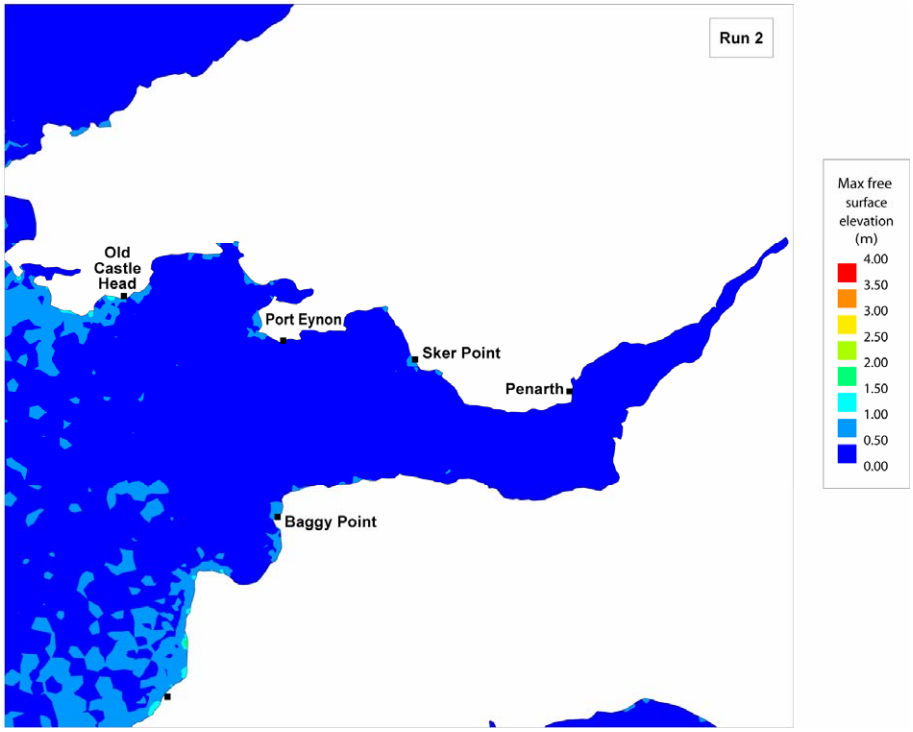

Figure 4.2 Maximum water elevation around the Bristol Channel above still water level (Tsunami source B2)

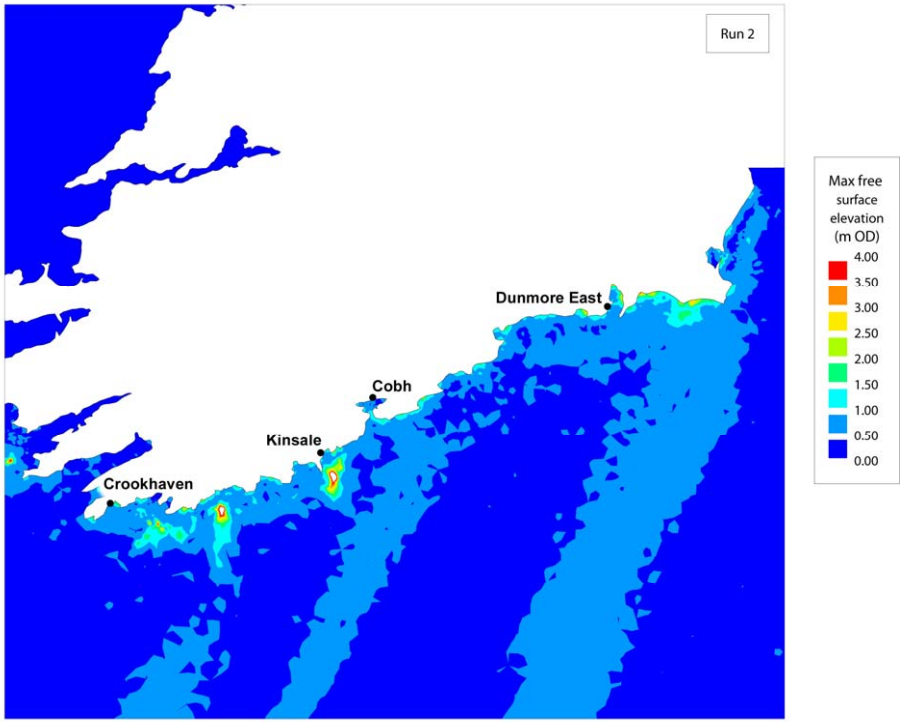

Figure 4.3 Maximum water elevation along the Southern Irish coast above still water level (Tsunami source B2)

These maximum elevations (some locations given by a range of values) assumed firstly to occur at mean high water springs (MHWS) and secondly to occur at mean height water neaps (MHWN). These values are compared to the 1:50 and 1:100 year extreme sea levels (Dixon and Tawn, 1997) for the Cornish coast and the

Bristol Channel and the estimated 1:50 year extreme sea levels along the southern Irish coast in Tables 4.1 to 4.3, respectively.

Table 4.1 Comparison of computed tsunami maximum elevations and extreme sea levels around the Cornish coast

Location	Tide levels plus tsunami wave elevation (mODN)		Extreme sea levels (mODN) (Dixon and Tawn, 1997)	
	MHWS	MHWN	1:50 year	1:100 year
Crackington Haven	4.3	2.6	5.1	5.2
Kesley Head	4.1 to 4.8	2.4 to 3.1	4.5	4.6
Cape Cornwall	4.2 to 4.8	2.5 to 3.1	3.6	3.7
Gwennap Head	5.0 to 5.4	3.7 to 4.1	3.9	4.0
Lizard Point	5.0	3.9	3.5	3.6
Dodman Point	3.4 to 3.8	2.3 to 2.7	3.4	3.6

Table 4.2 Comparison of computed tsunami maximum elevations and extreme sea levels around the Bristol Channel

Location	Tide levels plus tsunami wave elevation (mODN)		Extreme sea levels (mODN) (Dixon and Tawn, 1997)	
	MHWS	MHWN	1:50 year	1:100 year
Old Castle Head	4.6 to 5.2	2.5 to 3.1	5.1	5.2
Port Eynon	5.0 to 5.2	2.6 to 2.8	5.4	5.5
Sker Point	5.2 to 5.3	2.8 to 2.9	6.8	7.0
Penarth	6.0 to 6.1	3.0 to 3.1	7.9	8.1
Baggy Point	5.0 to 5.2	2.7 to 2.9	6.0	6.2

Table 4.3 Comparison of computed tsunami maximum elevations and extreme sea levels along the Southern Irish coast

Location	Tide levels plus tsunami wave elevation (mODD)		Estimated extreme sea levels (mODD)
	MHWS	MHWN	1:50 year
Crookhaven	4.6	3.9	3.8
Kinsale	5.7	5.0	4.9
Cobh	5.2	4.3	5.2
Dunmore East	6.3	5.3	5.3

NB These estimates of extreme sea levels combine estimated HAT levels at the locations specified and the 50 year surge elevations predicted by Flather *et al* (1998)

Extreme sea levels around the Cornish coast range from 3.4m – 5.2m, Table 4.1. The maximum tsunami wave elevation computed in this study, at MHWS, exceeds the 1:100 year extreme sea level at the Cornish peninsula (Cape Cornwall, Gwennap Head, Lizard Point). Further along the northern Cornish coast, Crackington Haven, the tsunami elevation at MHWS is approximately 1m lower that the extreme sea levels predictions.

Under the MHWN tidal conditions the tsunami elevation is in the vicinity of the predicted 1:100 year extreme sea levels or lower.

In the Bristol channel, even at MHWS, the tsunami wave elevation is less than the predicted 1:100 year extreme sea level predictions.

For the southern Irish coast, the maximum tsunami wave elevation exceeded the 1:50 year estimated extreme sea level at MHWS. Under the MHWN tidal condition, the tsunami wave elevations were approximately equal to the estimated 1:50 year extreme sea level elevations, except at Cobh, were the tsunami wave elevations were 1m less than than the 1:50 year extreme.

It should be noted that the mean high water springs tidal level is obtained or exceeded on approximately 26 occurrences per year (twice a month), for possible up to 3 hours at a time. These high tidal levels are obtained approximately 1% of the time per year (this value may actually be exceeded nearer 2% of the year if we include surges on low atmospheric tides). In addition to the low probability of a tsunamigenic event creating significant waves at the UK coast, the probability of the tsunami reaching the coast at MHWS is extremely low. A more appropriate tidal level, to review the effect of the tsunami at the coast, would be mean high water neaps. This tidal level is exceeded approximately 25% of the time per year.

Reviewing the impact of the largest simulated tsunami wave in this study at MHWN, indicates that only the most south-westerly coast of the UK may incur sea level elevation marginally in excess of the 1:100 year extreme sea level predictions.

It should be noted that the extreme sea levels of Dixon and Tawn are anticipated to cover up to approximately three tide cycles each rising from a minimum to maximum water level over a period of 11 hours. Under the tsunami inundation, the wave period is assumed to be approximately 20 minutes, significantly shorter than the tidal cycle. This shorter event time, for a tsunami, could possible lead to areas of significant scour around the coast, caused by the high flow velocities induced by a tsunami as it propagates inshore and then retreats.

4.2 Water elevation and flow velocities on beaches

In section 4.1, water elevations around the coastline for a 50 and 100 year extreme sea level were reviewed and compared to the maximum water surface elevations computed for our Lisbon type tsunami. It is not just the water elevation around the coastline that is important though; the flow velocities are also of consequence. The profile modelling for the North Sea event provided predictions of the flow velocities up a 1:60 beach slope. These, in combination with the water depths, are now investigated.

Recently, a flooding risk to people project (FD2321) was completed for Defra (Wade, 2006). One of the outcomes of this report was a simple formula

$d * (v + 0.5)$

where d = water depth (m) and v = flow velocity (m/s), which could be used to identify the degree of hazard associated with steady-state flows. The degree of hazard, associated with the numerical value from the equation above, is defined in Figure 4.4.

d x (v + 0.5)	Degree of Flood Hazard	Description
<0.75	Low	Caution *"Flood zone with shallow flowing water or deep standing water"*
0.75 - 1.25	Moderate	Dangerous for some (i.e. children) *"Danger: Flood zone with deep or fast flowing water"*
1.25 - 2.5	Significant	Dangerous for most people *"Danger: flood zone with deep fast flowing water"*
>2.5	Extreme	Dangerous for all *"Extreme danger: flood zone with deep fast flowing water"*

Figure 4.4 Hazard associated with combinations of flow depth and velocity

This simple approach was used to assess the degree of hazard for an individual standing on the shoreline for the simulated North Sea event. Water depth against flow velocity for the run-up and run-down of the initial tsunami wave, at the shoreline, is plotted in Figure 4.5 for the inundation of a 1:60 beach slope. The colour code, taken from Figure 4.4, is used to identify the hazard associated with the flow conditions.

It can clearly be seen that the hazard associated with the tsunami inundation of a 1:60 beach slope for the North Sea event, is classified as low.

The Lisbon-type event, covered in Chapter 2, indicated significantly larger tsunami wave elevations at the coast than the 0.3m elevation of the North Sea event. The hazard levels associated with tsunami inundation on a typical 1:60 sloping beach around the Cornish coast and south coast Ireland for a 1m and 2m wave elevation are presented in Figures 4.6 and 4.7, respectively.

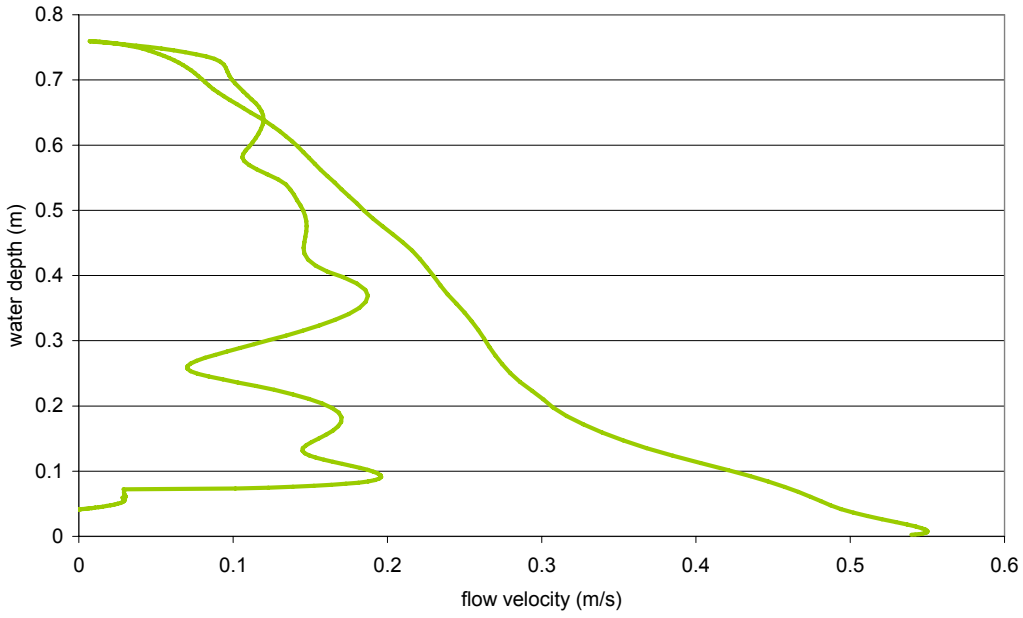

Figure 4.5 **Hazard associated with the North Sea event (1:60 beach slope, tsunami wave elevation = 0.3m). Colour scale from Figure 4.4.**

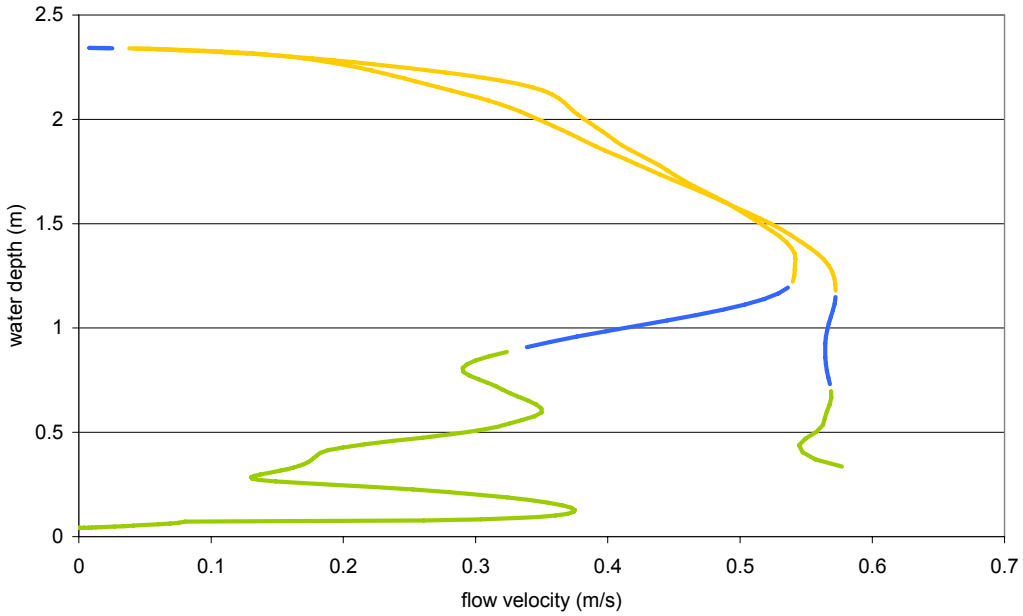

Figure 4.6 **Hazard associated with the Lisbon-type event (1:60 beach slope, tsunami wave elevation = 1.0m). Colour scale from Figure 4.4**

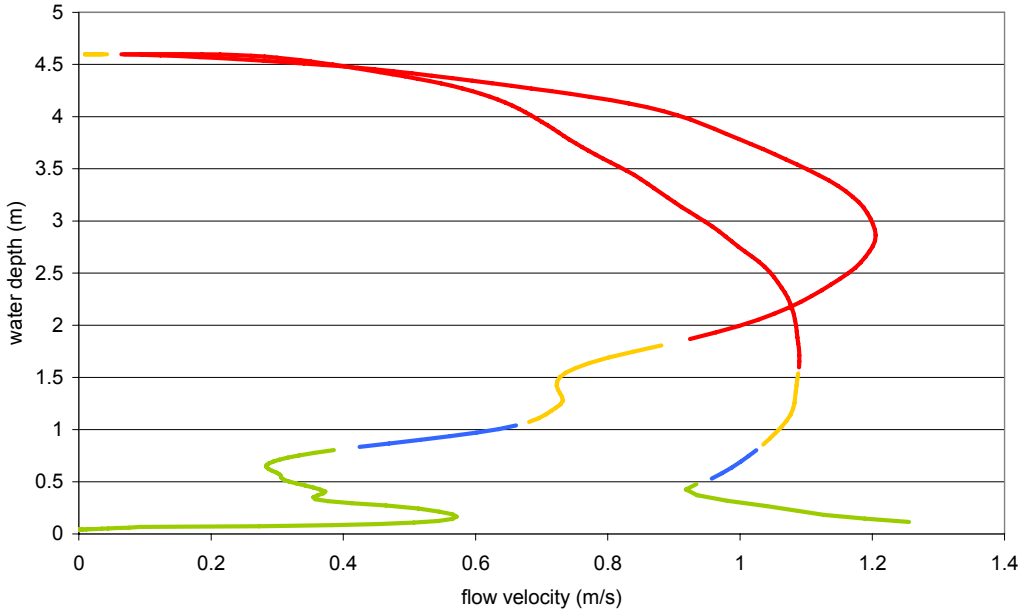

Figure 4.7 **Hazard associated with the Lisbon-type event (1:60 beach slope, tsunami wave elevation = 2.0m)**

These larger wave heights clearly infer greater hazard to individuals, specifically once the water depth is greater than 1m, for whatever the associated flow velocity. This indicates that should such a tsunami hit the Cornish coast or Southern Ireland, then all individuals would be in extreme danger regarding the hazard associated with the incoming wave.

4.3 Arrival times to the UK coastline

Arrival times of the tsunami at the coast, from the respective source origins could also play an important role. The original study (Kerridge, 2005) reviewed the possibility of a warning system for the UK. It was decided that events which would require warnings to be used for the UK would be extremely rare.

This study has reviewed two potential origins for tsunami sources generation. In the North Sea, a tsunamigenic event would create a relatively small amplitude wave which could impact upon the coastline within 30 minutes. There would probably be insufficient time from detection of the seismic event to impact on the coast to issue a warning, should such system be in place, although the hazard associated with such an event would be low.

For a Lisbon-type event, the travel time of the resulting wave from source to the Cornish coast is expected to be approximately four and a half hours. The source parameters modelled, indicate that waves reach the continental shelf after approximately two hours. Due to the significantly reduced water depth over the continental shelf, the wave speed decreases and takes a further two and a half hours to reach Cornwall and southern Ireland. The tsunami reaches the Welsh coast, six hours after the original seismic event. If a potential Lisbon-type event occurred, of tsunamigenic magnitude and for a potentially dangerous orientation, there should be sufficient time to disseminate information to the public, assuming an appropriate mechanism.

5 Conclusions

A review of the available data and proposed models for the 1755 Lisbon earthquake has shown that the problem of determining the earthquake location, source mechanism and rupture dimensions is poorly constrained. As a result, a large number of models have been proposed that partially fit the available macroseismic and tsunami observations. The tsunamigenic earthquake of 1969 (Fukao, 1973) highlights this problem. Gjevik *et al*. (1997) find that even for this, relatively well-recorded event, the problem of determining the source parameters from tsunami observations is non-unique. A number of the proposed models are controversial, including subduction along the western Iberian margin (Gutscher, 2004), or unrealistically complex, involving composite slip on unrelated fault systems (Vilanova, 2003).

Given this, we have proposed three simple source models that can be used to study the impact on the United Kingdom of a tsunamigenic earthquake of a similar size, and in a similar region to the 1755 source. Model A is an earthquake southeast of the Gorringe Bank, with the same epicentre and mechanism as the 1969 earthquake. Model B is an earthquake north of the Gorringe Bank, similar to that proposed by Johnston (1996). Models A and B are in good agreement with the compressional tectonics of the eastern Azores-Gibraltar fault zone and correspond to significant tectonic features where there is known earthquake activity. Both these models provide a reasonable fit to the macroseismic intensity observations, but the modelled tsunamis generated by these events do not fully fit the sparse available observations of the 1755 tsunami (Baptista *et al*., 1998b).

Model C is similar to a model proposed by Baptista *et al*. (1998b) and involves an earthquake offshore / southwest of Lisbon, closer to the Iberian shore than Models A and B, on a fault that strikes at N340E and dips at 45˚. Baptista *et al* (1998b) find that this model provides a better match to the observed tsunami arrival times on the Iberian Peninsula, than models A and B. However, this model is not clearly associated with any well-defined tectonic structure or strong earthquake activity. Model C allows us to examine the effect of source orientation on tsunami waves reaching the UK and Irish coasts.

We calculate fault dimensions and slip using an upper and lower limit for the earthquake magnitude of 8.3 and 8.7 M_W, respectively, by applying a scaling relationship for intraplate earthquakes. The choice of an intraplate scaling relationship strongly affects the source dimensions and slip, allowing us to find smaller fault lengths but larger slips. This is in keeping with our tectonic understanding of the source region. A magnitude of 8.3 M_W gives a source length of 105km and slip of 6.8m and a magnitude 8.7 M_W gives a source length of 210km and slip of 13.6m. Applying this to the three different sources gives us six models that can be used to examine the likely tsunami impact on the UK and Irish coasts. Surface deformations calculated for all models show significant areas of uplift and subsidence that are likely to generate tsunami. Magnitudes of 8.3 and 8.7 M_W give maximum vertical uplifts of approximately 3m and 7 - 8m, respectively.

These vertical displacements of the water surface were input into the POL CS3 extended 12km model, which resolves the non-linear shallow water equations, as initial conditions. The propagation of the resulting waves, created by these initial surface displacements, was then modelled up to the UK continental shelf break.

The results from the CS3 model indicated that the 8.3 M_W earthquakes produced maximum surface elevations, of the waves at the shelf break, in the region of 0.1m. For the larger magnitude (8.7 M_W) disturbances the maximum elevation at the shelf break was in the region of 0.5m. The orientation of the fault is also significant in the elevation of the resulting tsunami waves as they propagate towards the UK and Irish coasts.

Wave data from the POL CS3 model was extracted and used as boundary conditions for the TELEMAC modelling of wave propagation to the coastline. Wave transformation up the continental shelf, refraction and diffraction across the shelf and at the coastline, together with localised shoaling, increased the sea elevations at the Cornish coast to generally 2m above the still water level. In certain, localised regions, the sea level at the coast increased by 4m.

The effect of the tide appeared to have little impact on the initial tsunami wave propagation from source in the CS3 model. Additional TELEMAC runs were performed to review the water elevation at the coastline, for both a low and high tide condition at Cornwall. The effect on the maximum wave elevation around the coast was minimal, although locations of maxima elevation shifted around the Cornish peninsula.

For the North Sea event, wave run-up and inundation, of two relatively flat beach slopes, were reviewed. The source origin in the North Sea produced a significantly smaller wave amplitudes, although similar wave period to the Lisbon event. Results indicated that run-up levels were approximately 2.5 (for a 1:60 beach slope) - 3.0 (for the 1:200 beach slope) times the offshore wave amplitude.

Following the model simulations for the Lisbon-type and North Sea events, an assessment of hazard was undertaken. Water elevation for the Lisbon-type tsunami wave elevation occurring initially at mean high water springs and then at mean high water neaps, was compared against extreme sea levels predicted by Dixon and Tawn. It is argued that it is more appropriate to compare the tsunami elevation at mean high water neaps with the 50 year and 100 year extreme sea levels. Consequently only the most south-westerly coast of the UK may incur sea level elevation marginally in excess of the 1:100 year extreme sea level predictions. Along the Southern Irish coast, tsunami sea level elevations are approximately equal to (or less than) the estimated 1:50 year extreme sea level predictions.

Another assessment of hazard, is to review the water depth and associated flow velocities of the tsunami wave, at the still water level, as it runs up and down the beach. These values were placed into a simple formula to assess the degree of hazard. The outcome of this analysis indicated that the hazard level for the North Sea event, with an offshore wave height of approximately 0.3m, was “low”. The same approach was applied to tsunami waves of 1m and 2m which may reach the Cornish coast and Southern Ireland for the Lisbon-type event. For these larger waves, the hazard levels reached “significant” and “extreme”, which indicated that the flow inundation on the beach would be dangerous for most individuals.

Finally, the travel time of the simulated tsunami events, from origin of source to the UK coast were reviewed. If a tsunamigenic event was to occur in the North Sea, then there would probably be insufficient time (< 0.5 hours) to warn the general public. That said the hazard level for such an event has previously been defined as

low. For a Lisbon-type event, the travel times to the UK should be sufficient to allow warning of the general public of the approaching danger. The time between the seismic event and waves reaching the UK coast would be approximately four and a half hours. This assumes a suitable mechanism is in place to detect the tsunami at the time it is generated, relaying this to the UK and disseminating the information to the public.

The main conclusions of the study are presented below:

- Three potential models for the 1755 Lisbon event have been proposed.
- The most exposed areas of the UK and Ireland, for a Lisbon-type event, are the Cornish coast and southern Ireland.
- Simulated wave elevations on the Cornish and southern Irish coasts are typically in the range of 1-2m, with localised amplification enhancing the elevations to approximately 4m.
- Effects of the tide have been studied on the initial propagation and inundation of the tsunami wave, no significant effect on the wave elevation has been noted.
- Result of the North Sea inundation study show that the effect of relatively flat beach slopes has little effect on the wave run-up level, which is approximately 2.5-3.0 times the offshore wave height.
- Assessment of hazard results indicate that only the most south-westerly coast of the UK may incur sea level elevation marginally in excess of the 1:100 year extreme sea level predictions.
- The hazard level for the beach inundation of the North Sea event could be classified as “low”. For an 8.7 M_W Lisbon-type event the hazard level could be “extreme”, dangerous for all, over much of the Cornish coast and southern Ireland.
- If a Lisbon event, large enough to be tsunamigenic, occurred then the travel time for the wave to the UK coast should be sufficient to warn the general public, assuming a mechanism is in place.

References

Abe, K., 1979. Size of great earthquakes of 1837-1974 inferred from tsunami data*, Journal of Geophysical Research*, Vol. 84, 1561-1568.

Abercrombie, R.E., and Ekstrom, G., 2001. Earthquake slip on oceanic transform faults, *Nature*, Vol. 410, 74-77.

Argus, D. F., Gordon, R. G., DeMets, C., and Stein, S., 1989. Closure of the Africa-Eurasia-North America plate motion circuit and tectonics of the Gloria Fault, *Journal of Geophysical Research*, Vol. 94 (B5), 5585-5602.

Baptista, M. A., Heitor, S., Miranda, J. M., Miranda, P., and Mendes Victor, L., 1998a. The 1755 Lisbon tsunami; evaluation of the tsunami parameters*, Journal of Geodynamics*, Vol. 25, 143-157.

Baptista, M. A., Miranda, P. M. A., Miranda, J. M., and Mendes Victor, L., 1998b. Constrains on the source of the 1755 Lisbon tsunami from numerical modelling of historical data on the source of the 1755 Lisbon tsunami, *Journal of Geodynamics*, Vol. 25, 159-174.

Baptista, M. A., Miranda, J. M., and Gutscher, M. A., 2002. A subduction source for the great Lisbon earthquake and tsunami of 1755? *AGU Fall Meeting*, 2002, abstract #S11B-1139.

Baptista, M. A., Miranda, J. M., Chierici, F., and Zitellini, N., 2003. New study of the 1755 earthquake source based on multi-channel seismic survey data and tsunami modelling, *Natural Hazards and Earth System Sciences*, Vol. 3, 333-340.

Baptista, M A, and Miranda, J M. 2005. Evaluation of the 1755 earthquake source using tsunami modelling. *Proceedings of the International Conference of the 250th Anniversary of the 1755 Lisbon Earthquake*, Lisbon, 574-577.

Bergeron, A., and Bonnin, J., 1991. The deep structure of Gorringe Bank (NE Atlantic) and its surrounding area, *Geophysical Journal International*, Vol. 105, 491-502.

Borges, J. F., Fitas, A. J. S., Bezzeghoud, M., and Teves-Costa, P., 2001. Seismotectonics of Portugal and its adjacent Atlantic area, *Tectonophysics*, Vol. 337, 373-387.

Borlase, W., 1755. Letter to the Rev. Charles Lytteton, *Philosophical Transactions of the Royal Society of London,* Vol. 49, 373-378.

Borlase, W., 1758. Observations on the Islands of Scilly. Frank Graham, Newcastle upon Tyne.

Buforn, E., Udías, A., and Colombás, M. A., 1988. Seismicity, source mechanisms and tectonics of the Azores-Gibraltar plate boundary, *Tectonophysics*, Vol. 152, 89-118.

Buforn, E., Bezzeghoud, M., Udias, A., and Pro, C., 2004. Seismic sources on the Iberia-African plate boundary and their tectonic implications, *Pure and Applied Geophysics,* Vol. 161, 623-646.

Bundgaard H.I., Warren I.R and Barnett A., 1991. Modeling of tsunami generation and run-up. *Science of Tsunami Hazards*, 9, 23-30.

Cabral, J, Ribeiro, P, Figueiredo, P, Martins, A, Pimentel, N, Moniz, C, Carvalho, J, Carrilho, F, Dias, R, Matias, L M, Terrinha, P, Torres, L, and Senos, L. 2005. Active tectonic structures in the Lower Tagus Valley: State of the art, Unpublished.

Carvalho, A, Campos Costa, A, and Sousa Olivera, C. 2004. A stochastic finite-fault modelling for the 1755 Lisbon earthquake. *Proceedings of the 13th Word Conference of earthquake Engineering*, Vancouver, 2194.

Carvalho, A, Campos Costa, A, and Sousa Olivera, C. 2005. A finite-fault modelling of the 1755 Lisbon earthquake sources. *Proceedings of the International Conference of the 250th Anniversary of the 1755 Lisbon Earthquake*, Lisbon, 578-583.

Choi B.H., Pelinovsky E., Hong S.J. and Woo S.B., 2003. Computation of tsunamis in the East (Japan) Sea using dynamically interfaced nested models. *Pure and Applied Geophysics*, 160, 1383-1414.

Edmonds, R., 1869. An account of an extraordinary movement of the sea in Cornwall, in July 1843, with notices of similar movements in previous years, and also of earthquakes which have occurred in Cornwall, *Report of the British Association of the Advancement of Science,* Vol. 38, 112-121.

Flather, R., Smith, J., Richards, J., Bell, C. and Blackman, D., 1998. Direct estimates of extreme storm surge elevations from a 40-year numerical model simulation and from observations, *The Global Atmosphere and Ocean System,* Vol. 6, pp 165-176.

Flather, 2000. Existing operational oceanography. *Coastal Engineering*, 41, 13-40.

Fonseca, J. F. B. D., 2005. The source of the Lisbon earthquake, reply to What caused the great Lisbon earthquake?, Gutscher, M. A., 2004. *Science* (letters), Vol. 308, 50.

Frankel, A. 1994. Implications of felt area-magnitude relations for earthquake scaling and the average frequency of perceptible ground motion. *Bulletin of the Seismological Society of America*, Vol. 84, 462-465.

Fukao, Y., 1973. Thrust faulting at a lithospheric plate boundary: the Portugal earthquake of 1969*, Earth and Planetary Science Letters*, Vol. 18, 205-2016.

Gjevik, B., Pedersen, G., Dybesland, E., Harbitz, C. B., Miranda, P. M. A., Baptista, M. A., Mendes-Victor, L., Heinrich, P., Roche, R., and Guesmia, M., 1997. Modeling tsunamis from earthquake sources near Gorringe Bank southwest of Portugal, *Journal of Geophysical Research*, Vol. C102, 27931-27949.

Gràcia, E., Dañobeita, J., Vergés, J., and the PARSIFAL team, 2003. Mapping active faults offshore Portugal (36ºN-38ºN): implications for seismic hazard assessment along the southwest Iberia margin, *Geology*, Vol. 31, 83-86.

Gutscher, M. A., 2004. What caused the great Lisbon earthquake? *Science*, Vol. 305, 1247-1248.

Gutscher, M. A., Malod, J., Rehault, J.-P., Contrucci, I., Klingelhoefer, F., Mendes-Victor, L., and Spakman, W., 2002. Evidence for active subduction beneath Gibraltar, *Geology*, Vol. 30, 1071-1074.

Hayir, A., 2004. Ocean depth effects on tsunami amplitudes used in source models in linearized shallow-water wave theory. *Ocean Engineering*, 31, 353-361.

Hayward, N., Watts, A. B., Westbrook, G. K., and Collier, J. S., 1999. A seismic reflection and GLORIA study of compressional deformation in the Gorringe Bank region, eastern North Atlantic, Geophysical Journal International, Vol. 138, 831-850.

Heinrich, P., Baptista, M. A., and Miranda, P., 1994. Numerical simulation of the 1969 tsunami along the Portuguese coasts. Preliminary results, *Science of Tsunami Hazards*, Vol. 12, 3-23.

Henni, P. H. O., Fyfe, C. J., and Marrow, P.C., 1998. The BGS World Seismicity Database, *British Geological Survey Technical Report*, WL/98/13.

Jiménez-Munt, I., Fernàndez, M., Torne, M., and Bird, P., 2001. The transition from linear to diffuse plate boundary in the Azores-Gibraltar region: results from a thin-sheet model, *Earth and Planetary Science Letters*, Vol. 192, 175-189.

Johnston, A. C., 1996. Seismic moment assessment of earthquakes in stable continental regions – III. New Madrid 1811-1812, Charleston 1886 and Lisbon 1755, *Geophysical Journal International*, Vol. 126, 314-344.

Kerridge, D., 2005. *The threat posed by tsunami to the UK*. Study commissioned by Defra Flood Management and produced by British Geological Survey, Proudman Oceanographic Laboratory, Met Office and HR Wallingford. 167pp.

Kowalik Z., 2001. Basic relations between tsunami calculations and their physics. *Science of Tsunami Hazards*, 19, 99-115.

Levret, A., 1991. The effects of the November 1, 1755 “Lisbon” earthquake in Morocco, *Tectonophysics*, Vol. 193, 83-94.

López Casado, C., Sanz de Galdeano, C., Molina Palacios, S., and Henares Romero, J., 2001. The structure of the Alboran Sea: an interpretation from seismological and geological data, *Tectonophysics*, Vol. 338, 79-95.

Machado, F., 1966. Contribuição para o estudo do terramoto de 1 de Novembro de *1755. Revista da Faculdade de Ciências de Lisboa* , (2C), Vol. 14, 19-31

Mader, C. L., 2001. Modeling the 1755 Lisbon tsunami, *Science of Tsunami Hazards*, Vol. 19, 93-98.

Maldonado, A., Somoza, L., and Pallarés, L., 1999. The Betic orogen and the Iberian-African boundary in the Gulf of Cadiz: geological evolution (central North America), *Marine Geology*, Vol. 155, 9-43.

Marchuk A.G., Chubarov, L.B. and Shokin, L.L., 1983. *Numerical Modelling of Tsunami Waves*, Nauka Press, Novosibirsk. 282pp.

Matias, L M, Ribeiro, A, Zitellini, N, Miranda, J M, Baptista, M A, Teves Costa, P, Terrinha, P, Cabral, J, and Fernandes, R M. 2005. The Tagus Valley seismic hazard and the 1755 earthquake: A critical review. *Proceedings of the International Conference of the 250th Anniversary of the 1755 Lisbon Earthquake*, Lisbon, 584-591.

Matias, L M, Ribeiro, A, Baptista, M A, Zitellini, N, Cabral, J, Terrinha, P, Teves Costa, P, and Miranda, J M. 2005. Comment on: Lisbon 1755: A case of triggered onshore rupture? by Vilanova, S.P., Nunes, C.F. and Fonseca, J.F.B.D. *Bulletin of the Seismological Society of America*, In press.

Mendes, V. L., Baptista, M. A., Miranda, J. M., and Miranda, P. M. A., 1999. Can hydrodynamic modelling of tsunami contribute to seismic risk assessment? *Physics and Chemistry of the Earth (A)*, Vol. 24, 139-144.

Milne, D. 1841. Notices of earthquake-shocks felt in Great Britain, and especially in Scotland, with inferences suggested by these notices as to the causes of the shocks. *Edinburgh New Philosophical Journal*, Vol. 31, 259-309.

Moreira, V. S., 1989. Seismicity of the Portuguese continental margin, in *Earthquakes at North Atlantic Passive Margins: Neotectonics and Postglacial Rebound*, S. Gregersen and P. W. Basham (eds), Kluwer, Massachusetts, US.

Morel, J. L., and Meghraoui, M., 1996. Goringe-Alboran-Tell tectonic zone: a transpression system along the Africa-Eurasia plate boundary, *Geology*, Vol. 24, 755-758.

Okada, .Y.,1985. Surface deformation due to shear and tensile faults in a half-space, Bull. Seis. Soc. Am., Vol. 75, 4, 1135-1154.

Pagarete, J, and Ruegg, J. 2005. Simulated displacements for the 1755 Lisbon earthquake: Study of conformity with proposed source mechanisms, Unpublished.

Pinheiro, L. M., Whitmarsh, R. B., and Miles, P. R., 1992. The ocean-continent boundary off the western continental margin of Iberia – II. Crustal structure in the Tagus Abyssal Plain, *Geophysical Journal International*, Vol. 109, 106-124.

Platt, J., and Houseman, G., 2003. Evidence for active subduction beneath Gibraltar: COMMENT, *Geology*: online forum, e22.

Purdy, G. M., 1975. The eastern end of the Azores-Gibraltar plate boundary, *Geophysical Journal of the Royal Astronomical Society*, Vol. 43, 973-1000.

Rabinovich, A. B., Miranda, P., and Baptista, M. A., 1998. Analysis of the 1969 and 1975 tsunamis at the Atlantic coast of Portugal and Spain, *Oceanology*, Vol. 38, 513-520.

Reid, H. F., 1914. The Lisbon earthquake of November 1, 1755. *Bulletin of the Seismological Society of America*, Vol. 4, 53-80.

Sartori, R., Torelli, L., Zitellini, N., Peis, D., and Lodolo, E., 1994. Eastern segment of the Azores-Gibraltar line (central-eastern Atlantic): an oceanic plate boundary with diffuse compressional deformation, *Geology*, Vol. 22, 555-558.

Sborschikov, I. M., Shreyder, A. A., Rimskiy-Korsakov, N. A., and V. S. Yastrebov, 1988. The Gorringe Bank and the tectonics of the Azores-Gibraltar fracture zone, *Oceanology*, Vol. 28, 742-746.
Scholz, C. H., 1982. Scaling laws for large earthquakes: consequences for physical models, Bull. Seis. Soc. Am., Vol. 72, 1-14.

Scholz, C. H., Aviles, C. A. and Wesnousky, S. G., 1986. Scaling differences between large interplate and intraplate earthquake, Bull. Seis. Soc. Am., Vol. 76, 65-70.

Scholz, C. H., 2002. The mechanics of earthquake faulting, 2nd ed., Cambridge University Press, Cambridge, UK.

Stich, D., Mancilla, F. de L., and Morales, J., 2005. Crust-mantle coupling in the Gulf of Cadiz (SW-Iberia), *Geophysical Research Letters*, Vol. 32, L13306, doi: 10.1029/2005GL023098.

Terrinha, P., Pinheiro, L. M., Henriet, J.-P., Matias, L., Ivanov, M. K., Monteiro, J. H., Akhmetzhanov, A., Volkonskaya, A., Cunha, T., Shaskin, P. and Rovere, M., 2003. Tsunamigenic-seismogenic structures, neotectonics, sedimentary processes and slope instability on the southwest Portuguese margin, *Marine Geology*, Vol. 195, 55-73.

Tortella, D., Torne, M., and Pérez-Estaún, A., 1997. Geodynamic evolution of the eastern segment of the Azores-Gibraltar zone: the Gorringe Bank and the Gulf of Cadiz region, *Marine Geophysical Researches*, Vol. 19, 211-230.

Vilanova, S. P., Nunes, C. F., and Fonseca, J. F. B. D., 2003. Lisbon 1755: a case of triggered onshore rupture? *Bulletin of the Seismological Society of America*, Vol. 93, 2056-2068.

Wade, S., 2006. *Flood Risks to People.* Study commissioned by Defra and Environment Agency and produced by HR Wallingford, Middlesex University and Risk and Policy Analysts Ltd.

Walters R.A., 2002. From river to ocean: a unified modelling approach. In Spaulding, M.L. (Ed.) *Estuarine and Coastal Modelling*: Proceedings of the 7th International Conference, ASCE, New York, pp. 683-694.

Walters R.A., 2005. Coastal ocean models: two useful finite element methods. *Continental Shelf Research*, 25, 775-793.

Ward, S.N and Day, S.J., 2001. Cumbre Vieja volcano – potential collapse and tsunami at La Palma, Canary Islands. Geophysical Research Letter, 28: 3397-3400.

Zahibo N., Pelinovsky E., Yalciner A., Kurkin A., Koselkov A. and Zaitsev A., 2003. The 1867 Virgin Island tsunami: observations and modelling. *Oceanologica Acta*, 26, 609-621.

Zitellini, N. 2005. New approaches to the seismogenesis of the 1755 Lisbon earthquake, Unpublished.

Zitellini, N., Chierici, F., Sartori, R., and Torelli, L., 1999. The tectonic source of the 1755 earthquake and tsunami, *Annali di Geofisica*, Vol. 42, 49-55.

Zitellini, N., Mendes, L. A., Cordoba, D., Danobeitia, J., Nicolich, R., Pellis, G., Ribeiro, A., Sartori, R., Torelli, L., Bartolome, R., Bortoluzzi, G., Calafato, A., Carrilho, F., Casoni, L., Chierici, F., Corela, C., Correggiari, A., Della Vedova, B., Gracia, E., Jornet, P., Landuzzi, M., Ligi, M., Magagnoli, A., Marozzi, G., Matias, L., Penitenti, D., Rodriguez, P., Rovere, M., Terrinha, P., Vigliotti, L., and Zahinos Ruiz, A., 2001. Source of the 1755 Lisbon earthquake and tsunami investigated, *EOS, Transactions*, Vol. 82, 285, 290-291.

Appendices

Appendix A Tectonics of the Azores-Gibraltar fault zone

The tectonic evolution of the AGFZ and its surrounding area has been somewhat complex due to the interactions between three plates: Africa, Eurasia, and the Iberia microplate. The break-up of the super continent Pangaea in the Permo-Triassic initiated the formation and evolution of the South Iberia passive margin (a continental margin that is not also a plate margin), and the opening of the central and northern Atlantic Ocean in the Mesozoic (Tortella *et al.*, 1997).

Compared to the Mid Atlantic ridge (MAR), motion along the Africa-Eurasia plate boundary is poorly described by magnetic profiles, oceanic strike slip (transform) faults or focal mechanisms (Argus *et al.*, 1989). Geophysical studies of the point where the North America, Africa and Eurasia plates meet (the Azores triple junction) suggest that the spreading rate of the MAR south of the Azores is lower than that observed on the northern segment, which results in right-lateral transcurrent movement along the AGFZ at a slow rate of approximately 4 mm/yr (Argus *et al.*, 1989; Jiménez-Munt *et al.*, 2001). The current tectonic configuration of the AGFZ as shown in Figure 2. is unusual in that extension (directed approximately NNE-SSW), WNW-ESE oriented convergence and E-W strike-slip movement are all observed within a distance of about 3000 km (Buforn *et al.*, 1988; Argus *et al.*, 1989; Jiménez-Munt *et al.*, 2001).

The eastern segment of the AGFZ extends eastwards from the Madeira Tore rise to the Strait of Gibraltar (see Figure 2. and Figure 2.). Structurally, this segment is more complex than the western segments (Sborshchikov *et al.*, 1988; Sartori *et al.*, 1994; Tortella *et al.*, 1997). It is characterised by a series of ridges and seamounts (the Gorringe Bank, the Coral Patch and Ampere seamounts) shown in Figure 2.. These NE-SW and ENE-WSW trending basement highs are separated by significant depressions such as the Horseshoe and Tagus abyssal plains. The major structural features of this area are discussed individually below. Here, the plate boundary (shown as a dashed line in Figure 2.) has been obscured by geological structures formed during successive periods of convergence (Sborshchikov *et al.*, 1988; Sartori *et al.*, 1994; Morel and Meghraoui, 1996), and the character of the plate boundary here is not well understood. The diffuse distribution of seismicity suggests that there is a wide transpressional zone between the Gorringe Bank and the Tell Atlas mountains (Morel and Meghraoui, 1996). Sartori *et al.* (1994), Maldonado *et al.* (1996), Hayward *et al.* (1999) support similar models.

Seismicity on the eastern segment (Figure 2.) indicates active WNW-ESE oriented compressional deformation involving oceanic lithosphere, an extremely rare occurrence in either inter- or intraplate settings (Sartori *et al.*, 1994). Crustal shortening is accommodated on numerous thrust faults, which affect both the basement and sedimentary cover (Buforn *et al.*, 1988; Sartori *et al.*, 1994; Morel and Meghraoui, 1996; Tortella *et al.*, 1997). Consequently, earthquakes occur over a much broader region on this segment (~ 250 km) as shown in Figure 2.. The average spacing between these thrust faults is about 10-15 km and they appear to sole out on intra-crustal discontinuities or at the base of the crust (Sartori *et al.*, 1994). Focal mechanisms indicate right lateral and reverse faulting on roughly east - west oriented structures. The presence of both strike-slip and oblique

compression is consistent with transpressive regional tectonics (e.g. Buforn *et al.*, 1988; Morel and Meghraoui, 1996).

Gorringe Bank Region

The Gorringe Bank is a large, northeast trending, asymmetric, ridge-like uplifted block of oceanic lithosphere (crust and brittle uppermost mantle) approximately 180 km long and 60-70 km wide (Sborshchikov *et al.*, 1988; Sartori *et al.*, 1994). Bathymetric data (Figure 2.) show that the highest summit on the ridge (the Gettysburg seamount) rises to a depth of 25 m below sea level (Sborshchikov *et al.*, 1988; Borges *et al.*, 2001). The second highest summit is associated with the Ormonde seamount, and reaches a depth of 60 m (Sborshchikov *et al.*, 1988).

Between the two seamounts, an almost continuous section of oceanic crust and upper mantle is exposed (Bergeron and Bonnin, 1991). Generally, these types of rocks are only exposed in ophiolite complexes emplaced by subduction. Whether ocean-ocean subduction occurs, or has occurred, in this part of the AGFZ is debateable. Sartori *et al.* (1994) suggest that subduction cannot occur here because the two converging plates are similar in terms of age, density, rigidity and thickness, and because the overall rate of convergence is low (~ 4 mm/yr; Argus *et al.*, 1989). Under such circumstances, stresses are released from the whole lithosphere across wide sectors of the converging plates without a well-defined plate margin (Sartori *et al.*, 1994; Hayward *et al.*, 1999). This conclusion is supported by the results of deep multi-channel seismic profiling in the area (Tortella *et al.*, 1997).

Given the lack of evidence for subduction, it is perhaps more likely that the Gorringe Bank originated from uplift associated with plate convergence: Sartori *et al.* (1994) propose regional buckling and the reactivation of a former transform discontinuity as a mechanism for uplift. Fukao (1973) suggests that the Gorringe Bank originated as a block of crust bounded by two thrust faults cutting through the crust. Shortening (or extension) on either one of these faults would result in the uplift (or subsidence) of the block of crust. Hayward *et al.* (1999) estimate that a maximum of 50 km shortening has occurred at the Gorringe Bank through thickening, folding and thrusting since the mid Miocene.

The Gorringe Bank is also associated with an anomalously high free-air gravity anomaly (300 mgal), which indicates the presence of a thick, high-density body immediately beneath the surface (Sborshchikov *et al.*, 1988; Bergeron and Bonnin, 1991; Sartori *et al.*, 1994). The Moho configuration across the Gorringe Bank suggests that across its peak, the oceanic crust is either very thin or completely absent with non-reflective lithospheric mantle directly overlain by sediment (Sartori *et al.*, 1994).

Tagus Abyssal Plain

The Tagus abyssal plain (Figure 2..2) lies to the north of the Gorringe Bank. It is bounded by the continental margin of Portugal to the east and the Madeira Tore rise to the west. The Eurasia/Africa plate boundary may form its south - west and north - east margins (Pinheiro *et al.*, 1992). At its southern boundary, there is a large olistostrome (a chaotic sedimentary deposit formed by gravitational sliding) within the Miocene sedimentary sequence, which is thought to have discharged from the Gorringe Bank (Sartori *et al.*, 1994).

Purdy (1975) estimated crustal thickness in the Tagus abyssal plain to be around 8 km from seismic refraction experiments. A NNE trending refraction line in the northern sector of the plain indicates that the crust here is only 2-4 km thick and is underlain by a low-velocity upper mantle (Pinheiro *et al.*, 1992). Pinheiro *et al.* (1992) suggest that this is where the transition from oceanic to continental crust occurs (and circumstantial evidence suggests that the transition may lie at about 11.5ºW). A similar crustal structure is also seen close to the ocean-continent transition off the whole of western Iberia (Pinheiro *et al.*, 1992).

Sartori *et al.* (1994) did not find compressional structures on a seismic profile extending into the southeastern sector of the plain.

Horseshoe Abyssal Plain

The Horseshoe abyssal plain (HAP; Figure 2.) is an elongate feature bounded by the Ampere and Coral Patch seamounts to the south, the Gorringe Bank and Tagus abyssal plain to the north, the Madeira Tore rise to the west and the Iberian continental margin to the east. In the deep waters of the plain, the crust is around 15 km thick (Gonzalez *et al.*, 1996).

There is strong evidence for active compressional deformation in the HAP east of 12º W (Sartori *et al.*, 1994) although there is no evidence of major recent tectonic activity in the western sector (Purdy, 1975). In the eastern part of the plain, the oceanic basement is affected by large vertical offsets along both the north and south boundaries (Sartori *et al.*, 1994). Numerous low angle thrusts or reverse faults at kilometre spacing are found across the entire plain, which affect both the oceanic basement and sedimentary cover, and accommodate plate convergence. The amount of crustal shortening accommodated by individual faults is modest but geological evidence suggests that compressional tectonism has prevailed in this area for a long time and is still active. Sartori *et al.* (1994) argue that the overall pattern of deformation in the HAP is inconsistent with subduction in this area.

Gulf of Cadiz

The Gulf of Cadiz (Figure 2..2) lies in the continental domain of SW Iberia and appears to represent the continuation of the Guadalquivir basin onto the continental margin (González *et al.*, 1998). It is thought to have developed as a result of interaction between the southern end of the Iberia palaeo-margin, the westward displacement of the Gibraltar arc, and the convergence between the Africa and Eurasia plates (Tortella *et al.*, 1997). Tortella *et al.* (1997) find evidence for three main phases of deformation in this area in the upper Neogene crustal structure: a mountain building phase in the early to mid Miocene, a period of distension in the late Miocene-Pliocene, and a period of Quaternary compression.

At the eastern end of the AGFZ lies the Gibraltar arc. The Alboran Sea lies further east between the Betic Cordillera to the north and the Rif and Tell fold and thrust belt in northern Morocco to the south. The western Alboran Sea is a zone of E-W oriented extension (López Casado *et al.*, 2001). The regional geodynamics are not well understood and numerous models have been proposed to account for the observed extension, the distribution of seismicity, and the results of travel time tomography. López Casado *et al.* (2001) summarise these models, which include subduction of Africa beneath Iberia with the Alboran Sea being a back-arc basin, the existence of a broken subducted sheet causing extension, active continental subduction of the Iberia plate beneath the Betic Cordillera and the Alboran Sea, collapse of a large dome in the Alboran Sea driven by mantle convection, and

lithospheric delamination (separation of part or all of the upper crust from the lower crust and mantle as a result of plate convergence).

Earthquakes in the Gulf of Cadiz and Cape St. Vincent region occur to depths of around 100 km due to coupling between the crust and brittle upper mantle (Stich *et al.*, 2005). Stress tensors obtained for shallow to intermediate depth (6-60 km) earthquakes are similar and display sub-horizontal σ_1 axes oriented NNW. Stich *et al.* (2005) conclude that this similarity indicates that deformation is analogous in both domains and that deeper earthquakes are unrelated to any active subduction process.

Appendix B

HR Wallingford

Dr Stephen Richardson	Project Manager
Christopher Hutchings	Project Director
Dr Alan Cooper	Principle Scientist
Dr Doug Cresswell	Senior Scientist
Dr Jane Smallman	Managing Director
Dr Michael Turnbull	Senior Scientist
Matthew Wood	Senior Scientist

British Geological Survey

Dr Brian Baptie	Seismologist
Dr David Kerridge	Programme Manager
Dr Roger Musson	Seismologist
Dr Lars Ottemöller	Seismologist
Dr Suzanne Sergeant	Seismologist

Proudman Oceanographic Laboratory

Dr Kevin Horsburgh	Ocean Modeller
Dr Chris Wilson	Ocean Modeller

Appendix C Possible source models for the 1755 Lisbon earthquake

Gorringe Bank Source Models

Similarities between the isoseismals for the 28 February 1969 and the 1755 earthquakes (Figure B1) have led many researchers to conclude that the earthquakes occurred on the same structure and had the same rupture mechanism (Levret *et al*., 1991; Heinrich *et al*., 1994; Rabinovich *et al*., 1998; Mendes *et al*., 1999). Several models have been constructed on this supposition. Johnston (1996) estimates that for a lithospheric depth of at least 50km, a down-dip fault width of 80km should be within the brittle regime for a dip-slip fault dipping in a southeasterly direction at an angle of about 40º (the south dipping plane found by Fukao, 1973). He finds, for average slip of around 12m and moderate stress and strain drops, a fault length of approximately 200km (Figure B2). This is comparable to the axial length of the Gorringe Bank. A thrust-faulting model for an M 8.7 earthquake in which the Gorringe Bank is in the hanging wall (the block lying above an inclined fault surface) provides a reasonable fit to the tectonics of the region, and the known strong ground motion and tsunami effects (Johnston, 1996). Johnston (1996) points out that given the greater rigidity of oceanic crust, an earthquake that occurs at the Gorringe Bank will require smaller fault dimensions and larger slip to generate a given seismic moment.

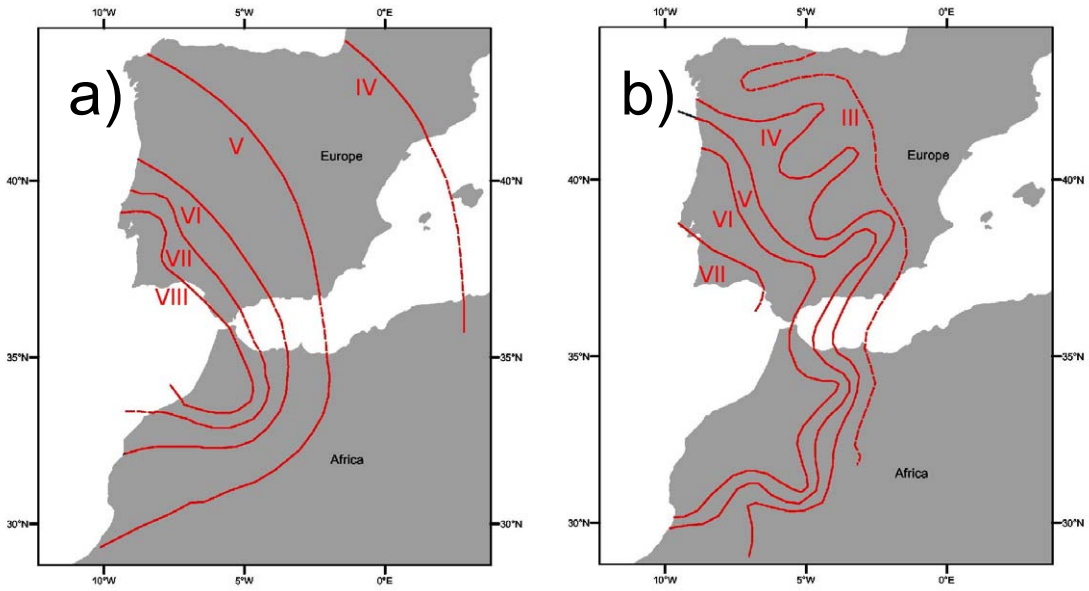

Figure B1 Modified Mercalli isoseismal sketch maps for (a) the 1755 earthquake, and (b) the 1969 event (after Johnston, 1996).

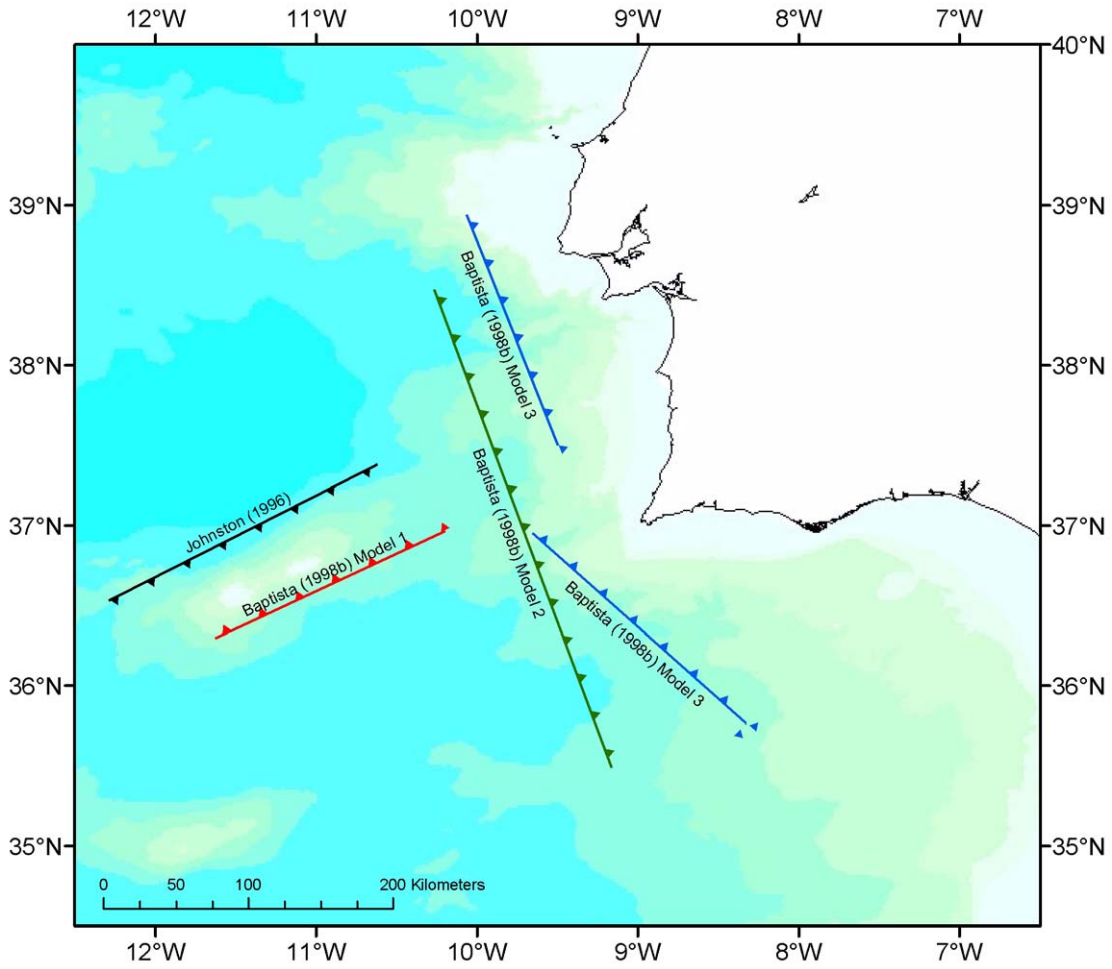

Figure B2 **Source models for the 1755 earthquake proposed by: Johnston (1996), black line; Baptista *et al.* (1998b) model 1, red line; Baptista *et al.* (1998b) model 2, green line; and, Baptista *et al.* (1998b) model 3, blue line. Bathymetry data is from Figure 2.2.**

Levret (1991) also assumes that the 1755 earthquake had the same origin, focal zone and focal mechanism as the 1969 earthquake, and uses an intensity attenuation function derived from the 1969 data to calculate intensities for the 1755 earthquake. In accord with Johnston (1996), the author finds that the pattern of intensities for the 1755 earthquake approximates the Moroccan isoseismals for the 1969 event reasonably well. However, Levret (1991) identifies a number of discrepancies between the model and observations at several locations in Morocco: on the western coast at El Jadida there is a two-degree difference between observed and computed intensity.

Baptista *et al*. (1998b) also examine a source on the Gorringe Bank, with a rupture mechanism similar to the 1969 earthquake and a source of 120km × 120km striking at N55º E (Figure B2). They find that this model does not reproduce the observed distribution of wave heights and travel times along the Iberian coast, and conclude that this rules out a 1969-type source for the 1755 earthquake.

Iberian Margin Source Models

Baptista *et al*. (1998b) use backward ray tracing and shallow water simulations to investigate two models on the Iberian margin also shown in Figure B2: (1) An elongated source 360km long and 100km wide with a strike angle of N160º located

along the western Iberian margin; and (2) a double rupture with one segment measuring 260 km (N-S) × 100 (E-W) km, and a second 160 km long and 135 km wide. The first model is inconsistent with some of the tsunami observations and historical reports from the Moroccan coast. Both Baptista *et al*. (1998b) and Mendes *et al*. (1999) find that the L-shaped composite rupture model accurately reproduces the observed travel-times at locations north of Lisbon, on the Algarve coast and in the Gulf of Cadiz, and the large wave amplitudes observed along the Iberian coast and the west coast of Morocco. This model implies under-thrusting between the Gorringe Bank and Iberia at the south Iberia margin oriented at N160º and N135º, respectively.

Zitellini *et al*. (1999, 2001) report the results of a multi-channel seismic reflection survey between the Madeira Tore rise and the Gulf of Cadiz. They detect a large thrust structure, the Marques de Pombal fault [MPF] (Figure B3), the location of which coincides with the source area identified by Baptista *et al*. (1998b). The deformed area associated with the MPF is approximately 200km long and numerous earthquakes have been located on it and associated structures. Zitellini *et al*. (1999) conclude that this is the most probable source of the 1755 earthquake and this model is consistent with the findings of Baptista *et al*. (1998b). However, although the projected length of the MPF may be sufficient, the imaged part of the MPF is too small to have accommodated the 1755 earthquake even with the high stress drop that might be expected for an intraplate earthquake (Zitellini *et al*., 2001).

Terrinha *et al*. (2003) suggest that the MPF could be connected to the Pereira de Souza fault [PSF] by means of a transfer fault. They propose that if the MPF and the PSF are connected at depth, it is possible to enlarge the rupture area proposed for the 1755 earthquake from 7,000km^2 to at least 19,000km^2. However, the PSF and associated structures acted as extensional faults in the rifting of the western Iberian margin and do not show any evidence of compression (Terrinha *et al*., 2003). Carvalho *et al* (2004, 2005) use a stochastic finite element approach to simulate the intensity distribution in Portugal using a variety of models, and incorporating the direction of rupture propagation. They obtained the best fit using a MPF-PSF model, with a nucleation point 120 km away from Lisbon and southward rupture propagation.

Gràcia *et al*. (2003) propose that the 1755 earthquake might have involved rupture on the east-dipping San Vincente and Horseshoe faults as well as the MPF. These faults are parallel and near to the MPF (Figure B3). Matias *et al* (2005a) also prefer the MPF-HF model on the grounds that both are reverse faults, and recent studies (as yet unpublished) on bathymetric data indicate a transfer fault joining the two. However, Pagarete and Ruegg (2005) consider that the MPF-HF model is too small to accommodate the 1755 event.

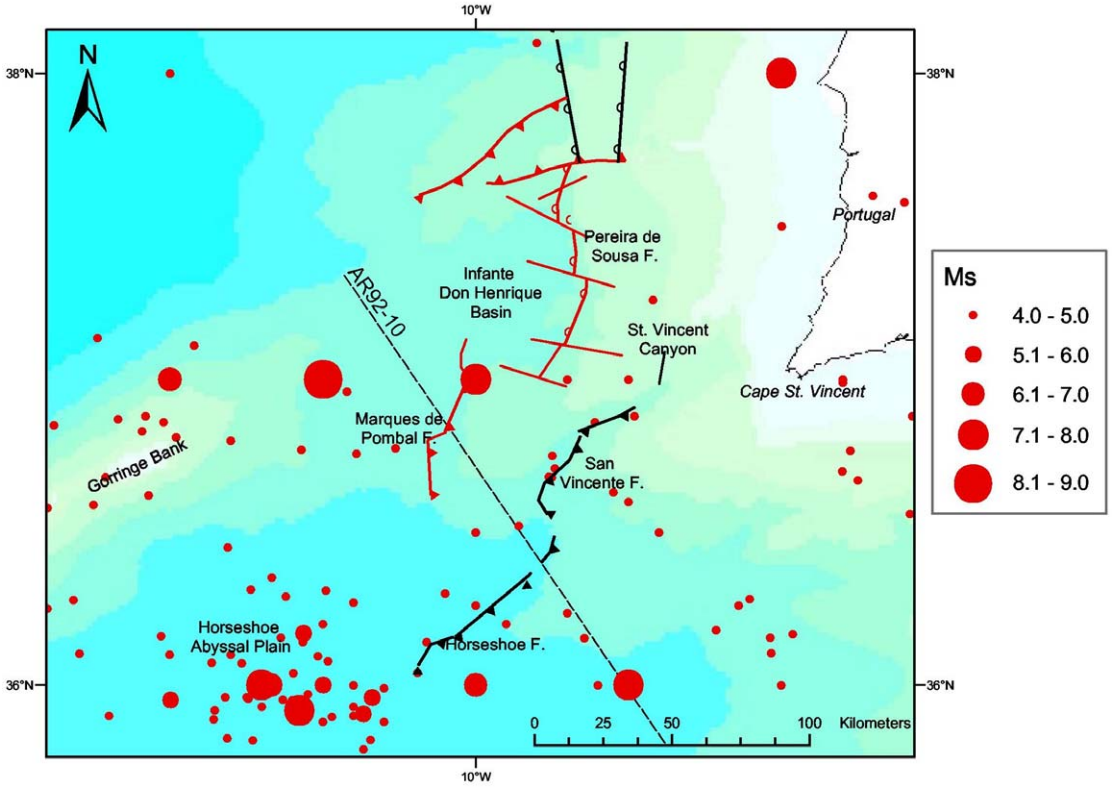

Figure B3 **Structural map of the MPF-PSF region showing major structures including the Marques de Pombal and Pereira de Sousa faults (after Terrinha *et al.*, 2003). Earthquake epicentres (symbols scaled to magnitude) are also plotted. AR92-10 is the seismic line on which the Marques de Pombal fault was first detected. Earthquake data are from the BGS World Seismicity Database (Henni *et al.*, 1998).**

Composite Source Models

Baptista *et al*. (2003) propose a composite source consisting of two segments: one following the MPF and another on the southern flank of the Guadalquivir Bank [GB]. In their model, the MPF segment is 105km long and 55km wide, dipping at 24º and with a strike of 21.7º. The GB segment is 96km long and 55km wide, dips at a steeper angle (45º) and strikes at 70º. Baptista *et al*. (2003) assume an average slip of 20m on both segments in order to reproduce wave heights at the nearest locations in south – west Iberia and for consistency with the magnitude estimate for the earthquake. Pagarete and Ruegg (2005) found that this model had too small a source and involved too high a slip to be credible.

The synthetic tsunami travel times for this source fit the data well at most locations with exceptions being at Huelva (southern Spain) and Safi (west coast of Morocco). At these locations, the synthetic arrivals are very late. According to Baptista *et al*. (2003), the discrepancy at Huelva is probably due to its location on a shallow estuary. The model substantially underestimates reported wave heights at Cadiz (~ 15 m). This may be due to the original wave height being overestimated in historical reports or the result of strong local bathymetric effects. Baptista *et al*. (2003) also attempt to model distal observations of the 1755 tsunami from the UK and the Caribbean. For these locations, synthetic wave heights and arrival times are smaller and shorter than observed. Baptista *et al*. (2003) attribute this to insufficient source dimension and lack of detailed bathymetry for these areas.

In an effort to explain eyewitness reports of more than one ground shaking event and the high intensity observations from the area NE of Lisbon, Vilanova *et al*. (2003) propose a composite rupture model for the 1755 earthquake involving the Lower Tagus Valley fault [LTVF]. In this model, an initial shock occurs on a fault in the Gorringe Bank region, following Johnston (1996). Then a secondary shock is triggered onshore on the LTVF through either static and/or dynamic stress changes. The LTVF is thought to have been the source structure for several destructive earthquakes around Lisbon, including a powerful shock in 1531. Vilanova *et al*. (2003) show that when the intensity observations from the 1969 Gorringe Bank and 1531 Lisbon earthquakes are superimposed, the result is close to the distribution of intensities seen for the 1755 earthquake. However, Matias *et al* (2005a) suggests that the offshore sources cannot produce a large enough variation in Coulomb failure stress in the LTV to advance it to failure. Also, Cabral *et al* (2005) discuss the potential for seismicity in the Lower Tagus Valley, noting an absence of any surface faulting in Quaternary deposits. The segmented fault system in this part of Portugal imposes an upper magnitude bound of around 6.5, unless there is some merging of structures at depth.

A Subduction Source

Gutscher *et al*. (2002) propose a model in which there is an active subduction zone beneath the Strait of Gibraltar associated with an almost vertical subducting slab. This model was constructed in order to account for global and regional travel time tomography results that they claim shows a slab of oceanic lithosphere descending from the Gulf of Cadiz, passing through intermediate depth seismicity (60-120km) beneath the Gibraltar arc and the western Alboran sea, and merging with a cluster of deep earthquakes (600-660km) located below Granada in southern Spain.

The model is controversial because it is not fully consistent with the relative motions of Africa and Eurasia, nor is it consistent with estimates of Miocene crustal shortening in this area (Platt and Houseman, 2003). Furthermore, Platt and Houseman (2003) argue that the tomographic images interpreted by Gutscher *et al*. (2002) only bear a superficial resemblance to a subducting slab, and that the intermediate and deep seismicity west of the Strait of Gibraltar is highly localised, in no way resembling a Wadati-Benioff zone. Buforn *et al*. (2004) suggest that these deep earthquakes may actually be related to older subduction processes. There are no instrumental records of earthquakes associated with this subduction zone. Gutscher (2004) interprets this as evidence to suggest that the subduction zone (if it exists and is active) is currently locked.

Baptista *et al*. (2002) investigate the possibility of a rupture 180km $\times$ 210km on a shallow east dipping fault plane with an average slip of 20m. Tsunami modelling results for this type of source are consistent with arrival times and amplitudes observed in the Gulf of Cadiz, Madeira and Porto Santa. However, the model underestimates amplitudes and overestimates arrival times at locations on the west coast of Portugal. Furthermore, this type of model is hard to reconcile with the available intensity data from Spain, Portugal and Morocco (Fonseca, 2005). Baptista *et al*. (2002) conclude that a subduction source for the earthquake implies a second simultaneous source closer to the western margin of Iberia in order to be consistent with the observations.